Insights into fluoroquinolones uptake: a biophysical and biochemical approach

Mariana Santos Ferreira de Sá

PhD thesis submitted to
Faculdade de Ciências da Universidade do Porto,
Faculdade de Ciências e Tecnologia da Universidade Nova de Lisboa,
Universidade de Aveiro
Medical Biochemistry and Biophysics

2019

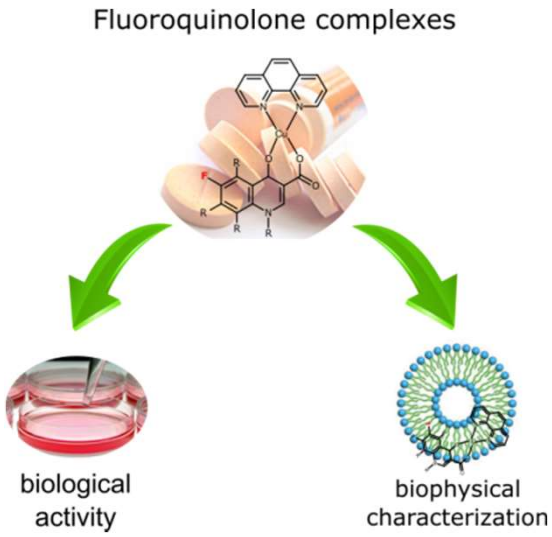

Insights into fluoroquinolones uptake: a biophysical and biochemical approach

Mariana Santos Ferreira de Sá
Programa Doutoral em Química Sustentável
Departamento de Química e Bioquímica
2019

Orientador
Alberta Paula Lobo Machado Gameiro dos Santos, Professor Auxiliar com Agregação, Faculdade de Ciências da Universidade do Porto


M2B-PhD
Medical Biochemistry & Biophysics
International Doctoral Programme


requimte
LABORATÓRIO ASSOCIADO
PARA A QUÍMICA VERDE


FCT
Fundação
para a Ciência
e a Tecnologia


COMPETE
2020
PORTUGAL
2020
UNIÃO EUROPEIA
Fundos Europeus Estruturais
e de Investimento

Acknowledgments

No final deste trabalho gostaria de agradecer a todas as Instituições e pessoas, sem as quais este trabalho não teria sido desenvolvido:

À Fundação para a Ciência e Tecnologia (FCT) pelo financiamento e atribuição da bolsa de doutoramento (SFRH/BD/52382/2013).

Ao Programa Doutoral em Química Sustentável (PDQS) e ao Medical Biochemistry & Biophysics International Doctoral Programme (M2B-PhD), que me proporcionaram formação de excelência e permitiram contactar com investigadores e docentes de elevada relevância nas suas áreas de investigação.

Ao REQUIMTE, que assegurou as condições técnicas à realização deste trabalho.

À Faculdade de Ciências da Universidade do Porto por me ter aceitado como aluno de Doutoramento.

À Dra. Paula Marques, por todo o apoio administrativo neste processo.

À minha grande parceira de trabalho e amizade, a Professora Paula, que me orienta e acompanha. Obrigada pela amizade e oportunidades que me tem dado e, claro, pelas gargalhadas e discussões mais intensas.

À Professora Eulália, cujo espaço é constantemente invadido pela minha energia e ruído! E pelas ajudas várias, entre as quais boas sugestões e sentido crítico.

To Dr. Stefania Stefani and Dr. Floriana Campanile that gave me the opportunity to learn microbiology in their laboratory, in Catania. And to Elena, Giusi, Dafne and all girls that helped me in the lab and that were good friends during the time I spent in Catania. Saudades of all!

To Dr. Reto Luginbuehl and the Cost Action that gave me the opportunity to go to Catania through financial support.

Aos elementos da minha comissão de acompanhamento, a Professora Doutora Conceição Rangel, a Professora Doutora Paula Gomes e o Doutor Jorge Oliveira, que acompanharam o desenrolar do trabalho.

À Iva Fernandes e ao Professor Nuno Mateus, pela oportunidade e apoio para realizar os ensaios de toxicidade.

À D. Aurora, por toda a ajuda e boa disposição.

Aos meus amigos de laboratório, a Sílvia, a Carla, a Lucinda, a Ritinha e o Miguel. Obrigada por toda a ajuda, por me aturarem (tarefa árdua, muitas vezes) e por fazerem do nosso grupo um grupo coeso, apesar das tantas diferenças que nos distinguem.

À Alex, pela amizade e boa disposição.

Aos meus Gambozinos e à Suzana e ao Rui, que me acompanham há anos e que me aquecem o coração. E à musica, sem a qual eu não imagino o meu dia-a-dia!

Ao Daniel, aos meus pais e ao Gonçalo, que são constantemente bombardeados com as novidades e ansiedades do dia-a-dia e que me dão suporte. E à nossa Kikas, que me aumentou o tamanho do coração e cujo sorriso torna cada dia ainda mais luminoso.

E a Deus, que me tem dado tantas oportunidades e me tem trazido tanta gente boa à minha vida!

Abstract

Fluoroquinolones (FQs) are antibiotics widely used in the clinical practise due to the large spectrum of action against Gram-negative and some Gram-positive bacteria. The influx route of these drugs in the bacterial cells has been widely study and seems to depend on hydrophobic (through the membrane) and hydrophilic (through porins, especially OmpF and OmpC) interactions. Nevertheless, the misuse and overuse of antibiotics have triggered the development of bacterial resistance mechanisms.

The main bacterial resistance mechanisms described against FQs occur through i) the reduction of the intracellular concentration of the drugs, due to changes on membrane permeability (resultant from the decrease of the expression of porins usually involved in the translocation of the pure drugs) or via efflux pumps or ii) mutations of the target molecules, topoisomerase II (DNA gyrase) and topoisomerase IV.

One of the strategies to circumvent this problem is the complexation of FQs with divalent metal ions and phenanthroline (phen) since it forms very stable complexes, known as metalloantibiotics (M(II)/FQ/phen), with different activity and enhanced pharmacological behaviour. Although little is known on the influx of the metalloantibiotics, preliminary studies point out for an alternative translocation pathway through the bacterial membranes, independent of porins.

The main objective of the present work was the investigation of the translocation pathways of FQs and respective Cu(II)/FQ/phen. Five FQs (cpx, erx, lvx, mxfx and spx) and their respective metalloantibiotics were studied and the work was performed through biophysical studies, microbiological tests and activity and toxicity assays.

Biophysical studies on the determination of the partition coefficient (K_p) of these compounds show a greater K_p values for the metalloantibiotics, in *Escherichia coli* total extract liposomes. Location studies were further performed using different probes with known membrane location and by quenching by iodide. The obtained results pointed out for a deeper location of all metalloantibiotics and pure spx, in comparison to the rest of pure FQs. Lastly, the interaction of the compounds with OmpF was evaluated, using wild-type (WT) and mutants of the porin. The association constants (K_{ass}) determined for FQs and metalloantibiotics with OmpF WT were very similar. Additional quenching studies by iodide and acrylamide were also performed in the absence and presence of cpx and Cucpxphen. The obtained results demonstrated a stronger interaction of cpx near the centre of the porin, contrary to the Cucpxphen whose interaction was analogous in the centre of the channel and in the bilayer/protein

interface. The biophysical results support different translocation routes for FQs (with exception of spx) and metalloantibiotics, supporting a hydrophobic translocation pathway for the ternary complexes and for spx.

The microbiological section aimed to elucidate the role of porins in the influx of the compounds and to determine the antimicrobial activity against multidrug-resistant (MDR) clinical isolates. The compounds were tested against three parental *E. coli* strains and their porin deficient mutant derivatives, through the antimicrobial susceptibility testing. The minimum inhibitory concentration (MIC) values determined pointed out the need of porins for the translocation of cpx, erx, lvx, Cucpxphen and Culvxphen. On the contrary, the influx of mxfx, spx, Cuerxphen, Cumxfxphen and Cuspxphen seemed to occur through a porin-independent route. The growth inhibition zones obtained in the disk diffusion test displayed similar diameters for FQs and metalloantibiotics, not providing additional information.

The biophysical and microbiological results are clearly complementary, providing information that allow to infer the need of porins for the uptake of cpx, erx and lvx and a hydrophobic pathway for the influx of mxfx, spx, Cuerxphen, Cumxfxphen and Cuspxphen. Metalloantibiotics, as Cucpxphen and Culvxphen, might also diffuse into the membrane through the porin.

Subsequently, the antimicrobial activity of the compounds was evaluated against a panel of MDR clinical isolates. The MIC was determined for all compounds against several MDR isolates of Gram-negative (*E. coli* and *Pseudomonas aeruginosa*) and Gram-positive (methicillin-resistant *Staphylococcus aureus* - MRSA) bacteria. The obtained results showed comparable MIC values for FQs and metalloantibiotics against the Gram-negative strains. In turn, the metalloantibiotics exhibited a greater antimicrobial activity against the majority of the MRSA isolates, which suggests that these compounds might be a promising alternative to FQs against *S. aureus*.

The last section of this work explored the enzymatic inhibitory activity of the metalloantibiotics against the main targets of FQs, DNA gyrase and topoisomerase IV. The study was performed with two metalloantibiotics, Cucpxphen and Cuspxphen, against enzymes of *E. coli* and *S. aureus*. The results obtained were similar for both metalloantibiotics and proved their inhibitory activity, proposing a similar mechanism of action for FQs and metalloantibiotics. In addition, metalloantibiotics exhibited greater inhibitory activity against the Gram-positive enzymes, which corroborates the microbiological results. Finally, preliminary toxicity tests were performed, showing greater cytotoxicity for the metalloantibiotics against fibroblasts cells, comparing to pure

FQs. In turn, the hemolytic activity of the metalloantibiotics was comparable to the one of pure FQs, showing no significant erythrocyte lysis.

In summary, metalloantibiotics seem to be a promising alternative to pure FQs. In *E. coli*, their influx relies on hydrophobic pathways, favoured by electrostatic interactions with the surface of the bacterial membrane and/or by diffusion through the porin. Thus, metalloantibiotics may bypass the AMR mechanism based on changes on membrane permeability, commonly adopted by Gram-negative bacteria. In addition, these compounds revealed improved antimicrobial activity against MRSA strains. Although metalloantibiotics are more cytotoxic than FQs, the application of these compounds might be advantageous in the fighting of AMR mechanisms.

Keywords: Fluoroquinolones, Metalloantibiotics, Bacterial resistance, Liposomes, Gram-negative and Gram-positive bacteria, Porins, Fluorescence, Microbiology, DNA gyrase, Topoisomerase IV, *In vitro* cytotoxicity

Resumo

As fluoroquinolonas (FQs) constituem uma família de antibióticos de largo espectro de ação contra bactérias Gram-negativas e algumas Gram-positivas. As vias de permeação bacteriana destes fármacos, vastamente estudadas nos últimos anos, parecem depender de diferentes tipos de interações: interações hidrofílicas, via porinas (nomeadamente OmpF e OmpC) e hidrofóbicas, através da bicamada fosfolipídica. Contudo, a frequente utilização errática dos antibióticos, por uso inadequado ou abusivo, tem originado o célere desenvolvimento de mecanismos de resistência bacteriana a antibióticos. Os principais mecanismos de resistência bacteriana a FQs ocorrem, usualmente, através i) da redução da concentração intracelular dos antibióticos (por alteração da permeabilidade membranar resultante da diminuição da expressão de porinas ou via bombas de efluxo) ou ii) de mutações das enzimas-alvo, as topoisomerases II (DNA girase e topoisomerase IV).

Uma das estratégias de combate à resistência bacteriana a FQs baseia-se na complexação destes antibióticos com metais de transição e fenantrolina (phen), a qual origina complexos ternários (M(II)/FQ/phen) muito estáveis, com atividade antibacteriana e potencial farmacológico. As vias de translocação destes metaloantibióticos estão ainda pouco esclarecidas mas parecem assentar em mecanismos independentes de porinas.

O presente estudo teve como principal objetivo a investigação das vias de permeação membranar de FQs e respetivos complexos ternários de Cu(II)/FQ/phen. O estudo abrangeu cinco FQs (cpx, erx, lvx, mxfx e spx) e respetivos metaloantibióticos e reuniu ensaios biofísicos, microbiológicos, bioquímicos e testes de toxicidade.

Os estudos biofísicos de determinação de coeficientes de partição (K_p) evidenciaram maiores valores de K_p para os metaloantibióticos em lipossomas de extrato total de *Escherichia coli*. O estudo prosseguiu com ensaios de localização membranar dos compostos, recorrendo à utilização de sondas fluorescentes com localização conhecida na membrana e a ensaios de extinção de fluorescência pelo ião iodeto. Os resultados experimentais revelaram uma localização mais profunda da spx e de todos os metaloantibióticos, comparativamente às FQs puras. Por fim, estudou-se a interação dos vários compostos com a porina OmpF, utilizando proteína nativa e mutada. As constantes de associação (K_{ass}) determinadas com a proteína nativa revelaram-se muito semelhantes para FQs e metaloantibióticos. Adicionalmente, realizaram-se ensaios de extinção de fluorescência da OmpF pelos agentes extintores

iodeto e acrilamida, na ausência e presença de cpx e Cucpxphen. Os resultados experimentais revelaram que a interação da cpx com a porina é mais forte na zona central do canal, enquanto o metaloantibiótico interage de forma semelhante no centro do canal e na interface lípido/proteína. Desta forma, os estudos biofísicos sugerem diferentes vias de permeação para FQs (com exceção da spx) e metaloantibióticos, sustentando uma via de translocação hidrofóbica para a spx e para os metaloantibióticos.

O trabalho prosseguiu com os estudos de microbiologia, com vista à clarificação do papel das porinas na translocação dos compostos e ao estudo da atividade antimicrobiana dos compostos contra um painel de isolados clínicos multirresistentes. O teste de suscetibilidade antimicrobiana foi realizado para todos os compostos contra três estirpes parentais de *E. coli* e respetivos mutantes deficientes na expressão de porinas. Os valores da concentração mínima inibitória (CMI) determinados mostraram que as porinas são necessárias para a permeação de cpx, erx, lvx, Cucpxphen e Culvxphen. Contrariamente, a translocação de mxfx, spx, Cuerxphen, Cumxfxphen e Cuspxphen parece ocorrer através de uma via independente de porinas.

A realização de ensaios biofísicos e microbiológicos revelou-se uma mais-valia para o estudo das vias de permeação dos compostos. Os resultados obtidos são complementares e mostram que as porinas são necessárias para o influxo de cpx, erx e lvx. No entanto, a translocação de mxfx, spx, Cuerxphen, Cumxfxphen e Cuspxphen não necessita das porinas.

Seguiu-se a determinação da CMI para todos os compostos contra vários isolados multirresistentes de bactérias Gram-negativas (*E. coli* and *Pseudomonas aeruginosa*) e Gram-positivas (*Staphylococcus aureus* resistentes à meticilina - SARM). Os resultados experimentais revelaram valores de CMI semelhantes para FQs e metaloantibióticos contra estirpes Gram-negativas. No entanto, os metaloantibióticos evidenciaram atividade antimicrobiana melhorada contra a maioria dos isolados de SARM, o que sugere que estes compostos poderão constituir uma alternativa viável às FQs contra *S. aureus*.

A secção final deste trabalho abrangeu o estudo da atividade inibitória enzimática dos metaloantibióticos contra os principais alvos das FQs, a DNA girase e a topoisomerase IV. O estudo foi realizado com dois metaloantibióticos, Cucpxphen e o Cuspxphen, contra enzimas de *E. coli* e *S. aureus*. Os resultados obtidos foram semelhantes para ambos os metaloantibióticos e provaram que estes compostos têm atividade inibitória enzimática, o que aponta para um mecanismo de ação semelhante para FQs e metaloantibióticos. A atividade inibitória dos metaloantibióticos revelou-se,

ainda, superior contra as enzimas de bactérias Gram-positivas, o que corrobora os resultados de microbiologia. Por fim, o trabalho termina com testes de toxicidade, os quais evidenciaram maior citotoxicidade para os metaloantibióticos contra fibroblastos, comparativamente às FQs. Contrariamente, a atividade hemolítica dos metaloantibióticos é semelhante à das FQs, não tendo sido observada lise de eritrócitos.

Em suma, os metalontibióticos parecem constituir uma alternativa viável às FQs puras. Em *E. coli*, o seu influxo tem por base uma via hidrofóbica, favorecida por interações eletrostáticas com a superfície membranar das bactérias e/ou por difusão através das porinas. Desta forma, os metaloantibióticos poderão ser capazes de contornar o mecanismo de resistência bacteriana assente em alterações da permeabilidade da membrana, usualmente adotados por bactérias Gram-negativas. Adicionalmente, estes compostos exibiram atividade antimicrobiana melhorada contra estirpes de SARM. Embora a citotoxicidade dos metaloantibióticos seja superior à das FQs, a sua aplicação poderá ser vantajosa no combate a mecanismos de resistência bacteriana.

Palavras-chave: Fluoroquinolonas, Metaloantibióticos, Resistência bacteriana, Lipossomas, Bactérias Gram-negativas e Gram-positivas, Porinas, Fluorescência, Microbiologia, DNA girase, Toposisomerase IV, Citotoxicidade *in vitro*

Contents

List of Figures

List of Tables

List of Schemes

List of abbreviations

AMR - Antimicrobial resistance

ANOVA – Analysis of variance

BHI - Brain heart infusion

BSA - Bovine serum albumin

CAMH - Cation-adjusted Mueller-Hinton

CFU - Colony-forming units

CL – Cardiolipin

CLSI - Clinical and Laboratory Standards Institute

Cpx - Ciprofloxacin

DMPG - 1,2-dimyristoyl-s*n*-glycero-3-phospho-(1'-rac-glycerol)

DNA - Deoxyribonucleic acid

DOPG - 1,2-dioleoyl-s*n*-glycero-3-phospho-(1'-rac-glycerol)

DPH - 1,6-diphenyl-1,3,5-hexatriene

DSPG - 1,2-distearoyl-s*n*-glycero-3-phospho-(1'-rac-glycerol)

EARS-Net - European Antimicrobial Resistance Surveillance Network

EDTA - Ethylenediaminetetraacetic acid

Erx – Enrofloxacin

E. coli - *Escherichia coli*

ESBL – Extended-spectrum β-lactamase

EUCAST - The European Committee on Antimicrobial Susceptibility Testing

FQ – Fluoroquinolone

Gpfx – Grepafloxacin

HEPES - N-(2-hydroxyethyl) piperazine-N'-ethanesulfonic acid

K_p - Partition coefficient

K_{ass} - Association constant

Lmx - Lomefloxacin

LUV – Large unilamellar vesicle

Lvx - Levofloxacin

MDR – Multidrug-resistant

MHA - Mueller-Hinton agar

MHB - Mueller-Hinton broth

MIC - Minimum inhibitory concentration

MLV – Multilamellar vesicle

MRSA - Methicillin-resistant *Staphylococcus aureus*

MTT - Thiazolyl Blue Tetrazolium Bromide

Mxfx - Moxifloxacin

Nfx - Norfloxacin

Ofx - Ofloxacin

Omp – Outer membrane protein

oPOE - Octylpolyoxyethylene

PE - Phosphatidylethanolamine

PG – Phosphatidylglycerol

Phen – Phenanthroline

PMQR - Plasmid-mediated quinolone resistance

POPE - 1-palmitoyl-2-oleoyl-s*n*-glycero-3-phosphoethanolamine

POPG - 1-palmitoyl-2-oleoyl-s*n*-glycero-3-phospho-(1'-rac-glycerol)

P. aeruginosa - *Pseudomonas aeruginosa*

r_s - Steady-state fluorescence anisotropy

Spx – Sparfloxacin

SUV – Small unilamellar vesicle

SWR - Standard working reagent

S. aureus - *Staphylococcus aureus*

TAE - Tris acetate EDTA

TMA-DPH - 1,6-diphenyl-1,3,5-hexatriene-4′-trimethylammonium tosylate

T_m - Transition temperature

Tvx - Trovafloxacin

WHO – World Health Organization

WT - wild-type

2-AS - (±)-2-(9-Anthroyloxy) stearic acid

12-AS - (±)-12-(9-anthroyloxy) stearic acid

$< \tau >$ - Amplitude-weighted lifetime

$\bar{\tau}$ - Average lifetime

Introduction

1

1.1. **Gram-negative and Gram-positive bacteria**

The cell envelope of bacteria is the first natural barrier against antimicrobials and its characteristics enable the classification of bacteria into two groups, the Gram-negatives and Gram-positives, harbouring structural and chemical characteristics differences that can easily be noted after the Gram stain (Gram-positive bacteria retain this complex after treatment with alcohol and appear purple, whereas Gram-negative organisms decolorize following such treatment and appear pink).[1,2]

Briefly, Gram-positive bacteria are surrounded by a single membrane, the cytoplasmic membrane, while Gram-negative bacteria comprise two membranes, the cytoplasmic membrane (the inner membrane) and the outer membrane.[3] In general, bacterial membranes are rich in anionic and zwitterionic lipids, especially phosphatidylglycerol (PG), cardiolipin (CL) and phosphatidylethanolamine (PE).[3,4] Beyond the membrane, the bacterial wall encompasses the peptidoglycan, a layer that differs in location and thickness, according to the type of bacteria. Figure 1 shows the constitution and structure of the cell envelope of Gram-negative and Gram-positive bacteria.

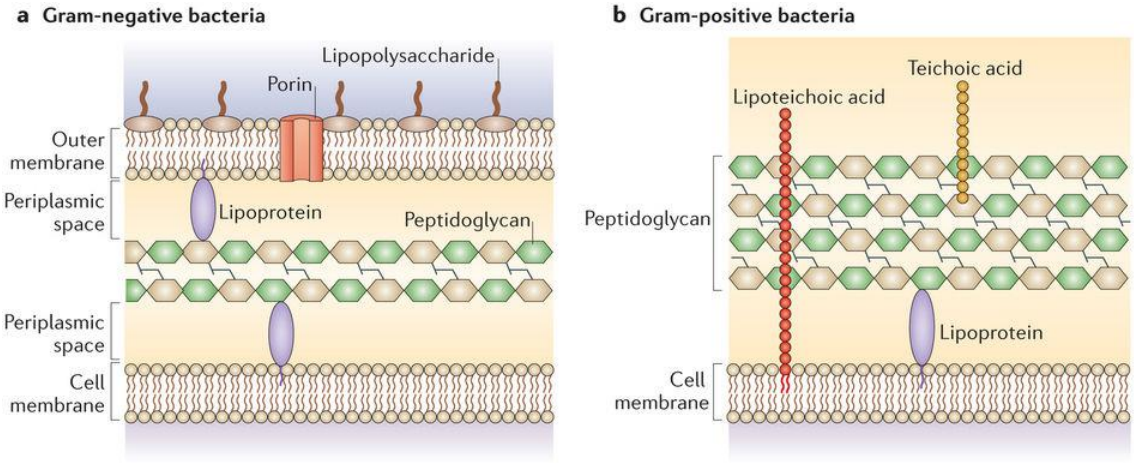

Figure 1 - Bacterial cell envelope of Gram-negative (a) and Gram-positive (b) bacteria, from [5].

Peptidoglycan is a polymer of repeated subunits of *N*-acetylglucosamine and *N*-acetylmuramic acid (two sugars) and several amino acids. The organization of this bacterial structure usually exhibits the alternation of the two sugars with the amino acids linked to the carboxyl group of the *N*-acetylmuramic acid. Some amino acids present in the peptidoglycan are not found in proteins, being characteristic of this

structure (as the *D*-glutamic acid, the *D*-alanine and the *meso*-diaminopimelic acid).[6] Gram-positive bacteria exhibit a thicker peptidoglycan (with around 30-100 nm), externally positioned to the cytoplasmic membrane, while in Gram-negative bacteria a thinner peptidoglycan layer (around scarce nm) is observed between the cytoplasmic and the outer membranes.[3,7] These distinctive characteristics justify the natural trend of Gram-negative bacteria to be more resistant to antimicrobial agents compared to Gram-positive bacteria.[8] Besides the structure, the composition of the membranes of Gram-positive and Gram-negative bacteria also differs in terms of phospholipids and other molecules.

Typically, the cytoplasmic membrane of Gram-positive bacteria is largely enriched with anionic phospholipids (around fifty-fifty of PG and CL), there being some species with a considerable percentage of zwitterionic phospholipids (around 40 to 60% of PE), as the *Bacillus spp*.[3,9] In turn, the peptidoglycan of Gram-positive bacteria is composed by several layers of disaccharide *N*-acetylglucosamine and *N*-acetylmuramic acid, cross-linked by pentaglycine interbridges, and among which there are anionic polymers, the teichoic and lipoteichoic acids.[3,6,7,10] These polymers are mainly rich in glycerol phosphate, glucosyl phosphate or ribitol phosphate and are covalently bonded to peptidoglycan (teichoic acids) or linked to the headgroups of phospholipids of the cytoplasmic membrane (lipoteichoic acids). The Gram-positive cell envelope also contains proteins, positioned in or near the cytoplasmic membrane, attached to lipid anchors, covalently bonded or linked to peptidoglycan or to teichoic acids.[7]

In Gram-negative bacteria, the inner membrane is a phospholipidic bilayer, mostly composed of zwitterionic and anionic phospholipids as PE (around 60-80%), PG (about 20%) and CL (up to 10%).[7,11,12] The peptidoglycan of Gram-negative bacteria is a simpler structure when compared to the one of the Gram-positive bacteria. Instead of the pentapeptide interbridges (of glycine) observed in the Gram-positive bacterial peptidoglycan, this structure exhibits direct cross-linking between the peptides attached to the disaccharide layers (commonly performed by the carboxyl group of the *D*-alanine with the amino group of the diaminopimelic acid). Furthermore, the teichoic and lipoteichoic acids are not present in this structural component.[6] The outer membrane is a complex and asymmetric bilayer that differs in the composition of the inner and outer leaflets. The inner leaflet is mostly composed by phospholipids, being extremely similar to the inner (cytoplasmic) membrane.[8] In this way, this bilayer contains mainly PE, PG and CL in its composition. In contrast, the outer leaflet of the outer membrane is enriched with glycolipids, mainly lipopolysaccharides (LPS), which are in fact specific lipids present in Gram-negative bacteria.[2,8,11,13] The outer membrane is also rich in

proteins (around 50%, w/w), as lipoproteins (attached to lipids) or integral membrane proteins, known as outer membrane proteins (Omps) or porins.[12,14]

Omps are general β-barrel proteins that grant high permeability to the outer membrane for hydrophilic molecules smaller than 600 Da (~ 1 Å).[12,15] These channels are responsible for the influx of nutrients and some antibiotics as fluoroquinolones (FQs) or β-lactams.[13,16,17] Usually, these porins do not show selectivity for substrates, only some discrimination concerning the charge of the molecules (cations or anions). The structure of these porins is homotrimeric and contains short loops between strands towards the periplasmic side and large loops orientated to the extracellular space.[3,14,15] Generally, each monomer is composed by 16 β-strands (general/non-selective porins) but some porins have 18 β-strands (selective porins).[12] The diameter of the pore also differs according to the specificity of the channel for the substrates, being around 15 Å for general porins and about 6 Å for the selective ones.[15] Although the functionality of the channel is assured by the existence of a trimer, each monomer is able to permeate independently of the others (but never in its absence).[16,18]

OmpF and OmpC are the main porins of *Escherichia coli* and have been well characterized by X-ray. These two proteins, composed of antiparallel 16 β-strands, are almost homologous, showing the main differences in the centre of the pore (Figure 2).[16,18,19] The positions and functions of the several loops that integrate these channels are well studied, being known that loops L1, L2 and L4 assure the trimer structure through the mediation of the interactions between monomers; loops L5, L6 and L7 are positioned in the superficial part of the barrel; loop L8 is located toward the interior and supports the functionalization of the aperture of the channel; loop L3 is a long and internal loop that, together with the adjacent barrel wall, forms the constriction zone, in the middle of the barrel.[15,16,20] The constriction zone exhibits a hourglass-like shape and has an active role in the influx due to its high compositional variability, that will determine the permeation selectivity of each protein.[12,16,17] OmpF and OmpC share a highly conserved sequence in loop L3 (Pro-Glu-Phe-Gly-Gly-Asp, conserved among enterobacterial porins), only diverging in the position of the residues.[12,17,21] This difference determines the strength of the electric field of the constriction zone and governs the permeation characteristics of each porin. In OmpF, the electric field results from the opposite location of charged residues, especially Asp113 and Glu117 (negative/acidic residues of the loop L3) and Lys16, Arg42, Arg82, and Arg132 (positive/basic residues located in the adjacent β-barrel wall).[16,21,22] In turn, the residues Asp18, Asp105 and Glu109 located oppositely to Lys16, Arg37, Arg74 and Arg124, are responsible for the electric field of the constriction zone of OmpC.[23] Although OmpF

and OmpC show a preference for the translocation of cations, OmpC is even more selective because its pore is more negative.[20,24] Furthermore, the diameter of the pore also differs between the two porins, being around 12 Å for OmpF and tighter for OmpC, and that may explain why OmpF is more permeable than OmpC, allowing the passage of larger solutes than OmpC.[19,21,24]

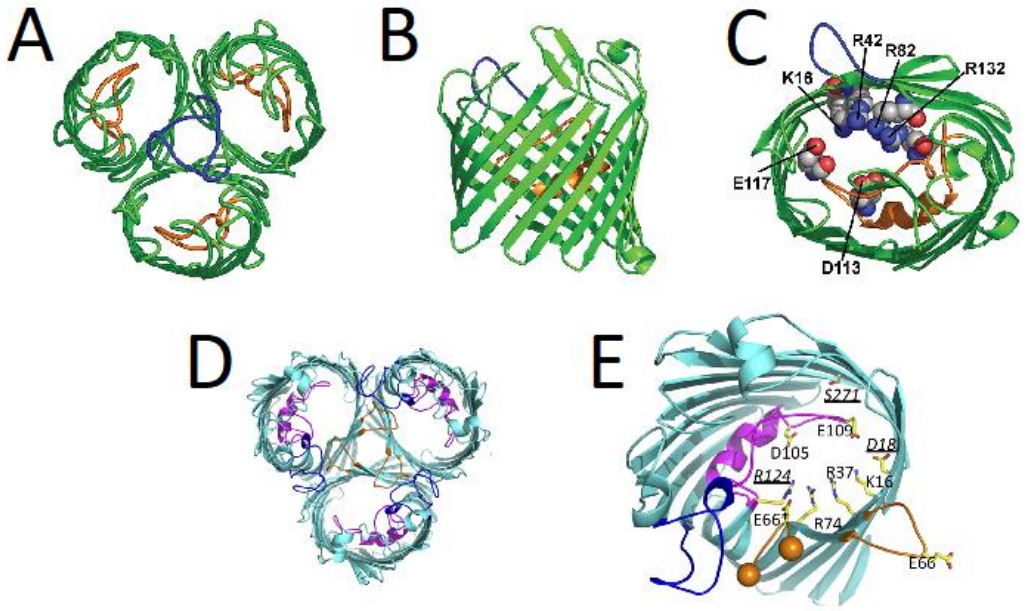

Figure 2 - Structures of OmpF (A, B and C) and OmpC (D and E) porins of E. coli, adapted from [21,23]. Top view of the trimer of OmpF (A), with Loop 2 coloured blue and Loop3 coloured orange; Side view of the barrel monomer of OmpF (B); Top view of a monomer of OmpF (C), highlighting the main residues of the constriction zone of the pore (Arg42, Arg82, Arg132, Lys16, Glu117 and Asp 113); Top view of the trimer of OmpC (D), with Loop 2 coloured orange and Loop3 coloured magenta; Top view of a monomer of OmpC (E), highlighting the main residues of the constriction zone of the pore (Arg37, Arg74, Arg124, Lys16, Glu109, Asp18, Asp105, Glu66 and Ser271).

Recent studies suggest that salt concentration has direct implications in the permeability of porins, showing that OmpC improves its influx ability under high salt concentrations, becoming similar to that of OmpF.[24] The osmolarity, temperature and ionic strength are also factors that play an important role in the regulation of the expression of these two porins, usually resulting in opposite effects in the two porins. As an example, if high osmolarity, high ionic strength and raised temperature results in the down-regulation of OmpF, it up-regulates OmpC.[24,25] This causality is used by bacteria in their own favour, as in the case of *E. coli*, which takes advantage of low temperatures and reduced ionic strength of natural waters to improve the uptake of nutrients through OmpF.[24]

1.2. **Phospholipids**

As previously mentioned, phospholipids constitute a great percentage of the lipidic composition of the cytoplasmic membrane of all bacteria and of the inner leaflet of the outer membrane of Gram-negative bacteria. These molecules are composed by an alcohol bound to a polar headgroup (phosphorus group) and a variable number of fatty acid chains. The contrast between the hydrophilic character of the headgroups and the hydrophobic nature of the aliphatic tails confers amphiphilic characteristics to phospholipids. The composition of the headgroups and of the hydrophobic tails can vary a lot, resulting in a great diversity of phospholipids.[26,27] According to the alcohol present in the molecule, phospholipids can be divided in two groups, glycerophospholipids, possessing a glycerol, and sphingomyelins, holding a sphingosine.

Glycerophospholipids are the predominant phospholipids in eukaryotic cells and bacteria.[26] As previously reported, PE, PG and CL are the most abundant phospholipids in bacteria, being PE zwitterionic, and PG and CL anionic. The chemical groups attached to the headgroup (phosphorus group) in each of these phospholipids are illustrated in Figure 3. However, there is a wide variety regarding the hydrophobic tails, mostly due to differences in length and saturation, resulting in several types of PE, PG and CL (as dipalmitoyl, dimyristoyl and dioleoyl, for example). Among these three phospholipids, CL is the most distinguishable due to its double negative charge and its four aliphatic chains (against the two characteristic of PE and PG).

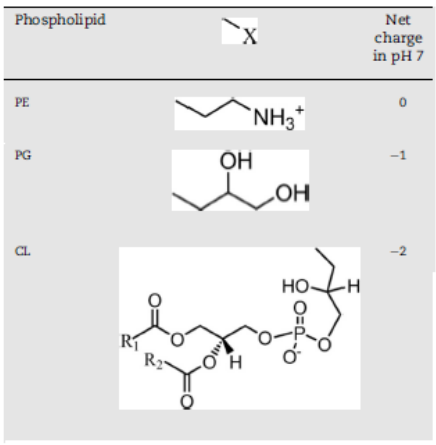

Figure 3 - The predominant phospholipids of bacteria, adapted from [26].

The characteristics of the hydrophobic tails and their proportion relative to the headgroup influence the molecular shape/architecture of phospholipids. Commonly, PE possesses the cone shape, while PG and CL assume the cylinder shape. Thus, the assembling of phospholipids with different molecular shapes results in diverse architectures. As shown in Figure 4, PG and CL usually form planar structures, the traditional bilayers (lamellar phase), while PE typically results in tubules with an aqueous channel in the middle (the hexagonal phase or cubic phase).[26,27]

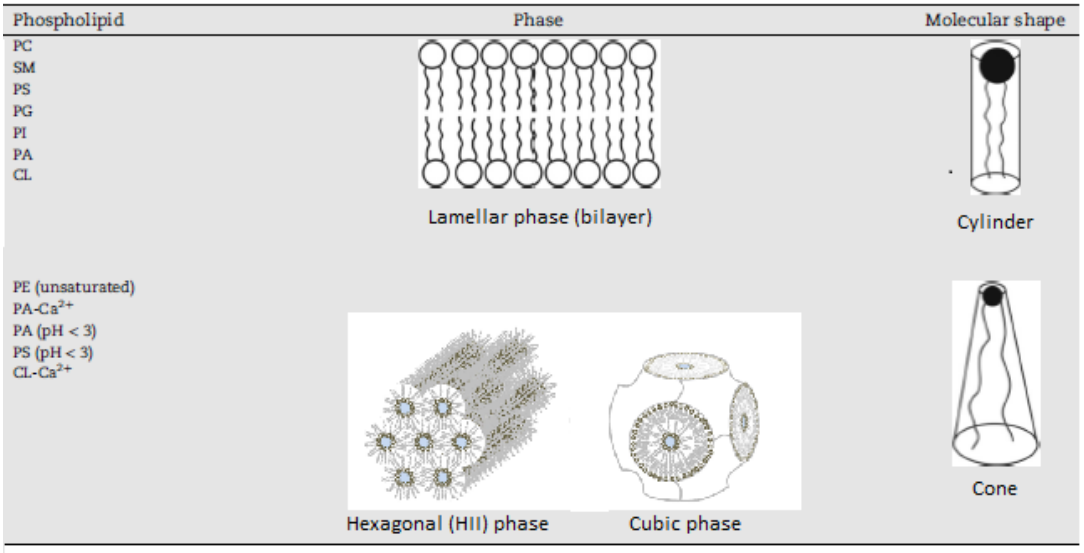

Figure 4 - The polymorphic phases and molecular shapes of phospholipids, adapted from [26,27].

However, variations in the length and degree of saturation of the aliphatic chains have direct implications in the architecture adopted by phospholipids. The hexagonal phase is privileged by longer aliphatic chains and higher numbers of unsaturation. For this reason, the same phospholipid can form different structures, depending on the characteristics of the fatty acid chains. For example, saturated PE tends to form a lamellar phase instead of the hexagonal phase usually observed. Furthermore, variations in temperature may result in phase changes, for instance alteration from a hexagonal to a lamellar phase can happen by the decreasing of temperature.[27] The architecture of the phospholipids can be related to the rigidity degree of the membranes. The lamellar phase, usually encompassing saturated aliphatic chains, is more rigid, while the hexagonal phase, enriched with unsaturated fatty acid chains, is more fluid.[27,28]

Besides shape and phase, phospholipids exhibit diverse physical properties as permeability and phase transition temperature (T_m). Once again, these characteristics depend mainly on the length and saturation degree of the aliphatic chains and on the present polar headgroups. Furthermore, the addition of other molecules, as proteins, to membrane bilayers also affects the thermodynamic behaviour of these systems.

Membrane bilayers can exhibit two main thermodynamic phases, a gel phase (more rigid and ordered phase) and a liquid-disordered or liquid crystalline phase (more fluid and disordered phase). The intra- and intermolecular interactions observed in these two phases differ, especially in the flexibility of the fatty acid chains, being more limited in the gel phase and more unrestricted in the liquid crystalline phase. In both cases, the preservation of the structure of the bilayer is assured by the electrostatic interactions between the water molecules and the polar headgroups of phospholipids. The transition between these two phases may still result in an intermedium phase, characterized by moderate fluidity and order, so-called liquid-ordered phase.[4,27,29] The T_m, specific of each lipidic system, is the temperature at which the phase change occurs. The nature, unsaturation and heterogeneity degree of the membrane bilayer define the T_m of the system. For example, although the only difference between 1-palmitoyl-2-oleoyl-s*n*-glycero-3-phosphoethanolamine (POPE) and 1-palmitoyl-2-oleoyl-s*n*-glycero-3-phospho-(1'-rac-glycerol) (POPG) is the polar headgroup, the T_m of POPE is 25 ºC, while the one of POPG is -2 ºC.[30] However, a POPE/POPG (0.75/0.25) mixture has a T_m of ~ 21ºC.[31] In turn, and besides the unique difference between 1,2-distearoyl-s*n*-glycero-3-phospho-(1'-rac-glycerol) (DSPG) and 1,2-dimyristoyl-s*n*-glycero-3-phospho-(1'-rac-glycerol) (DMPG) is the length of the saturated fatty acid chains, DSPG has a higher T_m (55 ºC), compared to DMPG (23 ºC), due to its longer aliphatic chains.[30] The presence of unsaturation in the fatty acid chains of phospholipids also affects the T_m, decreasing it, as is observed by the higher T_m of saturated DSPG (55 ºC), compared to the one (- 18 ºC) of the unsaturated 1,2-dioleoyl-s*n*-glycero-3-phospho-(1'-rac-glycerol) (DOPG).[29,30] As the heterogeneity of the systems increases, the existence of a single T_m is unlikely, being expected a temperature range between the gel phase and the liquid crystalline phase, corresponding to the coexistence of these two phases (in different proportions) and that may encompass more than one T. This evidence is well observed in liposomes composed by total lipid extract of *E. coli*.[29,31]

Natural phospholipids are mainly unsaturated, which positively contributes to the fluidity and permeability of the biological membranes allowing the diffusion of solutes and other biological processes.[27]

Although biological membranes are complex systems whose composition is extremely varied and random, these biological systems usually preserve the liquid crystalline phase. In the last decades, highly ordered lipidic domains were described specifically for eukaryotes. The so-called lipid rafts were described as lipidic spots, usually enriched with cholesterol, with different composition and physical properties from the rest of the membrane. Nowadays, the concept of lipid rafts was extended to bacteria, existing some molecules, different from cholesterol (only present in eukaryotes), responsible for the improvement of the order of specific regions of the bilayer in these organisms.[4,27]

1.2.1. **Mimetic membrane model systems**

The extraordinary complexity of the membranes, both in structure and composition, makes it difficult to create appropriate models for their study. For this reason, the development of different models has been explored during the last decades, being the liposomes and the proteoliposomes the predominant membrane mimetic model systems.[32-34]

Liposomes are spherical particles, comprising one or more lipidic bilayers that surround an aqueous compartment. The lipidic bilayers are mainly composed by phospholipids whose polar headgroups are faced to the aqueous environments (the interior compartment and the exterior of the particle). In turn, the middle region of the bilayers encompasses the hydrophobic tails of the phospholipids. This arrangement confers an amphiphilic character to liposomes and is responsible for the structural similarity of these particles to membranes.[28,32,35]

According to the characteristics of the membrane which is intended to mimic, liposomes can differ in size, number of bilayers, lipidic composition, lipidic source and method of preparation.[28] The classification of these particles is commonly based on the number of the bilayers and on the size of the vesicles. Liposomes containing a single bilayer are denominated unilamellar, while multilamellar vesicles (MLVs) are composed of more than one bilayer, resembling an onion. The size of the liposomes can vary from 25 nm to 2.5 μm and the unilamellar particles are classified as small unilamellar vesicles (SUVs), with a diameter smaller than 100 nm, large unilamellar vesicles (LUVs), exhibiting a diameter between 100 and 1000 nm, and giant unilamellar vesicles (GUVs), whose diameter is greater than 1 μm. In turn, according to the number of the bilayers, the size of the MLVs may be significantly variable.[28,33] With respect to

composition, liposomes can be prepared using a single lipid or a mixture of several lipids, which may be of natural or of synthetic source. The natural lipids are the most expensive ones.[26,28]

The preparation of a homogenous suspension of liposomes is simple and easy, especially of SUVs and LUVs.[33] There are various methods developed for liposome preparation, being the hydration method, also known as film dispersion method, the simplest and largely used (Figure 5). This method starts with the solubilisation of the lipids in an organic solvent (usually chloroform or methanol), followed by its evaporation along the walls of a round-bottomed flask, under inert atmosphere (usually nitrogen or argon). This step results in the formation of a lipidic film along the walls of the flask, which is submitted to a period of vacuum to ensure the total removal of the organic solvent. The method continues with the hydration step that consists in the dispersion of the lipidic film in a solution buffer, using vortex if necessary.[35] It has been well described that during the hydration step phospholipids naturally form closed particles, usually MLVs.[28,35] The achievement of an homogeneous suspension of liposomes is only assured with the third step that encompasses several cycles of freezing and thawing (usually performed with liquid nitrogen and a water bath) and various cycles of extrusion. The thermal shocks increase the volume of the aqueous compartment, while the extrusion yields unilamellar vesicles with similar sizes. The size of the liposomes depends on the chosen polycarbonate membranes (with pores of 100 nm, 200 nm or 600 nm) and is influenced by the phospholipidic composition.[33,35] The homogeneity and polidispersion of the suspensions is usually evaluated by electron microscopy or light scattering.[33]

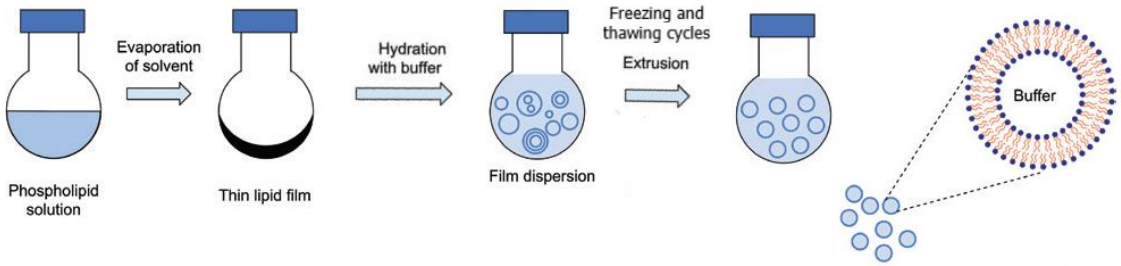

Figure 5 - Liposome preparation by film dispersion method, adapted from [35].

In addition to their similarity to biological membranes, liposomes are widely studied as propitious systems for drug delivery, due to their small size, amphipathic behaviour and promising characteristics of biocompatibility, biodegradability, and toxicity.[28,36,37]

However, liposomes just mimic the lipidic components of the membrane, ignoring the protein machinery present in biological membranes. For this reason, more complex mimetic systems, encompassing lipids and proteins, were developed. These membrane models systems are known as proteoliposomes and consist of unilamellar liposomes with proteins inserted in the lipid bilayer.[35,38] Nevertheless, there is a great challenge associated to the preparation of proteoliposomes because most of membrane proteins require a correct insertion with specific orientation to ensure their biological activity. Furthermore, the environment surrounding the inserted protein also affects the interactions and function of the protein, reason why the choice of the lipidic composition for the reconstitution is equally of great importance.[34,38,39]

Although there are several methods for the preparation of proteoliposomes (as mechanical methods, organic solvents, freeze/thaw and detergents), the fact that most membrane proteins are purified in detergents has direct implications in the chosen method. For this reason, membrane protein reconstitution is usually performed using detergents.[34] This methodology (Figure 6) starts with the preparation of a suspension of liposomes to which the protein (solubilized in detergent) and detergent are added. The total detergent concentration should not overpass the critical micellar concentration (CMC) characteristic of the chosen lipidic system, as above this concentration the vesicles became micelles.[29] During this step, the vesicles are perturbed to favour the protein insertion into the bilayers. After a period on ice, the excess of the detergent is removed using polystyrene beads (Bio-Beads), by adsorption.[34,35,40] Once again, the homogeneity and polidispersion of the suspensions should be evaluated (by electron microscopy or light scattering), in order to define if it is necessary to perform an extrusion of the proteoliposomes suspension.[33]

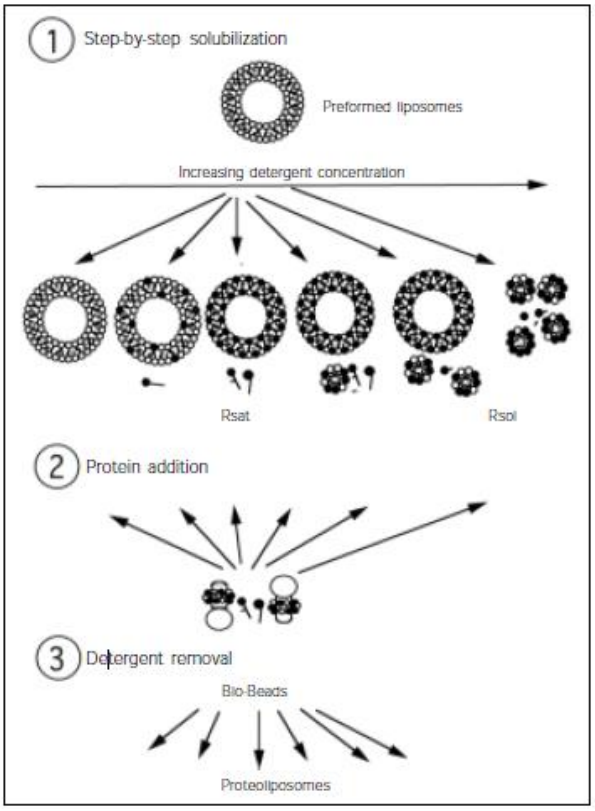

Figure 6 - Reconstitution of membrane proteins e preformed liposomes, from [34].

1.3. **Antimicrobial resistance**

Antimicrobial resistance (AMR) is one of the major public health threats of the 21st century, together with epidemics, outbreaks of infectious diseases and environmental hazards.[41,42] In 2009, the European Centre for Disease Prevention and Control (ECDC) pointed out for about 25,000 annual deaths in Europe directly related to infections caused by several resistant bacteria.[43,44] Due to its critical impact in the public health and expensive healthcare costs, AMR became a significant worldwide concern under systematic surveillance.[44] In Europe, the scrutiny of the incidence and dissemination of AMR is under the responsibility of the European Antimicrobial Resistance Surveillance Network (EARS-Net).[44]

AMR is the ability of a microorganism to circumvent the action of one or several antimicrobial agents.[44,45] It is a natural phenomenon, however, the overuse and misuse of antibiotics are stated as the main causes for accelerating the huge spreading of the bacterial resistance mechanisms.[42,46,47] The misuse of antibiotics is largely associated with inappropriate prescriptions (as in cases of viral infections), with self-medication (in

some countries, antibiotics are over-the-counter medicines), with unsuitable dosage or time of treatment, while overuse has been mostly seen in agriculture and in animal use.[48]

Bacterial resistance can arise from intrinsic characteristics, structural or functional, or from acquired mechanisms.[43,45] The diversity of lipidic composition of the cytoplasmic membrane of different bacteria (between Gram-negative and Gram-positive bacteria or among different species) has direct implications on the permeability of the membranes, being a good example of an intrinsic characteristic. For example, the reduced content of anionic phospholipids (~ 30%) in the Gram-negative cytoplasmic membrane directly reduces the entrance of daptomycin (Ca^{2+}-mediated process).[43,49] The structural differences between the cell envelope of Gram-negative and Gram-positive bacteria as well as the presence of genes encoding for specific functions can account for intrinsic characteristics that prevent the influx of some drugs.[43,46] Besides that, resistance to the antimicrobial agents can be acquired through vertical transmission (mutations in bacterial genes that are transferred to the following generations) or horizontal gene transfer. Horizontal gene transfer can occur via i) transduction, that implies the transference of resistance genes between two bacteria, through a bacteriophage (bacterial virus); ii) transformation, a process of acquisition of bacterial DNA (deoxyribonucleic acid) released in the extracellular space during cell lysis; iii) conjugation, that consists in the transference of a plasmid encompassing resistant genes, between two adjacent bacteria, through the cell surface (pili or adhesins); or iv) gene transfer agents, known as bacteriophage-like elements.[42,45,50,51] The Figure 7 shows the different types of horizontal gene transfer.

The emergence of AMR mechanisms walks along with the use of the antimicrobials, since the introduction of the first antibiotics, as penicillin. A good example of that is the discovery of penicillin by Alexander Fleming in 1928 that was promptly faced up with the evidence of bacterial resistance mechanisms against it (due to a penicillinase), in the decade of 40, approximately at the same time it started to be used clinically.[46,52]

There are several different mechanisms accounting for AMR, generally consisting in i) the reduction of the intracellular concentration of the antibiotic, ii) the alteration of the antibiotic target and iii) the inactivation of the antibiotic.[43,53] The reduction of the intracellular concentration of the antimicrobial can be achieved by drug extrusion, via efflux pumps, or reduction of the drug influx, through changes in the lipidic composition of the membrane or by decreased expression of porins. Modification of the drug target may occur due to mutations in the genes encoding the target site, by enzymatic

alterations of the binding site, and/or by replacement or bypass of the original target.[54] In the case of deactivation of the antimicrobial, the drug is modified by enzymes produced by bacteria causing hydrolysis, phosphorylation or acetylation, rendering the antibiotic ineffective.[1,45,53]

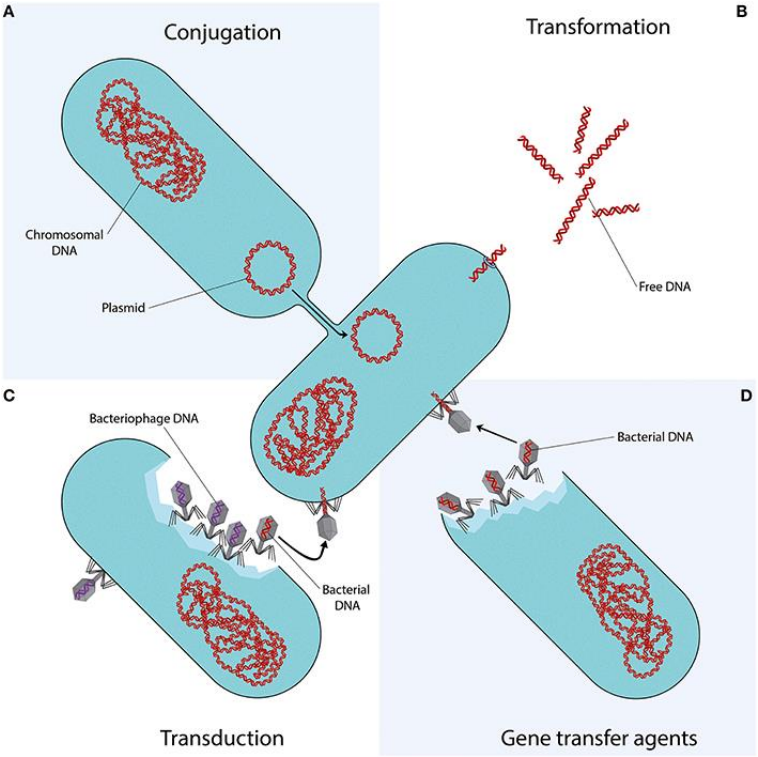

Figure 7 - Horizontal gene transfer can occur via: A. Conjugation; B. Transformation; C. Transduction; D. Gene transfer agents. Image from [2].

1.4. **Priority pathogens towards which new antibiotics are needed**

In February 2017, the World Health Organization (WHO) published its first ever list of antibiotic-resistant "priority pathogens" for which new antibiotics are urgently needed. The classification of pathogens by the different priority stages, published in 2017, is presented in Table 1.[41] The list highlights in particular the threat of Gram-negative bacteria that are resistant to multiple antibiotics, which are categorized with critical priority.

Table 1 - WHO priority pathogens list for Research & Development of new antibiotics, adapted from [41].

Priority 1: Critical
Acinetobacter baumannii, carbapenem-resistant *Pseudomonas aeruginosa*, carbapenem-resistant *Enterobacteriaceae* (*Klebsiella pneumonia*, *Escherichia coli*, *Enterobacter spp.*, *Serratia spp.*, *Proteus spp.*, *Providencia spp.* and *Morganella spp.*), carbapenem-resistant, 3rd-generation cephalosporin-resistant
Priority 2: High
Enterococcus faecium, vancomycin-resistant *Staphylococcus aureus*, methicillin-resistant, vancomycin intermediate and resistant *Helicobacter pylori*, clarithromycin-resistant *Campylobacter*, fluoroquinolone-resistant *Salmonella spp.*, fluoroquinolone-resistant *Neisseria gonorrhoeae*, 3rd-generation cephalosporin-resistant, fluoroquinolone-resistant
Priority 3: Medium
Streptococcus pneumoniae, penicillin-non-susceptible *Haemophilus influenzae*, ampicillin-resistant *Shigella spp.*, fluoroquinolone-resistant

E. coli, *Pseudomonas aeruginosa* and *Staphylococcus aureus* are three bacterial strains of clinical importance due to their multifaceted resistance mechanisms that result in raised resistance to one or several antimicrobials. In particular, extended-spectrum β-lactamase (ESBL) – producing *E. coli* and methicillin-resistant *S. aureus* (MRSA) are responsible for numerous infections that are more and more observed, frequently exhibiting resistance to FQs.[47,51]

E. coli is a fermentative Gram-negative bacterium that integrates the humans and animals intestinal flora, although it can sometimes be a pathogen, causing neonatal meningitis, bloodstream and urinary tract infections, more and more difficult to treat mainly due to the *E. coli* high rates of resistance, widely disseminated, especially to

β-lactams and FQs.[44,55] Although FQs and β-lactams belong to different classes of antibiotics with distinct modes of action (FQs inhibit two enzymes responsible for the bacterial replication and β-lactams inhibit the synthesis of the bacterial cell wall), their influx is commonly performed via porins, as OmpF.[17]

The resistance to β-lactam agents, such as penicillins, cephalosporins and carbapenems, can be accomplished by several mechanisms, which can be present simultaneously, like the reduction of the intracellular drug concentration (through the overexpression of efflux pumps and/or the reduction of the expression of porins), by modifications of the penicillin-binding proteins or by the action of β-lactamases. Nonetheless, it is known that β-lactamases are the commonest single cause of bacterial resistance to β -lactam antibiotics. β-lactamases are enzymes that hydrolyse the β-lactam ring of these drugs, and they can be both chromosomal- and plasmid-encoded; there are around 900 different known β-lactamases.[56] For instance, ESBLs can hydrolyse advanced-spectrum cephalosporins, monobactams and carbapenemases that are responsible for resistance to almost all β-lactams, including the carbapenems.[44,57] In turn, resistance to FQs involves mutations of the target molecules, topoisomerase II (DNA gyrase) and topoisomerase IV, and/or the reduction of the intracellular concentration of the drug, by the decreasing of the expression of porins and/or by drug extrusion, mediated by efflux pumps.[44,58]

Data from EARS-Net, referring to the year 2015, reports resistance to aminopenicillin and FQs as the most recurrently observed in *E. coli* isolates. The same report points out for 22.8% of *E. coli* isolates with resistance to FQs, although this percentage remains similar since 2012. On the contrary, the number of *E. coli* isolates with resistance to 3rd-generation cephalosporin and with combined resistance to FQs, 3rd-generation cephalosporins and aminoglycosides increased considerably from 2012 to 2015.[44]

In contrast to *E. coli*, *P. aeruginosa* is a non-fermentative Gram-negative bacterium that is ubiquitous in aquatic environments, though not a human commensal, it can be an opportunistic pathogen responsible for pneumonia, bloodstream, skin and urinary tract infections and several infections in patients with immune deficit (hospitalised patients). In addition, this microorganism is a frequent chronic coloniser of the respiratory tract of patients with cystic fibrosis.[44,59] *P. aeruginosa* exhibits intrinsic resistance to numerous antimicrobials due to its astute ability to survive under extreme environmental conditions.[60,61] The resistance mechanisms developed by this pathogen to escape antimicrobial agents usually encompass mutations of the drug targets (the main mechanism against FQs and aminoglycosides), the reduction of the intracellular

concentration of the drug through the decreased expression of porins (as happens for carbapenems and FQs) or by its extrusion via efflux pumps (in the case of β-lactams, FQs and aminoglycosides) and/or the inactivation of the drug by enzymes encoded by plasmids (also in the case of β-lactams and aminoglycosides).[44] According to the EARS-Net (European Antimicrobial Resistance Surveillance Network) report of 2015, the percentage of isolates of *P. aeruginosa* with resistance to FQs and aminoglycosides has decreased from 2012 to 2015, with a significant reduction from 20.9% to 19.3%.[44]

S. aureus is a fermentative Gram-positive bacterium, abundant in human nasal vestibule and skin.[44,62] On the other hand, it can also be an opportunistic pathogen responsible for bacteremia (bacterial blood infection) and numerous infections in the skin, the soft tissue or the pleuropulmonary area, being one of the main microorganisms causing hospital and community-acquired infections in Europe.[47,62,63] MRSA represent a huge threat in the bacterial resistance field, since these microorganisms are resistant to several antibiotic classes, including β-lactams, FQs, macrolides, rifampicin and tetracyclines.[44,47] These pathogens express the mecA gene that encodes the low-affinity penicillin-binding protein (PBP2a), allowing the cell wall synthesis in the presence of β-lactam agents. The number of MRSA reported by EARS-Net has been decreasing since 2011 (from 18.8% in 2011 to 16.8% in 2015). However, the majority of the MRSA isolates (85.2%) remains resistant to FQs, restricting the treatment of numerous infections.[44]

1.5. **Quinolones and fluoroquinolones**

Quinolones, or 4-quinolones, are an antibiotic family, synthetized from antimalarial agents, widely used in the clinical practise.[64,65] These antimicrobials exhibit a structure derived from a 4-oxo-1,8-naphthyridine-3-carboxylic acid nucleus (Figure 8). This nucleus base has been the subject of several modifications, through the insertion of diverse substituent groups in different positions, with the exception of positions 3 and 4. Positions 3 and 4, exhibiting a carboxylic acid and an exocyclic oxygen, respectively, assure the antimicrobial activity of this family, reason for their conservation.[65] In addition, a carbon atom (unsubstituted or substituted) in the 8-position of the nucleus is also characteristic of quinolones.[64,65]

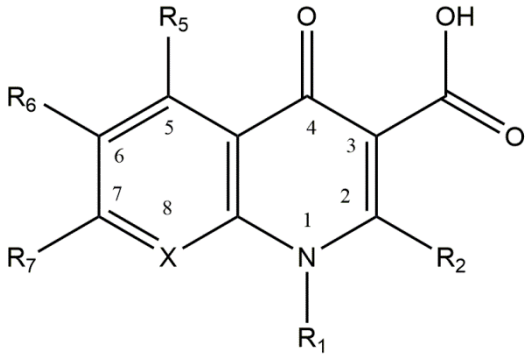

Figure 8 - Structure of the base nucleus of quinolones and naphthyridones, drawn using ChemDraw Professional 17.0. The position 8 is occupied by a carbon or a nitrogen atom (substituted or non-substituted), in the case of quinolones or naphthyridones, respectively.

The first quinolone (correctly, a naphthyridone), the nalidixic acid, was synthetized from a compound isolated from chloroquine, in 1962. In 1964, it was found that its mechanism of action involved the inhibition of the bacterial DNA gyrase synthesis.[66] Three years later, this drug was introduced in the clinical practise due to its antibacterial activity against Gram-negative bacteria (specially Enterobacteriaceae) but in a few years bacterial resistance mechanisms were observed in different strains, leading to the need to develop new drugs.[66] FQs appeared in the decade of 70, through the insertion of a fluorine atom at position 6 and a piperazinyl group at position 7.[64,65] The 6-fluorination of the nucleus resulted in improvements of up to 10 and 100-fold in the antimicrobial activity and in the minimum inhibitory concentration (MIC), respectively.[64] In turn, the introduction of the piperazinyl group at position 7 extended the antimicrobial activity to more Gram-negative species (as *Pseudomonas*) and some Gram-positive strains.[65] In addition, this substitution seemed to increase the potency of the other antimicrobials, when in combination, through the inhibition of the bacterial efflux pumps.[64] The influx in the bacterial cell was also facilitated by these two substitutions.[65,67]

These visible improvements triggered the development of different generations of quinolones, classified according to their potency, spectrum of action, pharmacokinetics and pharmacodynamics.[64,68] In this way, the 2nd generation of quinolones (the first FQs) appeared in the decades of 70 and 80, exhibiting effective antimicrobial activity against Gram-negative and some Gram-positive bacteria. The following decades were focused on the broadening of the antibacterial spectra and on the improvement of the potency and bioavailability of the compounds.[66,69] The decade of 90 marks the boom of the 3rd and 4th generation quinolones, opening doors to the fighting of several Gram-positive

species as well as anaerobic microorganisms.[64,68] 2nd generation of quinolones encompasses norfloxacin (nfx), ofloxacin (ofx), lomefloxacin (lmx), ciprofloxacin (cpx) and enrofloxacin (erx), among others. Grepafloxacin (gpfx), levofloxacin[1] (lvx) and sparfloxacin (spx) integrate the 3rd generation, while trovafloxacin (tvx) and moxifloxacin (mxfx) belong to the 4th generation.[69-71] The structures of the FQs used in this work (cpx, erx, lvx, mxfx and spx) are presented in Figure 9.

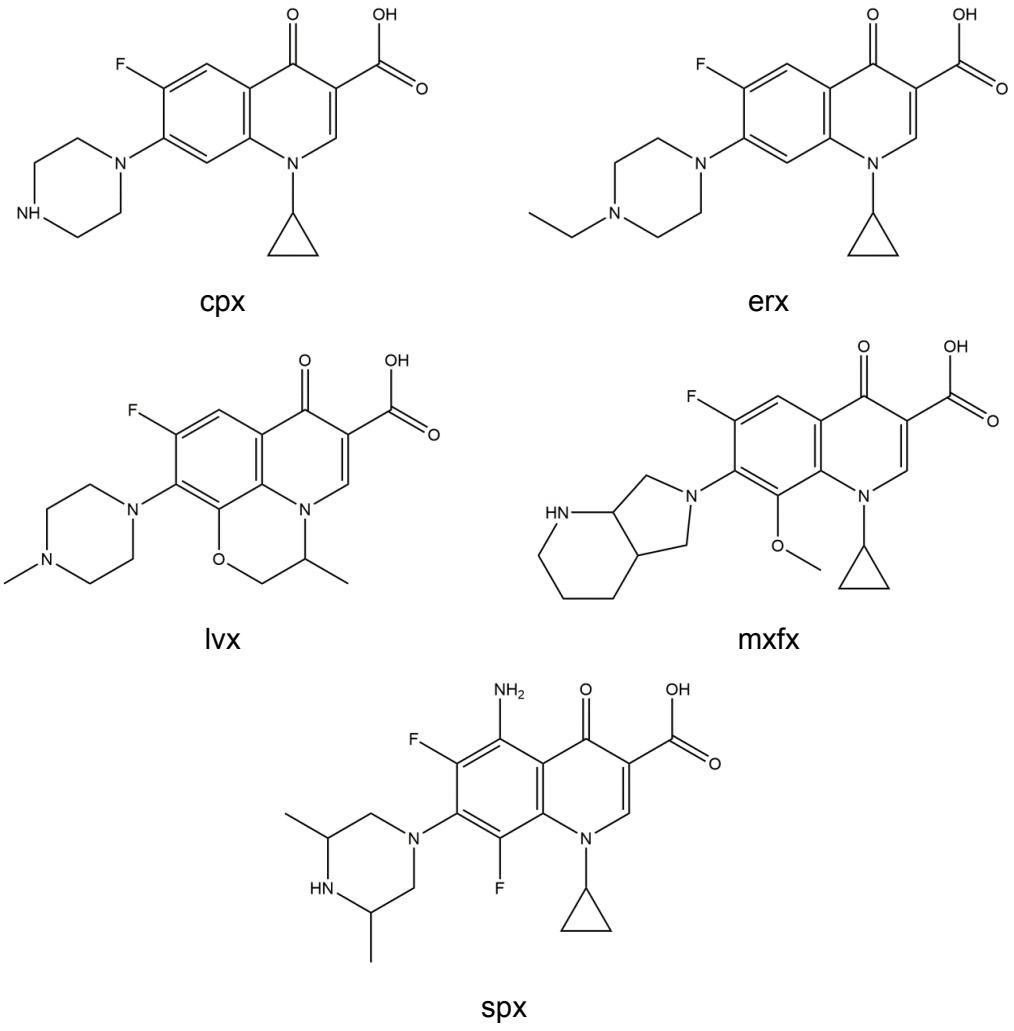

Figure 9 - Structures of cpx, erx, lvx, mxfx and spx, drawn using ChemDraw Professional 17.0.

[1] The classification of levofloxacin is ambiguous. Its chemical structure is typical of 2nd generation but its extended activity to Gram-positive species is characteristic of the 3rd generation.

The prompt development of so many compounds was only possible due to the knowledge acquired about the structure/activity relationship. The carboxylic acid and the exocyclic oxygen of the 3rd and 4th positions, respectively, are essential for the antimicrobial activity, as these two groups are responsible for the binding to the target molecule of FQs. For this reason, substitutions were not made in these two positions, maintaining these groups preserved along the several FQs.[65,72] Due to its proximity to the carboxylic acid and the exocyclic oxygen, the 2nd position is generally occupied by a hydrogen atom, since many explored substitutions had negative implications in the activity of the compounds. The 1-position usually encompasses a cyclopropyl group, as this substitution enhances the potency of the molecule. The substituent of this position might also allow a bridge with 8-position, likewise improving the activity of the compound (as observed in lvx).[65] The 7th position has direct implications in the potency, pharmacokinetics and permeation of the drugs. As described above, the piperazinyl group is regularly observed in this position (with some exceptions, as mxfx). By itself, the presence of this group confers high potency against Gram-negative bacteria, while the addition of methyl groups to the ring expands the activity to Gram-positive strains and improves the bioavailability.[65,67] The 5th and 8th positions affect the potency against Gram-positive and anaerobic bacteria. Together with the cyclopropyl group at 1-position, the addition of an amino group at 5-position and of a methoxy group at the C-8 results in the broadening of the spectrum of action and in the enhancement of the antimicrobial activity of the antibiotics. The introduction of a fluorine atom in the C-8 was also a good strategy in terms of potency but this substitution confers phototoxic characteristics to the compounds.[65,67,73] However, despite all advantages, the severe side effects and high toxicity of some FQs has restricted their used, such is the case of tvx and gpfx.[66,69]

Quinolones are bactericidal antibiotics that inhibit the bacterial replication, preventing the enzymatic activity of DNA gyrase (topoisomerase II) or topoisomerase IV.[65,68] DNA gyrase is involved in the introduction of the negative supercoils in the DNA strand, while topoisomerase IV performs the separation of the DNA molecules in the end of the replication (decatenation).[67,74] Quinolones intercalate reversibly with the bacterial DNA and the enzymes, establishing a ternary complex that cleaves the bacterial DNA and makes impossible the DNA synthesis.[51,68,75] Although exceptions may occur, quinolones preferentially target the DNA gyrase in Gram-negative bacteria and the topoisomerase IV in Gram-positive bacteria.[76-78]

DNA gyrase and topoisomerase IV are heterotetramers composed by two pairs of subunits. DNA gyrase has GyrA and GyrB subunits, each one composed of two

monomers, A and B, respectively. In turn, topoisomerase IV exhibits two subunits: ParC and ParE in Gram-negative bacteria or GrlA and GrlB in Gram-positive bacteria. GyrA is homologous to ParC and GrlA, while GyrB is homologous to ParE and GrlB.[67,72,79]

According to the target enzyme, quinolones bind to specific sites of each topoisomerase.[80] The carboxylic acid and the exocyclic oxygen of the 3rd and 4th positions of the quinolone bind to GyrA of DNA gyrase (or ParC of topoisomerase IV) through a water-Mg^{2+} bridge, while the substituent of the 7th position interacts with GyrB (or ParE) subunit.[72,75] The water-Mg^{2+} bridge also intervenes in the interaction of the drug with the DNA strand. For these reasons, the magnesium coordination-dependent positions (3rd and 4th) restrict the substitutions of the surrounding positions, as the 2nd position.[81] During the replication, the DNA strand interacts covalently with GyrA (or ParC) subunit, and the quinolone bind to this DNA/topoisomerase complex through a tyrosine residue of the active site of the enzyme (Tyr122 of GyrA or Tyr120 of ParC of *E. coli*).[79]

A recent study proposes an alternative binding mechanism, where the 7-position substituent of quinolones links to GyrA subunit of DNA Gyrase of *E. coli*.[75] Mustaev *et al.* suggest two possible pathways for this mechanism: i) the inversion of the orientation of the drug, promoting a magnesium bridge between the carboxylic acid and carbonyl groups of the quinolone and the Glu466 (or Lys447) of GyrB subunit and exposing the 7th group to the GyrA; or ii) the positioning of the quinolone in the interface of GyrA-GyrA subunits, through a magnesium bridge between the carboxylic acid of the quinolone and the Asp87 (of one subunit) and by the binding of the 7-position of the drug to Gly81 (of the other subunit).[75]

Pharmacokinetics properties of quinolones reveal excellent bioavailability (around 70-85% for cpx and about 100% for the recent FQs, as mxfx) after oral administration. The simultaneous ingestion of food doesn't seem to prejudice the absorption of these drugs, being even beneficial for the protection of the gastrointestinal tract.[68,82] The achievement of the maximum drug concentration in the serum happens between 1 and 3 hours after the administration. When compared to the serum levels, the drug concentrations reaching the kidney, liver, lungs, urine and faeces are quite high, facilitating the fight against pathogens located in the respiratory, gastrointestinal or urinary tracts.[68,82] The presence of serum proteins does not interfere with the bioavailability of FQs because most of these drugs do not show a high affinity to serum proteins (~ 20 to 30%), in contrast to what used to happen with the nalidixic acid (~ 95%).[82,83] However, the ability to chelate cations as iron, zinc, copper, cobalt and

nickel has negative implications in the bioavailability and penetration of FQs.[68] These family of antibiotics is metabolized in the liver or/and in the kidney. The produced metabolites vary according to the FQ but, with exception to ofx, all FQs are subject to oxidation reactions in the cytochrome P450.[84] FQs exhibit long half-lives, generally between 4 and 12 hours (20 hours for spx), originating raised elimination times and, consequently, the need of only one or two daily administrations.[68,83,85] The excretion of these drugs occurs mainly via the renal route.[68,82] However, the effects of the drugs are also dependent of each organism, being considered through the pharmacodynamics properties of the drugs. FQs are concentration-dependent drugs, meaning that the time of exposure of the drug is not a critical factor for the definition of the dosage. Besides this characteristic, these antimicrobials exhibit a relevant post-antibiotic effect, delaying the ability of bacteria to regrowth after the drug exposure. In this way, the key of the pharmacodynamics of the FQs is based on the definition of the maximum dose tolerated by the organism, a parameter that should take into account the toxicity versus the efficacy of the antibiotic.[85]

Drug combinations of agents of different classes of antibiotics represent an attempt to improve the effectiveness of these properties. Although FQs usually do not exhibit synergic activity with the majority of aminoglycosides, their combination with β-lactams (cephalosporins and carbapenems) usually results in synergistic effect.[59,86-88] Besides belonging to different classes of antibiotics, β-lactams and FQs also differ in the concentration-dependence as β-lactams are concentration-independent drugs. This additional difference also benefits the combination of these two antimicrobial families.[85] Although FQs do not have antifungal activity, their ability to bind to the topoisomerase of fungi may explain the synergistic activity resultant from their combination with some antifungal agents.[89]

As previously described, some FQs revealed high toxicity levels, which had implications in the approval and maintenance of some drugs. The *in vitro* toxicity of these drugs is usually evaluated through phototoxicity, cytotoxicity and hemolysis assays. Due to the variations in the substituent groups present in the FQs molecules, the structure/phototoxicity relation had been widely studied and the results described by some authors are described below. The irradiation of the FQs with UV light proved to be an inductive exponential factor of the toxicity of these molecules, being able to improve the cytotoxicity up to 90-fold.[90] Yamamoto *et al.* demonstrated that ofx, lmx and spx are FQs with severe cytotoxic effects when exposed to UV radiation.[90] In addition, the presence of specific substituents at positions 1 and 8 plays a crucial role in the phototoxicity of the FQs.[91,92] The presence of a halogen atom at 8th position

resulted in the enhancement of the phototoxicity of the FQs, contrary to the presence of a 8-methoxy (as observed in mxfx) that proved to confer resistance to photoirradiation.[91-93] The phototoxic activity resultant from presence of a halogen atom at 8th position derives from the photoinstability and consequent formation of ROS.[94,95] On the other hand, the presence of a hydrogen atom at 8th position also proved to increase the phototoxicity of the FQs. Combined with hydrogen at 8th position, a cyclopropyl or ethyl group at 1st position enhanced the phototoxicity of the molecules to a similar level to the presence of a halogen atom at 8th position.[91] On the contrary, the presence of a difluorophenyl or an oxetanyl at 1st position resulted in a moderation of the phototoxicity of the drugs.[91] Concerning the hemolytic activity, FQs only induce erythrocyte lysis in concentrations above 100 µg/ml. In addition, the presence of a non-substituted piperazinyl group at position 7 seemed to enhance the hemolytic activity.[90] Nevertheless, the results obtained *in vivo* are not always comparable to the ones previously determined *in vitro.*[93] Thus, the performance of both *in vitro* and *in vivo* assays is mandatory to evaluate safety of the drugs. The discrepancy observed between the *in vitro* and *in vivo* experiments explains why, besides the structure/phototoxicity relation, the majority of FQs is considered safe, making them widely used in the clinical practise.[44,70,96]

1.5.1. Mechanisms of resistance to fluoroquinolones

The main bacterial resistance mechanisms described against FQs encompass chromosomal mutations or plasmid-acquired resistance genes that confer alterations of the target molecule (DNA gyrase or topoisomerase IV) and the reduction of the intracellular concentration of the drug, through the decreasing of the influx or via the improvement of the efflux.[76,78]

Resistance mutations in the bacterial target enzymes of quinolones mainly vary according to the bacterial type (Gram-positive or Gram-negative). GyrA subunit of DNA gyrase is more susceptible to mutations in Gram-negative bacteria, while the Gram-positive species usually exhibit mutations in the correspondent subunit of topoisomerase IV, the ParC.[66,96] The substitution of specific residues of each enzyme reduces its affinity for the drug binding and avoids the formation of the water-Mg^{2+} bridge (Figure 10).[72,78,96] The common mutated residues are located in the “quinolone-resistance-determining region (QRDR)” that comprises the residues 51 to 106 of GyrA or 23 to 176 of ParC.[44,74,96] The substitution of Ser83 (serine, a polar amino acid, at

position 83) by a hydrophobic amino acid with a larger side chain (as tryptophan – Trp - or leucine) or the replacement of Asp87 (aspartate, an acidic amino acid, at position 87) for a polar amino acid (as tyrosine or glycine) of GyrA are vastly reported.[53,96] In turn, mutations of Ser80 (a polar amino acid, at position 80) by a hydrophobic amino acid (as isoleucine) or of Glu84 (glutamate, an acidic amino acid, at position 84) by basic (as lysine), hydrophobic (valine or alanine) or polar (as glycine) amino acids of ParC are the most described substitutions.[96,97] The concomitant mutation of GyrA and ParC potencies the bacterial resistance.[96] When subjected to mutations, the topoisomerases remain functional for the bacterial cell, only reducing the affinity for drug binding.[78]

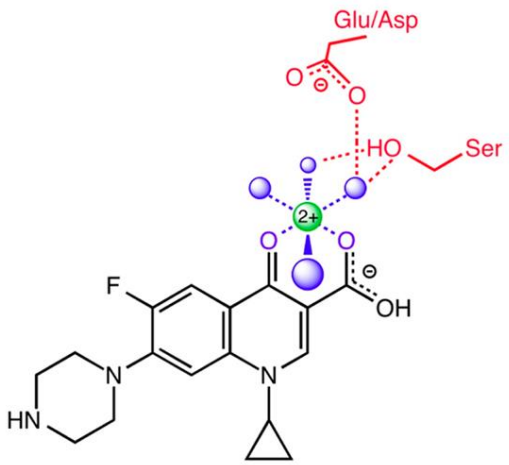

Figure 10 - Ciprofloxacin−topoisomerase binding, from [78].

Plasmid-mediated quinolone resistance (PMQR) consists in the transference of genes, encoding proteins that confer resistance to quinolones. Some PMQR genes are well characterized, as *qnrA*, *qnrS*, *qnrB*, *qnrC*, and *qnrD*. The *qnrA* gene, previously known as *qnr*, is responsible for the expression of a protein, Qnr, which binds DNA topoisomerases (DNA gyrase and topoisomerase IV) and prevents the quinolone action. Furthermore, the production of this protein also potentiates the acquisition of other resistance mutations.[44,46] Another PMQR strategy involves the inactivation of the quinolones by acetylation of the drugs at the amino group of the piperazinyl substituent. The acetylation is performed by an aminoglycoside acetyltransferase, encoded by *aac(6')-Ib-cr* gene.[44,98]

The reduction of the permeability of the bacterial membrane can arise from changes in the expression of porins, resulting in the decreasing of the influx of FQs that use these channels to translocate the membrane. The modifications can occur due to the reduction of the expression of the proteins, to the switch of the type of expressed porins or to the deactivation of pore functionality by gene mutation.[13]

In turn, the extrusion of several agents from the cytoplasm of bacterial cells consists of another strategy used by bacteria to escape antibiotics, like quinolones. The expulsion of the drugs is performed through efflux pumps, well identified for many bacterial species.[96] The major antibiotic efflux pump in *E. coli* is AcrAB-TolC, which is encoded, in part, by the acrAB operon. This operon is mainly regulated by two genes, *acrR* and *marR*, that usually repress acrAB operon expression. In this way, mutations in these genes result in the overexpression of acrAB, enhancing the pump expression and leading to the increasing of the drug efflux. The *marR* gene also has implications in the expression of OmpF. Mutations in *marR* decrease the expression of OmpF, reducing the influx of the drugs.[96,99] In the case of *P. aeruginosa*, the efflux of FQs is mostly performed by Mex-Opr efflux pumps (as MexAB-OprM, MexCDOpr-J, Mex-EF-OprN, MexXY-OprM, and MexVW-OprM), while MepA, NorA, NorB, and NorC represent the major pumps responsible for the efflux of quinolones in *S. aureus*.[96,100,101] The upregulation of efflux pumps generally enhances the MIC values 2 or more times, compared to strains that do not overexpress such efflux pumps.[102]

The drug extrusion of the bacterial cell can also arise from PMQR mechanisms, being OqxAB and QepA two well characterized efflux pumps.[44,96]

1.5.2. Metal complexes of fluoroquinolones

Among the main strategies to try to counteract AMR are the development of novel drugs or the improvement of drugs already used in the clinical practise. The first approach is more expensive and implicates more time, as the development of new drugs has to obey to well-defined stages. On the contrary, the improvement of compounds already in use in the market simplifies the process, being faster and avoiding some steps. In this way, one of the strategies to overcome the bacterial resistance to quinolones consists on the complexation of these antibiotics with transition metals.

During the last years numerous studies of complexation of FQs with transition metals have been performed.[70,71,95,103,104] Transition metals, as iron, zinc, copper,

cobalt, and nickel play an important role in several mechanisms of biological systems. In turn, the chemistry of FQs facilitates their complexation with various ligands. All FQs have two ionisable groups, the carboxyl group and the amino group, responsible for their amphoteric character. Each antibiotic has two specific pK_a values, corresponding to the ionisation of the carboxylic acid (pK_{a1}) and of the amino group (pK_{a2}).[69] In this way, the pH is a determinant factor for the protonation level and, consequently, for the species present in solution. At low pH ($pH < pK_{a1}$), FQs have both groups protonated, existing majorly in the cationic form (H_2FQ^+). With the increasing of the pH, the carboxylic acid deprotonates ($pH > pK_{a1}$) and there is a mixture of neutral (HFQ^0) and zwitterion forms ($HFQ^{\pm}$). At high pH ($pH > pK_{a2}$) the amino group also deprotonates and the drugs assume the anionic form (FQ^-) in solution.[105,106] The pK_{a1} and pK_{a2} values usually vary from 5.6 - 6.4 and 7.6 – 9.3, respectively, meaning that at physiological pH FQs exist mainly in a mixture of zwitterion and neutral forms.[69,105] When compared to other acids, the pK_{a1} value of FQs is increased, resulting from the intramolecular hydrogen bond existing between the carboxyl group (of the 4th position) and the exocyclic oxygen (of the 3rd position) of the drugs.[107]

The chelation of the transition metals to FQs occurs in the same groups responsible for the antimicrobial activity of the drugs, the exocyclic oxygen and the carboxyl group.[70,107,108] A compilation of studies comprising several FQs and numerous transition metals have been performed, showing that only copper(II) complexes are truly stable.[70,71,103,104] These results are in agreement with the Irving–Williams series that suggest that complexes of copper(II) are stronger and more stable than complexes of iron (II), cobalt(II), nickel(II) or zinc(II).

The significant roles of copper in the human organism encompass the production of haemoglobin, the preservation of tissues and blood vessels and the normal operation of several enzymes (as cofactor). This transition metal is mainly ingested through sea food, liver meat, green olives, chocolate, cocoa and black pepper, although its amount should be reduced (less than 30 mg/kg). After absorption in the intestine, copper reaches the liver, bounded to albumin, or is transported to several tissues, through ceruloplasmin, a plasma protein. The excretion of this metal occurs through bile and is a slow (around 10% in 72h) process.[109,110] The homeostasis of copper is crucial due to its ability of dual oxidizing behaviour, being able to avoid or to promote the production of free radicals. In the first case, its action as an antioxidant is beneficial to the organism, preventing the existence of free radicals and consequent damage. On the contrary, if copper acts as a pro-oxidant, it foments the production of free radicals, contributing for some diseases as the Alzheimer's disease.[109,110] The

important role of copper as cofactor of several enzymes involved in cell growth (among them the mitochondrial enzymes such as cytochrome c oxidase and superoxide dismutase) is transversal to bacteria and eukaryotes.[111,112] However, antimicrobial activity has been documented for this transition metal, being extremely important the maintenance of the homeostasis of copper in bacteria. Copper transporters and copper efflux systems, reported for several bacterial strains, are responsible for the regulation of the content of copper in bacteria.[112,113]

The antimicrobial activity of copper has been extensively studied and it was discovered that complexes of copper and 1,10-phenanthroline (1,10-phen) possess nuclease activity.[114-116] This finding has triggered the interest in complexes containing copper and phen (a nitrogen donor heterocyclic ligand) and several studies of synthesis and characterization of copper/phen complexes have been performed.[117,118]

The joining of the knowledge regarding the copper/FQ stability and the nuclease activity of copper/phen complexes opened doors to numerous studies concerning the complexation of FQs with copper and 1,10-phen.

Ternary complexes of copper(II), 1,10-phen and FQ have been subject of study during the last decade and the achieved outcomes suggest that these compounds are a potential alternative to pure FQs. The ternary complexes (CuFQphen) are cationic molecules that exhibit a square pyramidal geometry slightly distorted which lies on a five-coordinated metallic centre. The basal plane of the quadrangular pyramid is composed by two oxygen atoms of the FQ (one of the carboxyl group of the 4th position and other of the exocyclic oxygen of the 3rd position) and by two nitrogen atoms of the bidentate ligand phen. In turn, the axial plane of the pyramid is usually occupied by a water molecule, coordinated through the oxygen (Figure 11).[70,71,108,119,120]

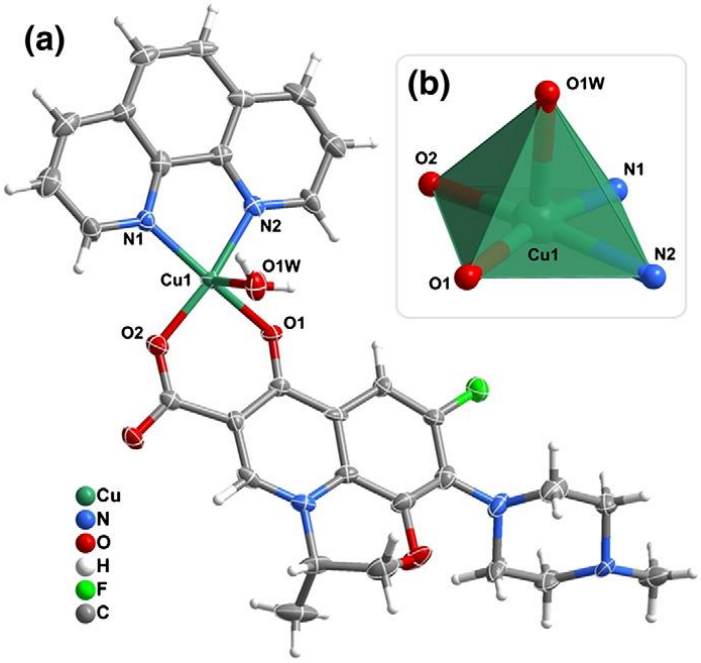

Figure 11 - Representation of (a) the cationic complex $[Cu(lvx)(phen)(H_2O)]^+$ and of (b) the copper(II) five coordinated centre $[CuN_2O_3]$ characteristic of the square pyramidal geometry slightly distorted of the CuFQphen complexes, from [71].

In the case of the Cucpxphen complex, instead of the water molecule, the fifth coordination of the metal occurs through a nitrogen atom of the piperazine ring of another FQ molecule (Figure 12). This specific coordination allows the formation of a polymeric chain composed of Cucpxphen cationic molecules (Figure 13).[70]

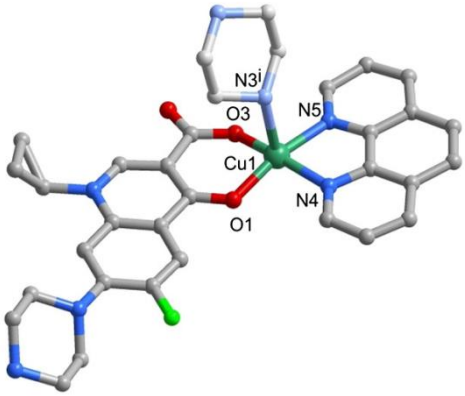

Figure 12 - Representation of the cationic complex $[Cu(cpx)(phen)]^+$, from [70].

The structures of the CuFQphen complexes are typically governed by C–H···O and weak C-H···F hydrogen bonds and π · · · π stacking interactions between the phen

rings of adjacent complexes. Furthermore, studies of the synthesis of these complexes show that counter-ions (usually NO_3^-) and crystallisation water molecules are involved in several interactions that assure the stability of the structures, specially through hydrogen bonds (O–H · · · O and O–H · · · N) with oxygen atoms of the FQs (of the 3rd and 4th positions), with nitrogen atoms of the ligands of the FQs or with the coordinated water molecules.[70,103]

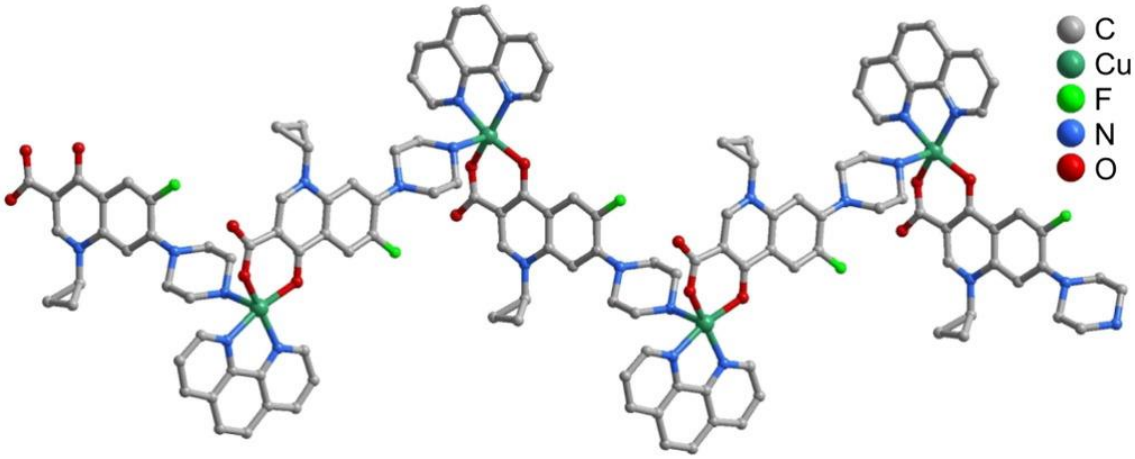

Figure 13 - Representation of the coordination chain of $[Cu(cpx)(phen)]^+$, formed in the crystal structure of Cucpxphen, from [70].

The high stability under physiological conditions of concentration, pH and temperature and the proven antibacterial activity (effectiveness comparable or improved, compared to pure FQs) anticipate that these complexes, known as metalloantibiotics, could be effective against bacterial strains resistant to FQs.[70,108,121] Furthermore, the differences of the chemical characteristics of the metalloantibiotics and FQs may implicate different influx mechanisms, possibly overcoming some bacterial resistance mechanisms developed to FQs.

The mechanism of action of these drugs is still not well known but it is expected to be similar to FQs, based on the nuclease activity and high affinity to intercalate into DNA reported for these complexes.[70,117] In turn, the toxicological safety of the metalloantibiotics still needs to be better studied, since there is some controversy.[70,122]

1.6. Aim of the study

This work was triggered by the growing problem of AMR, especially to FQs, a class of antibiotics widely used in the clinical practise. The goal of this work was to characterize ternary complexes of copper(II)/FQ/phen, pointed as promising alternatives to pure FQs during the last decades, and to evaluate if these metalloantibiotics could be a good choice to circumvent some of the antibiotic resistance mechanisms to FQs. The work comprised biophysical and biochemical studies, in order to i) clarify the influx route, ii) assess the antimicrobial activity against resistant strains, iii) infer possible mechanisms of action and evaluate the toxicological safety of five metalloantibiotics, always in comparison with the respective pure FQs (cpx, erx, lvx, mxfx and spx).

The first part of this work encompassed the determination of the partition coefficients (K_p), the assessment of the location in the membrane and the study of the interaction of these drugs with OmpF porin, through fluorescence spectroscopy. Some microbiologic studies were also performed in order to clarify the importance of the porins in the influx of these metalloantibiotics. The second part of the work proceeded with microbiological tests, by determining the MICs of FQs and respective metalloantibiotics, against several strains (reference and resistant strains) of *E. coli*, *S. aureus* and *P. aeruginosa*. The study of the mechanism of action of the ternary complexes was performed in a third part of the work, using topoisomerases of *E. coli* and *S. aureus*. Lastly, the evaluation of the toxicological safety of the drugs was performed through cell viability (Thiazolyl Blue Tetrazolium Bromide – MTT - assay) and haemolytic assays. As mentioned above, all studies were performed for pure FQs and respective metalloantibiotics.

Materials and Methods

2

2.1. Reagents

All compounds were used as received. Ciprofloxacin (cpx), enrofloxacin (erx), levofloxacin (lvx) and sparfloxacin (spx) (all >98.0%), were purchased from Sigma-Aldrich. Moxifloxacin (mxfx) was a gift from Bayer. Fluoroquinolones (FQs) were stored at room temperature (cpx, lvx, mxfx and spx) or at 4˚ C (erx), protected from light. *Escherichia coli* total lipid extract (PE 57.5%; PG 15.1%; CL 9.8%; unknown lipids 17.6%) was obtained from AVANTI Polar Lipids. Chloroform ($CHCl_3$, Reagent plus, purity ≥ 99.8%) was provided by Sigma-Aldrich. 1,10-phenanthroline (phen), NaCl and N-(2-hydroxyethyl) piperazine-N'-ethanesulfonic acid (HEPES) were from Sigma (grade pro analysis). Fluorescent probes 1,6-diphenyl-1,3,5-hexatriene (DPH) and (±)-12-(9-anthroyloxy) stearic acid (12-AS) were from Sigma-Aldrich, (±)-2-(9-Anthroyloxy) stearic acid (2-AS) was from Molecular Probes and 1,6-diphenyl-1,3,5-hexatriene-4′-trimethylammonium tosylate (TMA-DPH) was from Fluka. 2-AS and 12-AS probes were dissolved in absolute ethanol (grade *pro analysis* - PA) from Panreac and stored at -18˚C in the freezer prior to use. Potassium iodide was from AppliChem Panreac. Octylpolyoxyethylene (oPOE) was purchased from Bachem and Bio-Beads SM-2 from Bio-Rad. Polycarbonate filters were acquired from LIPEX Biomembranes. Ammonium molybdate, bicinchoninic acid solution, copper(II) sulphate solution, bovine serum albumin, Tris base, acetic acid glacial, and ethylenediaminetetraacetic acid (EDTA) were from Sigma-Aldrich. Fiske-Subarrow reducer was acquired from Fluka. All other chemicals were from Merck.

All solutions were prepared in 10 mmol dm^{-3} HEPES buffer (0.1 mol dm^{-3} NaCl; pH 7.4, using double deionised water), with the exception of copper solution that was prepared in double deionised water.

The metalloantibiotic solutions used were prepared by mixing the three components (FQ, Cu(II) and phen) in stoichiometric proportions (1:1:1), as previously reported for other FQs metalloantibiotics.[70,71,103,123-125] All compound solutions prepared were stored at 4˚C andprotected from light.

An analytical balance Mettler AT201 ($\pm 2\times10^{5}$g) was used to weight the compounds.

2.2. Strains and culture conditions

OmpF (outer membrane protein F) was a gift from Dr. Mathias Winterhalter (Jacobs University, Bremen, Germany) and from Dr. Ricardo Franco (Universidade Nova de Lisboa, Portugal). OmpF mutants (W61F and W214F) were a gift from Dr. Mathias Winterhalter and from Dr. Lorraine Benier (Jacobs University, Bremen, Germany). *E. coli* B_E strains (BL21(DE3), BL21(DE3)omp2 and BL21(DE3)omp8) were obtained from the Microbiology Department of the University of Basel (Switzerland); *E. coli* K12 (JF568, JF701 and JF703) were from *E. coli* Genetic Stock Centre (Yale University, USA); and the strains W3110, W3110 ΔC, W3110 ΔF and W3110 ΔFΔC were from the School of Engineering and Science (Jacobs University, Bremen, Germany).

All the bacterial reference strains are from ATCC (LGC Standards). Clinical isolates used were obtained from the two largest hospitals in Porto, "Hospital São João" (with authorization and approval by Dr. Cidália Pina-Vaz) and "Hospital Geral de Santo António" (with authorization and approval by Dr. Maria Helena Ramos).

Mueller Hinton Broth 2, cation-adjusted (CAMH broth) was obtained from Sigma-Aldrich and all other culture media used in the microbiology assays were purchased from Liofilchem. The media were acquired in dehydrated state and the preparation of the broths or agar plates was performed in the lab, according to the instructions of the products. Ciprofloxacin 5 µg disks were from Oxoid and blank paper disks from Liofilchem.

Supercoiling and relaxation assays were performed with *S. aureus* and *E. coli* gyrase supercoiling assay kits and with *S. aureus* and *E. coli* topoisomerase IV relaxation assay kits, from Inspiralis. GreenSafe Premium was purchased from NZYTech and Thiazolyl Blue Tetrazolium Bromide (MTT) was from Sigma-Aldrich.

2.3. Titration of copper and iodide solutions

The $Cu(NO_3)_2.3H_2O$ solution used to prepare the metalloantibiotics solutions was previously titrated in alkaline medium with EDTA and using murexide as indicator.

The iodide solution used in the location studies was prepared with sodium thiosulfate (10 mmol dm^{-3}) in order to avoid the rapid oxidation of potassium iodide solution.[126] The quantification of iodide in the potassium iodide solution was determined in acid medium, with potassium iodate and using carbon tetrachloride as indicator.

2.4. Quantification of phosphate in liposomes and proteoliposomes

The phospholipid concentration in the liposome suspensions was determined by phosphate analysis through a modified Bartlett method.[127,128] The Bartlett assay is a colorimetric method that allows the determination of the amount of inorganic phosphate of the samples. The procedure starts with the destruction of the phospholipids to inorganic phosphate, through the incubation of the samples with perchloric acid 70% v/v ($HClO_4$), for one hour, in a sand bath with controlled temperature between 180˚C and 200˚C. Parallel to the samples, a blank containing water and a set of standard solutions of potassium dihydrogen phosphate (concentrations between 0.05 and 0.3 mmol dm^{-3}) were prepared. All samples were prepared in replicates. After cooling to room temperature, ammonium molybdate and Fiske-Subbarow reagent were added and the samples were incubated for seven minutes, at 100˚C. During this reaction, inorganic phosphate is converted to phosphomolybdic acid, which is then reduced to a blue complex. After cooling to room temperature, the samples were vortexed and the amount of blue complex, which is proportional to the amount of phosphate, was determined by absorbance readings at 830 nm.

The concentration of phosphate was assessed for all liposomes and proteoliposomes prepared.

2.5. Quantification of total protein in purified samples and prepared proteoliposomes of OmpF

The protein concentration of OmpF, wild-type (WT) and mutants, was estimated using the bicinchoninic acid protein assay against bovine serum albumin (BSA) as standard. [129,130] This method consists is the addition of a standard working reagent (SWR) to the samples, in a proportion of 20 to 1 (v/v), respectively. Parallel to the samples, a blank containing HEPES buffer and a set of standard solutions of BSA (concentrations between 0.1 and 0.6 mg/mL) were prepared. All samples were prepared in replicates. The SWR was prepared by addition of 50 parts (v/v) of bicinchoninic acid solution (aqueous solution of 1% of BCA-Na_2, 2% of $Na_2CO_3.H_2O$, 0.16% of Na_2 tartrate, 0.4% of NaOH and 0.95% of $NaHCO_3$) to 3 parts (v/v) of copper(II) sulphate solution (4% aqueous solution of $CuSO_4.5H_2O$). After the addition

of the SWR, the samples were left to incubate at 37.0 ± 0.1˚C, for 30 minutes, followed by cooling to room temperature and absorbance readings at 562 nm.

The protein concentration was assessed for all received proteins and all prepared proteoliposomes.

2.6. Determination of the partition coefficient of sparfloxacin and its ternary copper/phen metalloantibiotic by time-resolved fluorescence spectroscopy

2.6.1. Liposome Preparation

Liposomes were prepared by incorporation of the fluorescent probes with known location (2-AS or 12-AS).[131] A solution of each fluorescent probe, previously prepared in ethanol, was added to the chloroform lipid solution containing the appropriate amount of *E. coli* total lipid extract. The final lipid:probe ratio was 100:1 and the final ethanol:chloroform ratio was 1% (v/v). The lipidic film was obtained by evaporation of the organic solvents, performed under inert atmosphere (nitrogen), followed by, at least, three hours of vacuum. MLVs were obtained by redispersion of the lipidic film in 10 mmol dm^{-3} HEPES buffer (0.1 mol dm^{-3} NaCl; pH 7.4). The samples were vortexed, and the vesicles were submitted to five freeze-thawing cycles. The freezing was done in liquid nitrogen and thawing in a boiling water bath. LUVs were obtained by 10 times MLVs extrusion through 100 nm polycarbonate filters on a LIPEX Biomembrane extruder attached to a water bath. The extrusions were performed above the phase transition temperature of the system (*E. coli* total lipid extract: ≈ 63°C).[31] The size distribution of the LUVs was determined by dynamic light scattering analysis using a MALVERN Instruments Zeta SizerNano ZS. For LUVs from *E. coli* total lipid extract the mean particle size was 130 ± 0.3 nm.[73] All liposome suspensions were stored at 4˚C, protected from light.

2.6.2. Fluorescence measurements

Fluorescence measurements were performed at 37.0 ± 0.1˚C using 1 cm quartz cells. Four sets of samples with a final volume of 1.5 mL were prepared by mixing a constant lipid concentration (between 100 μmol dm^{-3} and 650 μmol dm^{-3}) and increasing spx or Cuspxphen concentrations (from 0 to 80 μmol dm^{-3} for spx and from 0 to 25 μmol dm^{-3} for Cuspxphen). Samples were then vortexed, incubated at 37.0 ± 0.1˚C for 30 minutes and vortexed again prior to measurement. Time-resolved fluorescence measurements were performed on a Tempro single photon counting controller from HORIBA Jobin– Yvon attached to a temperature controller from JULABO. The fluorescence excitation was performed with a Nano LED source of 360 nm from HORIBA Jobin–Yvon and fluorescence emission was recorded at the maximum wavelength for each solution (458 nm and 455 nm for 2-AS and 12-AS, respectively). Time-resolved experiments were recorded using a window of 4024 channels, with a time calibration of 0.055 ns/channel and a peak count of 10,000. The lamp profile was recorded by inserting a scatter (diluted suspension of LUDOX in water) in place of the sample.[132] The antibiotic and metalloantibiotic concentrations used were chosen according to their Lambert-Beer law (absorbance value < 0.1 cm^{-1} at the excitation wavelength) in order to avoid the inner filter effect.[133,134] At least, three independent experiments were performed for each studied concentration.

2.6.3. Theoretical Methods

The partition coefficient (K_p) [2] of any compound between vesicle suspensions and an aqueous solution is defined as the ratio between the amount of drug present in the lipid and in the aqueous phase:[126,135]

$$K_p = \frac{(C_L/C_T)/[L]}{(C_W/C_T)/[W]} \quad (1)$$

in which C_T, C_L, and C_W are the total drug molar concentration and the drug molar concentration in lipid and in aqueous media, respectively; [L] and [W] represent lipid and water (55.3 mol dm^{-3} at 37˚C) [135] molar concentrations.

[2] The partition coefficient as defined by Eq. (1) is defined by IUPAC as the partition ratio; IUPAC does not recommend the use of the former definition. Its use throughout this work reflects the common practice in the biological literature.

The K_p of a fluorescent compound can be determined by fluorescence spectroscopy since the partition results in changes, extinction (quenching) or enhancement, in the fluorescence of the fluorophore. In this way, the analysis of the variations of the fluorescence of a fluorophore due to its incorporation in vesicle suspensions allows the assessment of its K_p.

The quenching process consists in the decrease of the fluorescence of a fluorophore and can arise from two different processes, known as static or collisional, being the contact between the quencher and the fluorophore molecules mandatory for both events.

The collisional quenching is characterized by the depopulation of the excited state as a consequence of contact between the quencher and the fluorophore in the excited state. After the interaction, the fluorophore returns to the ground state with no emission of a photon. For this reason, this process is also entitled dynamic quenching. The collisional quenching phenomenon is described by the Stern-Volmer equation:[126]

$$\frac{I_0}{I} = 1 + k_q\tau_0[Q] = 1 + K_D[Q] \quad (2)$$

where I_0 and I are the fluorescence intensities of the fluorophore in the absence and in the presence of the quencher (Q), respectively; k_q is the bimolecular quenching constant; τ_0 is the lifetime (average time that a molecule spends in the excited state) of the fluorophore in the absence of the quencher and $[Q]$ is the concentration of the quencher. The Stern-Volmer quenching constant is given by $K_D = k_q\tau_0$.

During the collisional quenching, there is a decrease of the fluorescence intensity of the fluorophore and of its lifetime due to the depopulation of the excited state, which means that:

$$\frac{I_0}{I} = \frac{\tau_0}{\tau} \quad (3)$$

where τ_0 and τ are the lifetimes in the absence and in the presence of the quencher, respectively. Rearrangement of Eq. (2) yields:

$$\frac{\tau_0}{\tau} = 1 + k_q\tau_0[Q] = 1 + K_D[Q] \quad (4)$$

The static quenching consists in the formation of a non-fluorescent complex between the quencher and the fluorophore in the ground-state. In this case, the

constant can be considered as the association constant (K_{ass}) for the complex formation:

$$K_{ass} = \frac{[F-Q]}{[F][Q]} \quad (5)$$

where $[F-Q]$, $[F]$ and $[Q]$ are the concentrations of the complex, of the uncomplexed fluorophore and of the quencher, respectively. As the total concentration of the fluorophore $[F]_0$ is given by:

$$[F]_0 = [F] + [F-Q] \quad (6)$$

Rearranging Eq. (5) with Eq. (6) and by substitution of the concentrations for fluorescence intensities yields:

$$\frac{I_0}{I} = 1 + K_{ass}[Q] \quad (7)$$

The lifetime of the fluorophore remains constant in static quenching, as the fluorescence observed comes from the uncomplexed fluorophores that have the unquenched lifetime (τ_0). For this reason, for static quenching:

$$\frac{\tau_0}{\tau} = 1 \quad (8)$$

Quenching data is usually presented as a Stern-Volmer plot of $\frac{I_0}{I}$ as a function of $[Q]$. Assuming a population of fluorophores with similar accessibility to the quencher, a linearity of the plot is expected. The Stern-Volmer constant is represented by K_D if the quenching is collisional or by K_{SV} in the case of static quenching.

The K_p can also be determined using a non-linear method, using the following equation:

$$\Delta I = \frac{\Delta I_{max} K_p [L]}{[W] + K_p [L]} \quad (9)$$

where ΔI is the difference between the fluorescence intensity of the fluorophore in the absence (I_0) and in the presence (I) of quencher (L); $[L]$ is the lipid molar concentration, $\Delta I_{max} = I_\infty - I_0$ where I_∞ is the limiting value of I and K_p is the association constant.

This non-linear method allows the calculation of the K_p in the case of either quenching or enhancement of the fluorescence of the fluorophore.

However, spx and Cuspxphen are non-fluorescent molecules, which means that the use of fluorescent probes is mandatory to assess their partition by fluorescence spectroscopy. These studies comprise the incorporation of a fluorescent probe in the lipid vesicles and the evaluation of the changes in its fluorescence due to the presence of the partitioning molecule in its surrounding. Generally, the partition of the non-fluorescent molecule results in the quenching of the probe and the decrease of its fluorescence intensity is proportional to the average number of the partitioning molecules.[135] In this way, this technique allows the calculation of the K_p through the quantification of the free and bound molecules to the membrane. In order to determine the values of K_p of spx and Cuspxphen, we used two fluorescent probes from the anthroyloxy fatty acids family, *n*-(9-anthroyloxy)-stearic acid (*n*-AS), incorporated in the lipid bilayer.[73] The *n*-AS probes are a set of probes with a fatty acid chain, aligned parallel to the phospholipid acyl chains during incorporation, attached to an anthroyloxy group, positioned at a well-known depth in the bilayer.[131,136] In this work we used 2-AS and 12-AS probes, whose anthroyloxy group is located ≈ 15.8 Å and 6 Å [3] from the centre of the bilayer.[137] Quenching of these probes is expected to occur by a collisional mechanism. For this reason, the experiments were carried out by time-resolved fluorescence spectroscopy.

Data analysis of the fluorescence intensity decays was carried out using a nonlinear least squares iterative convolution method with computer program DAS6 v6.5. Two exponentials were required to the fit, and its goodness of fit was assessed from the global Chi-square value ($\chi^2 \leq 1.3$ was considered acceptable), weighted residuals, and autocorrelation.[138-140] For a two-exponential decay, the amplitude-weighted lifetime of a fluorophore, $< \tau >$, is :[126]

$$< \tau >= \sum_i \alpha_i \tau_i \quad (10)$$

where τ_i represents each component of the fluorescence lifetime and $\propto_i$ the respective pre-exponential factor, which is proportional to the concentration of the component.

[3] Values referenced for phosphocholine (PC) vesicles at pH 5.

And the average lifetime, $\bar{\tau}$, for a two-exponential decay is :[126]

$$\bar{\tau} = \frac{\alpha_1\tau_1^2+\alpha_2\tau_2^2}{\alpha_1\tau_1+\alpha_2\tau_2} \quad (11)$$

As the drug-probe interaction resulted in a decreasing of the lifetime of the probe and the Stern-Volmer plot shows linearity, the experimental data were analysed using the equation described:[135]

$$\frac{<\tau_0>}{<\tau>} = 1 + K_{app}[Q]_t = 1 + {k_q}^{app}\,\bar{\tau}_0[Q]_t \quad (12)$$

where $<\tau_0>$ and $<\tau>$ are the fluorescence lifetimes of the probe in the absence and presence of the quencher, respectively; K_{app} is the apparent quenching constant, $[Q]_t$ is the total quencher concentration in the membrane and ${k_q}^{app}$ is the apparent bimolecular quenching constant. K_{app} and ${k_q}^{app}$ were calculated for the different lipid concentrations used.

For the calculation of the K_p', the presented equation was fitted to the experimental data:[135]

$$\frac{1}{{k_q}^{app}} = \alpha_m\left(\frac{1}{k_q} - \frac{1}{k_q K_p'}\right) + \frac{1}{k_q K_p'} \quad (13)$$

where $\frac{1}{{k_q}^{app}}$ is the reciprocal of the apparent bimolecular quenching constant calculated for each studied lipid concentration and considering that $\alpha_m = \frac{V_m}{V_t}$, where V_m is the membranar volume of *E. coli* and V_t is the total volume. The parameter V_m was determined assuming the value of 0.691 $dm^3\,mol^{-1}$ for the molar volume of *E. coli* (γ_L), calculated from [30,141]. k_q is the bimolecular quenching rate constant.

The K_p' value can be converted to K_p stated in Eq. (1), using the expression:

$$K_p = K_p'\,\frac{\gamma_L}{\gamma_w} \quad (14)$$

where γ_L and γ_w are the molar volumes of lipid and water, respectively.

All the experimental data were treated using the computer program Origin 7.

2.7. Location studies of the drugs in the mimetic membrane systems

2.7.1. *n*-AS probe/liposome preparation

Absolut ethanol solutions of the fluorescent probes (2-AS and 12-AS) were prepared. The incorporation of the probes was performed by the addition of a known volume of the probe solution in the lipid solution of chloroform. Lipid-probe LUVs were then prepared by the method described above for liposome preparation. The suspensions containing lipid and *n*-AS probe were prepared with a final concentration of liposome of 8.0 mmol dm^{-3} and a final lipid:probe ratio of 100:1.[73,142]

2.7.1.1. Fluorescence experiments with *n*-AS probes

The location studies with *n*-AS probes were performed with a set of samples with a final volume of 1.5 mL, prepared by adding a known volume of liposome/probe suspension and small volumes of antibiotic/metalloantibiotic solution in HEPES buffer. The samples were prepared for three different LUVs concentrations (265, 427 and 635 µmol dm^{-3}). The concentration range used for free and complexed FQs was from 0 to 20 (Cuerxphen) or 30 µmol dm^{-3} (Cucpxphen). The samples were incubated in a water bath, above the transition temperature of the lipidic system, for one hour, after which measurements were performed by steady-state and time-resolved fluorescence spectroscopy. The antibiotic and metalloantibiotic concentrations used were chosen according to their Lambert-Beer law (absorbance value < 0.1 cm^{-1} at the excitation wavelength) in order to avoid the inner filter effect.[133,134]

2.7.1.1.1. Steady-state fluorescence measurements

The steady-state spectra were recorded on a Varian Cary Eclipse spectrofluorometer equipped with a ‘‘single cell peltier accessory’’ temperature controller, at 37.0 ± 0.1˚C, in 1 cm quartz cuvettes, with a slit width of 5 nm for excitation and 10 nm for emission, and excitation and emission wavelengths of

363/458 nm and 363/455 nm for 2-AS and 12-AS, respectively. At least, three independent experiments were performed for each studied concentration.

2.7.1.1.1.1. Theoretical Methods

As the drug-probe interaction resulted in a quenching of the fluorescence, the experimental data can be analysed by a linear method, using Stern-Volmer equation, as described above by Eq. (2). However, as the quencher is distributed between the membrane and aqueous phase (partition coefficients), only the quencher molecules in the membrane are responsible for quenching. In this way, the effective concentration of the drug in the LUVs, $[Q]_m$, must be determined. The effective concentration is given by:[140,142]

$$[Q]_m = [Q]_t \left(1 - \frac{K_p \gamma_L L}{1-\gamma_L L+K_p \gamma_L L}\right) \frac{K_p}{1-\gamma_L L} \quad (15)$$

where $[Q]_t$ is total drug concentration, K_p the partition coefficient of the drug, γ_L the molar volume of the lipid and L the lipid concentration.

In this way, the experimental data were analysed by the following equation:

$$\frac{I_0}{I} = 1 + K_D [Q]_m \quad (16)$$

All the experimental data were treated by this linear graphical method, at the wavelength of maximum intensity, using the computer program Origin 7.

2.7.1.1.2. Time-resolved fluorescence measurements

Measurements were performed on a Tempro single photon counting controller from HORIBA Jobin–Yvon, attached to a temperature controller from JULABO. The fluorescence excitation was performed with a Nano LED source of 360 nm from HORIBA Jobin–Yvon, and fluorescence emission was recorded at the maximum wavelength of *n*-AS probes (458 and 455 nm for 2-AS and 12-AS, respectively). Time-resolved experiments were recorded using a window of 4024 channels, with a time calibration of 0.055 ns/channel and a peak count of 10000. The lamp profile was

recorded by placing a scatter (diluted solution of LUDOX in water) in place of the sample, as described above. At least, three independent experiments were performed for each studied concentration.

2.7.1.1.2.1. Theoretical Methods

Data analysis of the fluorescence intensity decays was carried out using a nonlinear least squares iterative convolution method with computer program DAS6 v6.5. Two exponentials were required to the fit. As the drug-probe interaction resulted in a decreasing of the lifetime of the probe and the Stern-Volmer plot is linear, the experimental data were analysed by a linear method, using the equation described:[143]

$$\frac{<\tau_0>}{<\tau>} = 1 + K_D[Q]_m \quad (17)$$

where $<\tau_0>$ and $<\tau>$ are the fluorescence lifetimes in the absence and presence of the quencher, K_D is Stern-Volmer constant and $[Q]_m$ is the effective quencher concentration in the membrane.

All the experimental data were treated by this linear graphical method, at the wavelength of maximum intensity, using the computer program Origin 7.

2.7.2. DPH and TMA-DPH probe/liposome preparation

Solutions of the fluorescent probes were prepared in chloroform (DPH) and in methanol (TMA-DPH). The incorporation of these probes was performed by the addition of a known volume of the probe solution in the lipid solution of chloroform. Lipid-probe LUVs were then prepared by the method described above for liposome preparation. The suspensions containing lipid and probe were prepared with a final concentration of liposome of 4.0 mmol dm^{-3} and a final lipid:probe ratio of 300:1.

2.7.2.1. Steady-state anisotropy measurements

The samples used in the anisotropy studies with DPH and TMA-DPH were prepared by incubation of the antibiotic/metalloantibiotic in the LUVs of liposome/fluorescent probe (with a final concentration of liposomes and antibiotic of 2 mmol dm^{-3} and 10 μmol dm^{-3}, respectively). The incubation was performed in a water bath, above the transition temperature of the lipidic system, for one hour, after which their steady-state fluorescence anisotropy (r_s) was measured. The measurements were performed on a Varian Cary Eclipse spectrofluorometer equipped with a ''single cell peltier accessory'' temperature controller, in 1 cm quartz cuvettes, with excitation and emission wavelengths of 360/427 nm and 365/426 nm for DPH and TMA-DPH, respectively, and with slits width of 5 nm for excitation and emission. The r_s values were recorded at 3˚C intervals within the 3˚C - 70˚C temperature range. The antibiotic and metalloantibiotic concentrations used were chosen according to their Lambert-Beer law (absorbance value < 0.1 cm-1 at the excitation wavelength) in order to avoid the inner filter effect.[133,134] At least, three independent anisotropy profiles were obtained for each studied compound.

2.7.2.2. Theoretical Methods

The steady-state fluorescence anisotropy (r_s) is defined by the following equation:[126]

$$r_s = \frac{I_{VV} - I_{VH}\, G}{I_{VV} + 2\, I_{VH}\, G} \qquad (18)$$

where I_{VV} and I_{VH} are the intensities measured in directions parallel and perpendicular to the excitation beam. The correction factor G is the ratio of the detection system sensitivity for vertically and horizontally polarized light, which is given by the ratio of vertical to horizontal components when the excitation light is polarized in the horizontal direction, $G = I_{HV}/I_{HH}$.[126]

Theoretically, the G factor value should be equal to one, as it is expected that $I_{HV} = I_{HH}$. Differences in I_{HV} and I_{HH} can be observed due to the specific characteristics of the detection system.

The r_s is a parameter widely used to evaluate the rigidity of molecular environments. The membrane-phase transition temperature (T_m) of a lipidic system can be assessed through the study of the r_s as a function of the temperature, due to its sensitivity to differences in the viscosity of the membranes.[31,144]

The following equation was fitted to the r_s versus temperature (T) data, in order to calculate the T_m:

$$r_s = r_{s2} + \frac{r_{s1} - r_{s2}}{1 + 10^{B'\left(\frac{T}{T_m} - 1\right)}} \quad (19)$$

where T is the absolute temperature, T_m is the midpoint phase transition and r_{s1} and r_{s2} are the upper and lower values of r_s; B' is the slope factor, related to the extent of cooperativity (B) by B = [1-1/(1+ B')]; the introduction of B yields a convenient scale of cooperativity ranging from 0 to 1.[144]

All the experimental data were treated using the computer program Origin 7.

2.7.3. Location studies with iodide

Iodide is a water-soluble quencher, widely used in location studies as it is able to quench fluorophores distributed in hydrophilic environments.[126,145,146] Time-resolved fluorescence was performed because the quenching by iodide is expected to occur by a collisional mechanism.[145-147]

The fluorescence excitation was made with a Nano LED source of 290 nm from HORIBA Jobin–Yvon, and fluorescence emission was recorded at the maximum wavelength of each metalloantibiotic solution (415 nm for Cucpxphen, 412 nm for Cuerxphen and 460 nm for Culvxphen and Cumxfxphen). Four sets of samples with a final volume of 1.5 mL were prepared by adding a known volume of metalloantibiotic solution (with a final concentration of 5.0 μmol dm^{-3} of Cucpxphen and 3.0 μmol dm^{-3} of Cuerxphen, Culvxphen or Cumxfxphen) and small volumes of iodide solution, in HEPES buffer. The experiments were performed with an iodide solution concentration range from 0 to 0.5 mol dm^{-3}. One of the sets was prepared in the absence of liposome suspension and the other three were prepared by adding a known volume of liposome suspension (≈ 250, 500 or 750 μmol dm^{-3}). The mixtures were incubated at 37.0 ± 0.1˚C for 30 minutes, after which the intensity decays were obtained. The antibiotic and metalloantibiotic concentrations used were chosen according to their

Lambert-Beer law (absorbance value < 0.1 cm-1 at the excitation wavelength) in order to avoid the inner filter effect.[133,134] At least, three independent experiments were performed for each studied compound.

2.7.3.1. Theoretical Methods

Data analysis of the fluorescence intensity decays was carried out using a nonlinear least squares iterative convolution method with computer program DAS6 v6.5. One exponential (in HEPES buffer experiments) or two exponentials (in *E. coli* liposomes) were required to the fit. As the presence of the iodide resulted in a decreasing of the lifetime of the drugs and the Stern-Volmer plot shows a linear relationship, the experimental data were analysed by a linear method, using the Eq. (4), previously described.

All the experimental data were treated by this linear graphical method, at the wavelength of maximum intensity, using the computer program Origin 7.

2.8. Quenching studies of OmpF by fluoroquinolones and metalloantibiotics

2.8.1. OmpF reconstitution into liposomes

OmpF proteoliposomes were prepared by protein incorporation into preformed liposomes. Protein reconstitution was performed by addition of OmpF solution (1% oPOE) and oPOE (with a final concentration of detergent lesser than the micellar critic concentration of *E. coli* ≈ 0.2%) to a LUVs suspension previously prepared. The mixture was incubated with gentle agitation at room temperature for 30 minutes, followed by one hour on ice. The excess of detergent was then removed by detergent adsorption on polystyrene beads, incubating the mixture twice with Bio-Beads SM-2, (75 mg per mL of the prepared proteoliposome) – addition for three hours with gentle agitation at room temperature, removal and second overnight at 4˚C.[148] The proteoliposome suspension was then submitted to a ten times cycle of frozen and thawed and extruded for 10 times through 100 nm polycarbonate filters on a LIPEX

Biomembrane extruder attached to a water bath, like previously described for liposomes. Once again, the extrusion was realized above the phase transition temperature of the lipidic system. The proteoliposomes were prepared with a final protein/lipid molar ratio of 1:1000, in HEPES buffer. During all the process, the size distribution of the particles was determined by dynamic light scattering on a Zeta Sizer Nano Zs of Malvern Instruments. The final mean particle size was ≈ 150 nm. All measurements were performed at 37.0 ± 0.1˚C.

2.8.2. Spectroscopic measurements

Absorption spectra were carried out on a UV-Vis-NIR (UV-3600) Shimadzu spectrophotometer equipped with a temperature controller (Shimadzu TCC-CONTROLLER). Spectra were recorded at 37.0 ± 0.1˚C, in 1 cm quartz cuvettes, with a slit width of 5 nm, in a wavelength range from 225 to 450 nm. Steady-state fluorescence measurements were performed on a Varian Cary Eclipse spectrofluorometer equipped with a "Single Cell Peltier Accessory" temperature controller, in 1 cm quartz cuvettes.

2.8.3. Drug-protein interaction

OmpF exhibits intrinsic fluorescence due to the fluorescent amino acid residues (as Trp) in its composition, which allow the study of drug-protein interaction by steady-state fluorescence spectroscopy. The study of the fluorescence of the protein was based on six Trp residues: three located at the interface bilayer/protein, near the phospholipid headgroups of the bilayer (Trp^{214} – W214) and three close to the centre of the porin channel (Trp^{61} – W61).[22,149] The determination of the interaction between cpx and its metalloantibiotic with OmpF Trp (W61 and W214) was achieved with *E. coli* total extract proteoliposomes of native protein (OmpF WT) and two OmpF mutants (W61F and W214F), lacking one of each Trp, which is substituted by phenylalanine (Phe). The OmpF-antibiotic association was also studied for erx, lvx, mxfx and respective metalloantibiotics in *E. coli* total extract proteoliposomes of native OmpF. Small aliquots (μL) of compund solution were successively added to an OmpF proteoliposome suspension of 1 mmol dm^{-3}/1 μmol dm^{-3} (lipid/protein). After each addition, the mixture was equilibrated for five minutes and the spectra were traced, at

37.0 ± 0.1˚C, under constant stirring. The interaction between cpx and OmpF (WT and mutants) was determined using a drug concentration range from 0 to 18 μmol dm^{-3}. In turn, the metalloantibiotic/OmpF (WT and mutants) interaction was studied with a compound concentration range from 0 to 5 μmol dm^{-3}. For the other experiments (OmpF WT), the compound concentration range used was 0-14 μmol dm^{-3} for erx, 0-3 μmol dm^{-3} for mxfx and Culvxphen, 0-4 μmol dm^{-3} for Cuerxphen and Cumxfxphen and 0-5 μmol dm^{-3} for lvx. The spectra were recorded with an excitation wavelength of 290 nm and emission wavelength range from 300 to 380 nm, an excitation slit width of 5 nm and an emission slit width of 10 nm, scan rate of 120 nm/minute and data range of 1 nm for *E. coli* total lipid extract/OmpF WT proteoliposomes. In turn, the spectra obtained for *E. coli* total lipid extract/OmpF mutant proteoliposomes were recorded with an excitation wavelength of 290 nm and emission wavelength range from 305 to 380 nm for W61F and an excitation wavelength of 287 nm and emission wavelength range from 300 to 380 nm for W214F, an excitation slit width of 5 nm and an emission slit width of 10 nm, scan rate of 120 nm/minute and data range of 1 nm. Due to the lower excitation wavelength of W61 (W214F) proteoliposomes, emission filters of 295-1100 nm were applied in order to avoid the excitation of tyrosine.[126] The antibiotic and metalloantibiotic concentrations used were chosen according to their Lambert-Beer law (absorbance value < 0.1 cm^{-1} at the excitation and emission wavelengths of OmpF) in order to avoid the inner filter effect.[133,134] All fluorescence experimental data were corrected for the dilution effect and three independent measurements were performed.[150]

2.8.3.1. Fluorescence quenching data analysis

Reported studies have showed the phenomenon of static fluorescence quenching on the interaction of FQs with OmpF protein.[151,152] As this interaction exhibits a linear plot of I_0/I vs.$[Q]$, the analysis of the quenching data was performed using the Stern-Volmer equation, described above by Eq. (7). The graphical methods were performed at the wavelength of maximum intensity of the protein (320 nm for WT, 318 nm for W214 - W61F - and 312 nm for W61 - W214F), using the computer program Origin 7.

2.8.4. Fluorescence quenching of OmpF by iodide and acrylamide

Fluorescence quenching of OmpF Trp residues (W61 and W214) by iodide and acrylamide were performed with *E. coli* total lipid extract proteoliposomes of native and mutant OmpF (W61F and W214F), in the absence and presence of compound solution. Small aliquots (μL) of quencher solution (iodide or acrylamide) were successively added to an *E. coli* total lipid extract/OmpF proteoliposome suspension of 1 mmol dm^{-3}/1 μmol dm^{-3} (lipid/protein), in a concentration range from 0 to 0.5 μmol dm^{-3}, in the absence or presence of cpx (≈ 30 μmoldm^{-3}) or Cucpxphen (≈ 8 μmoldm^{-3}) solution. After each addition, the mixture was equilibrating for five minutes and the spectra were traced, at 37.0 ± 0.1˚C, under constant stirring. The spectra were recorded using the conditions described above for each proteoliposome composition. All fluorescence experimental data were corrected for the dilution effect and three independent measurements were performed.[150]

The quenching of the cpx (≈ 30 μmoldm^{-3}) or Cucpxphen (≈ 8 μmoldm^{-3}) solutions by iodide and acrylamide (0 to 0.5 μmol dm^{-3}) were also studied. The spectra obtained for cpx and Cucpxphen solutions were recorded with an excitation wavelength of 290 nm and emission wavelength range from 305 to 550 nm with a slit width of 5 nm, scan rate of 120 nm/minute and data range of 1 nm.

2.8.4.1. Fluorescence quenching data analysis

Fluorescence experimental data were always corrected for the dilution effect [150] and for the inner filter effect, since under the established conditions, acrylamide absorbs light at the excitation wavelength of the protein and both cpx and Cucpxphen solutions absorb light at the emission wavelength of the protein. The inner filter effect artifact was corrected using the equation described below:[126,153,154]

$$I_{corr} = I_{obs} \times 10^{[(Abs_{ex}+Abs_{em})/2]} \quad (20)$$

where I_{corr} and I_{obs} are the corrected and observed fluorescence intensities, respectively; Abs_{ex} and Abs_{em} are the absorbance values at the excitation and emission wavelengths used. Absorbance values take in account the path length of the absorption of the excitation and emission light of the cuvette.

2.8.4.1.1. Linear Stern-Volmer plot

The Stern-Volmer equation, described above by Eq. (2), was fitted to the quenching data that exhibit a linear plot of I_0/I vs. $[Q]$, at the wavelength of maximum intensity of the protein (320 nm for WT, 318 nm for W214 - W61F - and 312 nm for W61 - W214F), or of the compound solution (415 nm for cpx and Cucpxphen), using the computer program Origin 7.

2.8.4.1.2. Deviations to Stern-Volmer plot

In some cases, deviations to the linearity were observed in the Stern-Volmer plot of the quenching by iodide.

An upward curvature concave toward the y-axis revealed in a Stern-Volmer plot is usually evidence of the occurrence of both dynamic and static quenching or of an apparent static quenching event known as the sphere of action model. The sphere of action model proposes a high spatial proximity between the quencher and the fluorophore at the moment of the excitation, resulting in the quenching of this pair. The model suggests a virtual “sphere” within which there is a high probability of contact between the quencher and the fluorophore. This probability enhances as the quencher concentration increases. Considering this model, the data can be treated according to this equation:[126]

$$\frac{I_0}{I} = (1 + K_a[Q])exp([Q]VN_A) \quad (21)$$

in which I and I_0 are the fluorescence intensities of the fluorophore measured in the presence and absence of the quencher Q, respectively; V is the volume of the sphere; N_A is Avogadro’s constant and K_a is the association constant of the quencher with the fluorophore.

Considering that $K_a[Q]$ is small enough, $1 + K_a[Q] \approx exp(K_a[Q])$, which is equivalent to $exp([Q]VN_A)$. In this case, the Eq. (21) can be rearranged as:[155]

$$\frac{I_0}{I} = exp(K_a[Q]) \quad (22)$$

where K_a can be easily calculated.

In turn, when the Stern-Volmer plot exhibits a downward curvature, it is expected to exist two different populations of fluorophores with distinct accessibilities to the quencher, what is in agreement with the different environments that surround W61 and W214. In this case, part of the total population is accessible to the quencher and other part is inaccessible:

$$I_0 = I_{0a} + I_{0b} \quad (23)$$

where I_0 is the total fluorescence intensity of the protein, in the absence of the quencher; $I_{0\,a}$ and I_{0b} are the fluorescence intensities of the accessible and inaccessible fractions, respectively.

Assuming that in the presence of the quencher the fluorescence intensity of the accessible fraction is quenched according to the Stern-Volmer equation, unlike the one of the inaccessible fraction that remains unaltered, the fluorescence intensity observed (I) is given by:

$$I = \frac{I_{0\,a}}{1+K_a[Q]} + I_{0\,b} \quad (24)$$

where K_a is the Stern-Volmer constant of the accessible fraction and $[Q]$ is the quencher concentration.

Subtraction of Eq. (24) to Eq. (23), yields:

$$\Delta I = I_0 - I = I_{0\,a}\left(\frac{K_a[Q]}{1+K_a[Q]}\right) \quad (25)$$

The inversion of the equation, followed by division by Eq. (23), results in the following equation that can be fitted to the experimental data:

$$\frac{I_0}{\Delta I} = \frac{1}{f_a\,K_a[Q]} + \frac{1}{f_a} \quad (26)$$

where f_a is the accessible fraction, given by $f_a = \frac{I_{0a}}{I_{0a}+I_{0b}}$.

The graphical methods were performed at the wavelength of maximum intensity of the protein (previously reported), using the computer program Origin 7.

2.9. Microbiological assays

2.9.1. Filter sterilized stock solutions

Stock solutions of phen, Cu(II)/phen (1:1), $Cu(NO_3)_2.3H_2O$, FQs (cpx, erx, lvx, mxfx and spx) and respective metalloantibiotics were prepared in HEPES buffer (with the exception of the copper solution, prepared in double deionised water), with a concentration of 2014 μg mL^{-1}. The solutions were sterilized by membrane filtration (≤ 0.22 μm nominal pore size) and stored in small aliquots, protected from light, at -80˚C. The stock solutions were then thawed as needed and used in the same day.

2.9.2. Bacterial strains and culture media

The bacterial strains used in the antimicrobial susceptibility testing performed by the broth microdilution method comprised i) four reference strains – *E. coli* ATCC 25922 and *Pseudomonas aeruginosa* ATCC 27853 (Gram-negatives), *Staphylococcus aureus* ATCC 25923 and ATCC 29213 (Gram-positives), ii) susceptible *E. coli* strains and their derived porin-deficient mutants and iii) 30 multidrug-resistant (MDR) isolates – four of *P. aeruginosa* (from Portugal), eight of *E. coli* (from Portugal) and 18 of methicillin-resistant *S. aureus* (MRSA) (14 isolates from Italy and four from Portugal). The susceptible *E. coli* strains used comprised the parental strain *E. coli* B_E BL21(DE3) and two mutants, *E. coli* BL21(DE3)omp8 (devoid of OmpC, OmpA and OmpF) and *E. coli* BL21(DE3)omp2 (devoid of OmpF); the parental strain *E. coli* JF568, derived from K12, and its derived mutants, *E. coli* JF701 (devoid of OmpC) and *E. coli* JF703 (devoid of OmpF); the parental strain *E. coli* W3110 and the three mutant strains, *E. coli* W3110 ΔC (devoid of OmpC), *E. coli* W3110 ΔF (devoid of OmpF) and *E. coli* W3110 ΔFΔC (devoid of OmpC and OmpF). All the strains and isolates were stored in glycerol, at - 80˚C, and thawed at room temperature before being plated on agar. Mueller-Hinton agar (MHA), a non-selective medium, was used for plating all studied strains in Portugal, while selective media were used in Italy: mannitol salt agar (MSA) for *S. aureus* and MacConkey agar (MCA) for *E. coli* strains. Fresh bacterial cultures were obtained by overnight incubation of agar plates, at 37 ± 0.1˚C.

The disk diffusion method was performed for *E. coli* ATCC 25922, the parental strain JF568 and the two mutant strains, *E. coli* JF701 (devoid of OmpC) and JF703 (devoid of OmpF).

2.9.3. Inoculum Preparation

The inoculum preparation was performed by the growth method, in Italy, and by the direct colony suspension method, in Portugal.

2.9.3.1. Growth Method

The growth method consists in the selection of three to five colonies (well-isolated and morphologically identical) from an agar plate culture and in their further suspension in a suitable broth medium, till the culture achieves the exponential growth stage. It is not mandatory that the culture is fresh, being possible to use colonies with more time than an overnight incubation, at 37 ± 0.1˚C. The colonies were isolated using a sterile loop and transferred to 3 mL of sterile brain heart infusion (BHI) broth. The bacterial suspension was incubated, at 37 ± 0.1˚C, for around four hours, in order to obtain a 0.5 McFarland turbidity that is equivalent to 1 to 2 x 10^8 colony-forming units (CFU) per mL. The suspension was then diluted ten times (≈ 10^7 CFU per mL) and the turbidity was evaluated by UV-vis spectrophotometry, at 450 nm, using a blank containing the BHI medium. The inoculum was then diluted in CAMH broth, according to the guidelines, in order to obtain ≈ 10^6 CFU per mL.[156] The bacterial cultures were prepared in aseptic conditions, at the Bunsen burner.

2.9.3.2. Direct Colony Suspension Method

In turn, the direct colony suspension method consists in the suspension of three to five fresh colonies from fresh cultures (in the exponential growth stage) directly to Mueller-Hinton broth (MHB). The colonies were obtained by overnight incubation of agar plates, at 37 ± 0.1˚C, and were transferred to 9 mL of MH broth, using a sterile loop. The turbidity of the bacterial suspension was assessed by measuring the optical density at 600 nm (OD_{600}), using a blank containing only medium, and adjusted to

OD_{600} = 0.1. This inoculum was then diluted in MHB, in order to obtain a final bacterial suspension with ≈ 10^6 CFU per mL.[157,158] The bacterial cultures were performed in aseptic conditions, in a Class II Biohazard Safety Cabinet from ESCO.

2.9.4. Antimicrobial susceptibility testing

The antimicrobial susceptibility testing was performed by the broth microdilution method and by the disk diffusion test.

2.9.4.1. Broth microdilution method

The antimicrobial susceptibility testing by the broth dilution method was performed with fresh CAMH broth (in Italy) or MHB (in Portugal). All antimicrobial stock solutions were diluted in order to obtain a solution that must be 2× more concentrated than the desired highest concentration to be tested. Once again, the protocol used in Italy and Portugal differs, as described below. Nevertheless, the susceptibility test is always performed in a 96-well plate, with a final bacterial concentration of ≈ 5 x 10^5 CFU per mL.[157]

The protocol used in Italy starts by dispensing 100 µL CAMH broth in all wells of the 96-well plate, followed by the addition of 100 µL of each compound solution to the column 1 (one row for each studied compound; maximum of 7 compounds per plate). This step consists in the two-fold dilution of the first column and was followed by a serial two-fold dilution from well 2 to well 12, using a multichannel pipette. The inoculum was finally dispensed into all wells (containing 100 µL of solution) by addition of 10 µL of the bacterial suspension of ≈ 10^6 CFU per mL, with the exception of the column 12 and half of the row H.[157] All the procedure was performed in aseptic conditions, near the Bunsen burner.

In turn, the procedure used in Portugal begins with the addition of 100 µL of each stock solution into the first column of a 96-wells plate (one row for each studied compound; maximum of 7 compounds per plate) and of 50 µL of the broth into all other wells (from the second column on). The compounds were then diluted in a serial two-fold dilution, using a multichannel pipette, from well 2 to well 12. The inoculum was then dispensed into all wells, by adding 50 µL of the bacterial suspension of ≈ 10^6 CFU per mL, with the exception of the column 12 and half of the row H.[157] All the procedure

was performed in aseptic conditions, in a Class II Biohazard Safety Cabinet from ESCO.

As contaminations can occur, it is necessary to assure their absence through the use of control wells of the broth, of the inoculum and of each compound solution used. In this way, and as it can be observed in the scheme below (Scheme 1), the column 12 works as the control for the compound and the row H contains the controls of the broth and of the inoculum. The controls were performed in both countries. In both cases, the 96-well plates were incubated at 37 ± 0.1˚C for 16 to 20 hours, after which the minimum inhibitory concentration (MIC) end points were determined.[157,159]

	1	2	3	4	5	6	7	8	9	10	11	12
A												**Compound solution control**
B												
C												
D												
E												
F												
G												
H	**Broth control**						**Inoculum control**					

Scheme 1 - Scheme used for each antimicrobial susceptibility testing. Each raw from A to G corresponds to a compound solution that is being tested.

2.9.4.1.1. Minimum inhibitory concentration (MIC) end points

The MIC is the lowest concentration of an antimicrobial agent that completely inhibits the bacterial growth, detected by the naked eye. The growth end points are determined by comparison of the amount of growth between the wells containing the antimicrobial agent and the wells of growth-control. At least, three independent experiments were performed for each compound tested.

The MIC ranges for quality control strains and susceptibility breakpoints are presented in Tables 2 and 3, respectively.

Table 2 - MIC quality control ranges (μg mL^{-1}) of FQs and copper salts against control strains (*E. coli* ATCC 25922, *P. aeruginosa* ATCC 27853, *S. aureus* ATCC 25923 and *S. aureus* ATCC 29213).

Compound	***E. coli*** **ATCC 25922** [a]	***P. aeruginosa*** **ATCC 27853** [a]	***S. aureus*** **ATCC 25923**	***S. aureus*** **ATCC 29213** [a]
cpx	0.004 – 0.016	0.25 – 1	0.125 - 0.5 [160-164]	0.125 – 0.5
lvx	0.008 – 0.06	0.5 – 4	0.125 - 0.5 [160,163-166]	0.06 – 0.5
mxfx	0.008 – 0.06	1 – 8	0.03 - 0.06 [160-164,167]	0.016 – 0.125
spx	0.004 – 0.015	0.5 - 2	0.06 – 0.125 [164,167]	0.03 – 0.12
Copper salt	≈ 128 (492 uM) for $CuCl_2.5\ H_2O$ [70]		250 for $Cu(NO_3)_2.2.5H_2O$ [168]	

[a] values defined as recommended by the European Committee on Antimicrobial Susceptibility Testing (EUCAST) and the Clinical and Laboratory Standards Institute (CLSI). [169,170]

Table 3 - MIC interpretive criteria (μg mL^{-1}) of FQs against *Enterobacteriaceae*, *P. aeruginosa* and *Staphylococcus spp.*

Antimicrobial agent	MIC breakpoint (*μ*g mL^{-1})					
	Enterobacteriaceae [b]		***P. aeruginosa*** [b]		***Staphylococcus* spp.**[b]	
	S	R	S	R	S	R
cpx [171]	≤ 0.25	> 0.5	≤ 0.5	> 0.5	≤ 1	> 1
lvx [171]	≤ 0.5	> 1	≤ 1	> 1	≤ 1	> 1
mxfx [171]	≤ 0.25	> 0.25			≤ 0.25	> 0.25
spx [169]					≤ 0.5	≥ 2

[b] values defined as recommended by the European Committee on Antimicrobial Susceptibility Testing (EUCAST) and the Clinical and Laboratory Standards Institute (CLSI). [169,171] S and R mean susceptible and resistant, respectively.

Due to the absence of standard MIC values of erx, the cpx standard MIC values were used to validate the CLSI methodology, as these two drugs show structural similarity. There is no MIC interpretative criterion for *S. aureus* ATCC 25923 as this strain is usually used for the disk diffusion method, while the *S. aureus* ATCC 29213 is commonly used for MIC assays.

2.9.4.2. Disk diffusion test

The disk diffusion test consists in inoculating a bacterial suspension of ≈ 1 to 2 x 10^8 CFU per mL on the surface of a MHA plate (150 mm diameter). Up to 3 paper disks containing a fixed concentration of a compound were placed on the inoculated agar surface and the plates were incubated at 37 ± 0.1˚C, for 16 to 20 hours. The study was performed with commercial cpx disks of 5 μg and with blank paper disks (of 6 mm) impregnated with the solutions being tested (including cpx) to reach 5 μg of each compound. The diameter of the zones of growth inhibition, obtained around each disk, were measured (in mm) and compared to the quality control ranges (Table 4).[159] Two independent experiments were performed to ensure assay reproducibility. The studies

were carried out in a Class II Biohazard Safety Cabinet from ESCO to assure the aseptic conditions.

Table 4 - Zone diameter interpretive criteria (mm) of cpx against *Enterobacteriaceae*.

	Quality control ranges of inhibition zones (mm) for *E. coli* ATCC 25922 [c]	
Antimicrobial agent	**EUCAST range**	**CLSI range**
cpx	29 - 37	30 - 40

[c] values defined as recommended by the Clinical and Laboratory Standards Institute (CLSI) and the European Committee on Antimicrobial Susceptibility Testing (EUCAST) for 5 µg of disk content.[169,170]

2.10. Activity and toxicity assays

2.10.1. Filter sterilized stock solutions

Stock solutions of phen, Cu(II)/phen (1:1), $Cu(NO_3)_2.3H_2O$, FQs and metalloantibiotics were prepared in HEPES buffer (with the exception of the copper solution, prepared in double deionised water), with a concentration of 2.5 mmol dm^{-3}. The solutions were sterilized by membrane filtration (≤ 0.22 µm nominal pore size) and stored in small aliquots, protected from light, at -80˚C. The stock solutions were then thawed as needed and used in the same day.

2.10.2. Enzymatic inhibitory activity assays

Type II topoisomerases, gyrase and topoisomerase IV, are the main targets of quinolones.[172] For this reason, the ability of the compounds to inhibit the bacterial toposiomerases II was assessed, both in *E. coli* and in *S. aureus*.

Gyrase supercoiling inhibition assays were performed by incubating relaxed pBR322 plasmid (0.5 µL per assay) with 1 unit of gyrase (prepared in the dilution buffer

supplied) and the assay buffer supplied, in the absence and presence of a concentration range of the solutions being tested. The mixing of the reagents was performed on ice and the reactions were carried out at 37.0 ± 0.1˚C, for 30 minutes. The reactions were then stopped by the addition of equal volume of STEB (40% w/v sucrose, 100 mmol dm^{-3} Tris-HCl pH 8, 10 mmol dm^{-3} EDTA pH 8 and 0.5 mg/mL bromophenol blue) and chloroform/isoamyl alcohol (24:1 v/v). Samples were vortexed and centrifuged (2,300 x g for two minutes) and run through a 1% (w/v) agarose gel in Tris acetate EDTA (TAE) buffer (40 mmol dm^{-3} Tris base, 20 mmol dm^{-3} acetic acid glacial and 1 mmol dm^{-3} EDTA) for two hours at 85 V, in an electrophoresis system from BioRad.

Topoisomerase IV relaxation assays were performed by incubation of supercoiled pBR322 plasmid (0.5 µL per assay) with 1.5 (*E. coli*) or 2 (*S. aureus*) units of topoisomerase IV (prepared in the dilution buffer supplied) and the assay buffer supplied, in the absence and presence of a concentration range of the compounds tested. The mixing of the reagents was performed on ice and the reactions were carried out at 37.0 ± 0.1˚C, for 30 minutes. The reactions were then stopped by the addition of equal volume of STEB (40% w/v sucrose, 100 mmol dm^{-3} Tris-HCl pH 8, 1 mmol dm^{-3} EDTA pH 8 and 0.5 mg/mL bromophenol blue) and chloroform/isoamyl alcohol (24:1 v/v). Samples were vortexed and centrifuged (2,300 x g for two minutes) and run through a 1% (w/v) agarose gel in TAE buffer for two hours at 85 V, in an electrophoresis system from BioRad.

All gels were stained with GreenSafe Premium, visualized and photographed under UV light, using an UV transilluminator (GenoSmart) from VWR. The study was carried out with two metalloantibiotics, Cucpxphen and Cuspxphen, and six compound concentrations were evaluated: 0.5; 1.0; 5.0; 10.0, 50.0 and 100.0 µmol dm^{-3}. Three controls were used in the study: a negative control, consisting of a mixture of the plasmid, water, assay buffer and dilution buffer (in the absence of the enzyme), and two positive controls, comprising a mixture of the plasmid, water, assay buffer and water or HEPES buffer (in the presence of the enzyme). Cpx was used as a control in all experiments, due to its known enzymatic inhibitory activity. All determinations were performed, at least, in three independent experiments to ensure assay reproducibility.

2.10.3. Cytotoxicity assay

The cytotoxic activity of the compounds was evaluated through the MTT assay, performed against an immortalized human fibroblasts cell line (HFF-1, ATCC number SCRC-1041). In metabolically active cells, MTT is reduced by mitochondrial enzymes and forms formazan crystals.[173] For this reason, this reagent is well used to evaluate the metabolic activity of cells in the presence of possible cytotoxic agents. Cells were maintained in 21 cm^2 culture flasks (TPP, Switzerland) at 37˚C, in 5% (v/v) CO_2, in Dulbecco's Modified Eagle's Medium (DMEM), from Sigma-Aldrich, supplemented with 15% (v/v) heat inactivated fetal bovine serum (Invitrogen, USA); 100 IU/mL of penicillin (~ 100 µg/mL); and 100 µg/mL of streptomycin. The attachment of the cells was performed in 96 well plates (TPP, Switzerland), 24 hours previously to the compound exposure, with a cell density of 5000 cells/well. The experiments encompassed one control group, containing cells only treated with media, and thirteen different compounds to which cells were exposed: cpx, erx, lvx, mxfx, spx, Cucpxphen, Cuerxphen, Culvxphen, Cumxfxphen, Cuspxphen, phen, Cu(II)/phen (1:1) and $Cu(NO_3)_2.3H_2O$ solution. The study was carried out with five compound concentrations: 1.56; 3.12; 6.25; 12.50 and 25.00 µmol dm^{-3}. After 24 hours of compound exposure (or media, in the case of the control), culture media was replaced by one containing MTT (0.5 mg/mL), for three hours, at the same culture conditions. After this period, the MTT was removed and the cells were treated with 100 µL of DMSO, for 10 minutes. The amount of the extracted formazan crystals was measured by optical density, at 540 nm, and correlated to the cell viability. The results were expressed as perceptual changes compared to control. All conditions were studied in six replicates and three independent experiments were performed.

2.10.3.1. Statistical Analysis

The statistical analysis was performed with two-way analysis of variance (ANOVA) with Bonferroni multiple comparison post-test, after normalization of the data, using GraphPad Prism version 5.00 for Windows (GraphPad Software, San Diego, California, USA). Statistical significance was considered when $p < 0.05$.

2.10.4. Hemolytic activity assay

The hemolytic activity of the compounds was tested against human red blood cells (RBCs). Peripheral blood, collected with EDTA, was obtained from healthy donors. The biological sample was centrifuged at 1,000 × g, for 10 minutes, at 4˚C, and the supernatant was replaced by PBS buffer. Three cycles of centrifugation/washing with PBS buffer were performed. A suspension of RBCs of 8% (v/v) was prepared and mixed with various concentrations of different compounds. The experiments were performed with a final concentration of RBCs of 4% (v/v) and five compound concentrations were evaluated (1.56; 3.12; 6.25; 12.50 and 25.00 μmol dm^{-3}). Two controls were used in the study: a negative control (considering 0% of hemolysis), comprising a suspension of RBCs in PBS buffer alone, and a positive control (assuming 100% of hemolysis), consisting of RBCs suspended in Triton X-100 (0.1% v/v). The study was carried out with seven different compounds: cpx, spx, Cucpxphen, Cuspxphen, phen, Cu(II)/phen (1:1) and $Cu(NO_3)_2.3H_2O$. The samples (400 μL) were incubated for one hour, at 37˚C, followed by centrifugation at 1,000 × g, for 20 minutes, at 4˚C. Supernatants (100 μL) were transferred to a 96-well plate and the optical density was measured at 450 nm (OD_{450}). The hemolytic activity of the compounds was quantified according to the following formula [174,175]:

$$hemolysis\ (\%) = \frac{OD_{\ drug} - OD_{\ negative\ control}}{OD_{\ positive\ control} - OD_{\ negative\ control}} \times 100 \quad (27)$$

All conditions were studied in duplicate and two independent experiments were performed.

2.10.4.1. Statistical Analysis

The statistical analysis was performed, after normalization of the data, and differences between mean values of groups were assessed by one-way ANOVA, using GraphPad Prism version 5.00 for Windows (GraphPad Software, San Diego, California, USA). A p-value < 0.05 was considered statistically significant.

Results and Discussion

3

This chapter, divided into three sections, presents the results obtained in the biophysical and biological studies performed with five metalloantibiotics and respective pure FQs (cpx, erx, lvx, mxfx and spx). The first section was dedicated to the study of the influx route of the FQs and metalloantibiotics in Gram-negative models. This section comprises the compilation of the partition coefficients, the study of the location in the membrane and the evaluation of the role of porins in the influx of the compounds, using fluorescence spectroscopy. The second section comprised microbiological tests and aimed to i) clarify the role of OmpF and OmpC in the influx route of the compounds in *E. coli* and ii) assess the antimicrobial activity of the compounds against resistant strains of Gram-negative and Gram-positive bacteria. The first part of the work was performed with susceptible *E. coli* strains and their derived porin-deficient mutants and the second part included reference and resistant strains of *E. coli*, *P. aeruginosa* and *S. aureus*. The third section of the work encompassed enzymatic studies in order to clarify the mechanism of action of the metalloantibiotics in Gram-negative and Gram-positive bacteria and preliminary studies of toxicological safety of the promising metalloantibiotics.

3.1. The influx route of FQs and metalloantibiotics in Gram-negative models

The influx of FQs has been widely studied in the last years, being known that these drugs use both lipid-mediated and porin-mediated pathways in the Gram-negative bacterial cells.[11] In this way, the knowledge of the properties of the bacterial membranes, concerning the lipid composition and the presence of porins, are crucial to understand the permeation of these antibiotics.[11,13,17] In turn, the protonation and lipophilicity of the FQs is also critical to the interaction and consequent translocation of the drugs.

The interaction of the drugs with the bacterial membrane is extremely important, especially for the lipid-mediated pathway.[11] The translocation process based on the drug-membrane interactions occurs via alterations on the membrane that enable the passive diffusion. The formation of hydrogen bonds between the piperazinyl group of the FQs (at position 7) and the polar headgroups of the lipids was described as the starting point of the drug-membrane interaction.[176] The protonation form of the drug has also direct implications in the diffusion of the FQs as it is related to the lipophilicity of the molecules.[176,177] Therefore, the characterization and speciation of the drugs is

mandatory as well as the determination of their interaction with the membrane, commonly assessed in terms of the K_p).[32]

This work was performed using five FQs (cpx, erx, lvx, mxfx and spx) and respective metalloantibiotics. The K_p constants are already determined for all studied compounds in *E. coli* liposomes, with the exception of spx and Cuspxphen. For this reason, the starting point of this work was the determination of the mentioned constants. Then, a compilation of the data available in literature and further comparison are presented.

3.1.1. Determination of the partition coefficient of sparfloxacin and its ternary copper/phen metalloantibiotic by time-resolved fluorescence spectroscopy

The vast majority of the FQs has intrinsic fluorescence, which enable the use of fluorescence techniques to perform numerous studies. However, some molecules, as spx and its metalloantibiotic, are non-fluorescent, being necessary the adoption of alternative strategies. Although it cannot be determined directly, the K_p of non-fluorescent molecules can be assessed by fluorescence spectroscopy through the incorporation of fluorescent probes with known location into the membrane. The partition is assessed by the changes observed in the fluorescence of the membrane probes arising from the presence of the drug.[135]

The *n*-(9-anthroyloxy)-stearic acids, as known as *n*-AS, are a series of fluorescent probes consisting of a fatty acid chain attached to an anthroyloxy group whose depth location in the bilayer is well known. When incorporated in the membrane, the fatty acid chains of the probes align parallel to the hydrophobic tails of the phospholipids, being known the distance of the anthroyloxy group to the centre of the bilayer.[131,136]

As the quenching of the *n*-AS probes usually occurs by a dynamic process, the experiments were carried out by time-resolved fluorescence spectroscopy. This technique relies on the lifetime of the fluorescent molecules, which varies with the environment and polarity of the surrounding medium.[131] The fluorescence lifetime of a fluorophore rises with the decrease of the polarity of the surrounding environment. For this reason, a fluorophore with a deeper location in the membrane bilayer exhibits a higher fluorescence lifetime.[131]

This work comprised two *n*-AS probes, 2-AS and 12-AS, whose anthroyloxy groups are located ≈ 15,8 and 6 Å [4] from the centre of the bilayer, respectively.[137]

The fluorescence lifetimes of 2-AS and 12-AS probes were determined in liposomes of *E. coli* total extract, with a two-exponential decay analysis, using Eq. (10) and Eq. (11), as summarized in Table 5. The two components of the lifetimes (τ_1 and τ_2) can be associated to different interactions, one related to an intermolecular hydrogen-bonded state (the shorter component, τ_1) and the other to an intramolecular hydrogen-bonded state (the larger component, τ_2), dependent on the polarity of the surrounding media.[178] As expected, the fluorescence lifetime of the 12-AS is higher than the one of 2-AS, due to its deeper location in the membrane. Although slightly smaller, the obtained fluorescence lifetimes are consistent with the values reported in the literature for the same probes in 1,2-dioleoyl-s*n*-glycero-3-phosphocholine (DOPC) liposomes: average lifetime ($\bar{\tau}$) of 6.30 and 12.21 ns for 2-AS and 12-AS, respectively.[131] The differences of the lifetime values indicate that the environment surrounding the probes is more polar in the case of the *E. coli* total extract liposomes, which can be attributed to the heterogeneous composition of this system.

Table 5 - Representative fluorescence lifetimes of *n*-AS probes determined in *E. coli* total extract liposomes (prepared in HEPES 10 mmol dm^{-3}, pH 7.4, NaCl 0.1 mol dm^{-3}), using a two-exponential decay. The amplitude-weighted and average lifetimes were calculated using Eq. (10) and Eq. (11), respectively.

Probe	α_1	τ_1 / ns	α_2	τ_2 / ns	$\langle\tau\rangle$ / ns [a]	$\bar{\tau}$ / ns [b]
2-AS	0.40	2.26	0.60	5.26	4.14 ± 0.24	4.68 ± 0.22
12-AS	0.40	2.89	0.60	10.35	7.73 ± 0.14	9.46 ± 0.20

[a] The amplitude-weighted lifetime, $\langle\tau\rangle$, calculated using Eq. (10).

[b] The average lifetime, $\bar{\tau}$, calculated using Eq. (11).

As previously mentioned, the use of florescent probes to determine the K_p of non-fluorescent drugs is an invasive method. For this reason, it is necessary to study the quenching of the probes for different liposome concentrations, always maintaining the lipid:probe ratio and the drug concentration range. The experimental data provide

[4] Values referenced for phosphocholine (PC) vesicles at pH 5.

different apparent quenching constants (K_{app}) and bimolecular quenching constants (${k_q}^{app}$), one for each specific studied condition, using Eq. (12). Afterwards, the K_p of the drug is determined using Eq. (13) and Eq. (14).

The experiments performed by time-resolved fluorescence spectroscopy with 2-AS probe did not allow the determination of the K_p, as the presence of both spx and its copper complex doesn't affect the fluorescence lifetime of this probe. These results indicate that the interaction of the 2-AS probe with spx and Cuspxphen doesn't occur by a collisional quenching. The location of this probe may explain these results, as the chromophore of the 2-AS probe is positioned in the interface between the membrane and the external environment.[179] This peripheral location may make it difficult to distinguish between the free drug (in solution) and the partitioned drug (in the membrane). The fluorescence of the probe may also be affected by interactions occurring in the neighbourhood of the chromophore, as interactions between the drugs and the polar headgroups of the membrane bilayer.

The same results were obtained for the interaction of spx with 12-AS probe, what demonstrates that this quenching cannot be described by a dynamic process. For this reason, partition studies of spx in *E. coli* total extract liposomes, published in the meantime, were performed by the quenching of this probe through steady-state fluorescence spectroscopy ($\log K_p$ = 4.61 ± 0.01) or by UV-vis spectroscopy ($\log K_p$ = 4.6 ± 0.2).[73]

In turn, changes in the fluorescence lifetime of the 12-AS probe were observed in the presence of increasing amounts of Cuspxphen. Therefore, the K_p of Cuspxphen in *E. coli* total lipid extract liposomes was determined by time-resolved fluorescence. The obtained results show a quenching of the fluorescence lifetime of 12-AS probe resultant from increasing amounts of Cuspxphen. And, as expected, the extension of the quenching is greater as lower the lipid concentration, for the same amount of metalloantibiotic (Figure 14 and Table 6). This trend occurs as the low concentrations host less lipid available for the partition of the compound. Thus, the addition of the same amount of quencher results in a higher extension of the occupancy of the membrane bilayer, which is measured by the apparent partition. The dependence of the apparent quenching constant on lipid concentration allows the determination of the K_p.[126]

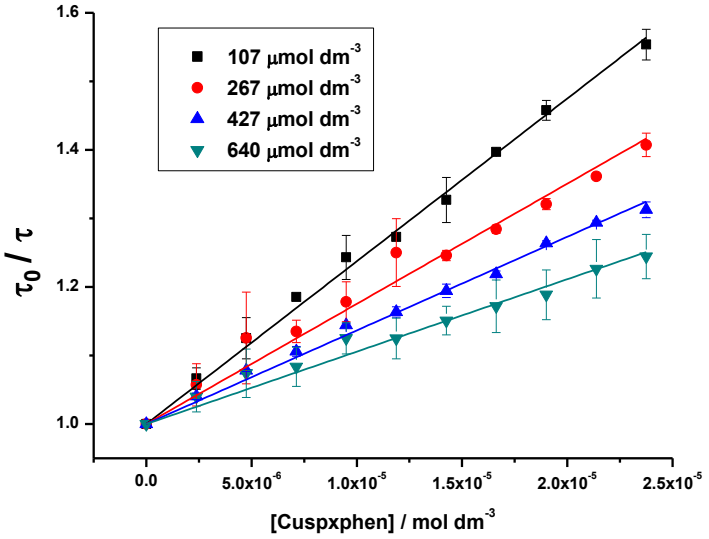

Figure 14 - Plots of τ_0/τ vs [Cuspxphen] concentration for 12-AS probe incorporated in different lipid concentrations of *E. coli* total extract liposomes (107, 267, 427 and 640 µmol dm^{-3} prepared in HEPES 10 mmol dm^{-3}, pH 7.4, NaCl 0.1 mol dm^{-3}). Eq. (12) was fitted to the experimental data. Data points are the mean of, at least, three independent experiments.

Table 6 - Detailed list of the used lipid concentrations, correspondent lipid volume fractions (α_m) and apparent bimolecular constants (k_q^{app}) obtained from the Stern-Volmer plots of τ_0/τ vs [Cuspxphen], calculated though the fitting of Eq. (12) and Eq. (13) to the experimental data.

[liposome] / µmol dm^{-3}	α_m / (x 10^{-4})	k_q^{app} / (x 10^{12}) dm^3 mol^{-1} s^{-1}
107	0.74	2.38 ± 0.03
267	1.85	1.76 ± 0.04
427	2.95	1.37 ± 0.02
640	4.42	1.06 ± 0.03

The determination of the K_p and of the k_q of Cuspxphen in *E. coli* total lipid extract liposomes was assessed using the lipid volume fraction (α_m) and apparent bimolecular constant (k_q^{app}) values obtained for each lipid concentration, using Eq. (12) and Eq. (13). The plot of $1 / k_q^{app}$ vs α_m allows the calculation of the K_p', which can be converted in the K_p (Figure 15 and Table 7), using Eq. (13) and Eq. (14).

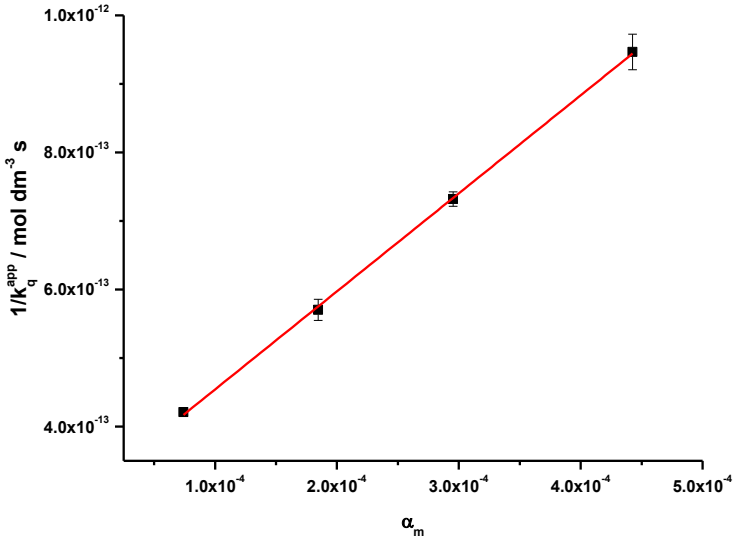

Figure 15 - Plot of the inverse of the apparent bimolecular constants (1 / k_q^{app}) vs lipid volume fraction (α_m) for *E. coli* total extract liposomes (prepared in HEPES 10 mmol dm^{-3}, pH 7.4, NaCl 0.1 mol dm^{-3}). Eq. (13) was fitted to the experimental data. Data points are the mean of, at least, three independent experiments.

Table 7 - Values of the partition coefficient (K_p) and bimolecular quenching constant (k_q) for the quenching of 12-AS, incorporated in *E. coli* total lipid extract liposomes (prepared in HEPES 10 mmol dm^{-3}, pH 7.4, NaCl 0.1 mol dm^{-3}), by Cuspxphen, obtained from the plot of the inverse of the apparent bimolecular constant (1 / k_q^{app}) vs the lipid volume fraction (α_m), through the fitting of Eq. (13) and Eq. (14) to the experimental data.

log K_p	5.24 ± 0.01
k_q / (x 10^8) dm^3 mol^{-1} s^{-1}	7.0 ± 0.1

When compared to the pure spx, the K_p of Cuspxphen is only slightly higher, not following the marked differences usually observed between metalloantibiotics and free FQs. Nevertheless, this result corroborates the hydrophobic route described for the influx of spx.[70,73]

The bimolecular quenching constant, k_q, discloses the accessibility of the quencher to the fluorophore and depends on the characteristics of the surrounding environment (solvent and viscosity).[126] Usually, diffusion-controlled quenching exhibits a k_q value around 1 x 10^{10} dm^3 mol^{-1} s^{-1}. However, this value can be highly decreased by steric shielding of the fluorophore, a phenomenon that occurs in the case of

fluorophores immobilised in lipid membranes.[126,180] This statement explains the smaller experimental value obtained in this work (k_q = 7.0 x 10^8 ± 0.1 x 10^8 dm^3 mol^{-1} s^{-1}), which is similar to what was described for other membrane lipidic systems: 3.86 - 5.26 x 10^8 dm^3 mol^{-1} s^{-1} in egg phosphatidylcholine liposomes [180] and 0.21 - 1.91 x 10^9 dm^3 mol^{-1} s^{-1} in dipalmitoyl phosphatidylcholine liposomes [181].

As a final conclusion, the obtained results demonstrate the collisional quenching of 12-AS probe by Cuspxphen in *E coli* total extract liposomes and support the hydrophobic influx pathway proposed for metalloantibiotics. The fluorescence method used in this work is highly sensitive and avoids the interferences resultant from the lipid scattering, usually described in the steady-state fluorescence measurements.[135]

With the K_p values determined for the non-fluorescent molecules (spx and Cuspxphen), it is now possible to analyse and make a comparison between the 10 compounds used in this work. Therefore, a compilation of the data available in the literature, concerning the pK_a and K_p values, is presented below, followed by a comparison analysis of all compounds.

As previously described, FQs have two ionisable groups, the carboxylic group of the 4th position and the amino group of the 7th position. The protonation level of these two groups depends on the pH of the medium and on the specific pK_a values characteristic of each drug (Table 8).

Table 8 - pKa of fluoroquinolones, from [70,71,103,145].

Antibiotic	pK_{a1}	pK_{a2}
cpx [70]	6.15 ± 0.01	8.95 ± 0.03
erx [103]	6.17 ± 0.01	7.72 ± 0.01
lvx [71]	6.02 ± 0.02	8.15 ± 0.04
mxfx [145]	6.23 ± 0.02	9.53 ± 0.03
spx [70]	6.13 ± 0.15	7.43 ± 0.04

According to the protonation level, FQs may exist in solution in four forms (Scheme 2): cationic (H_2FQ^+), zwitterionic ($HFQ^{\pm}$), neutral (HFQ^0) and/or anionic (FQ^-).[105,106,182]

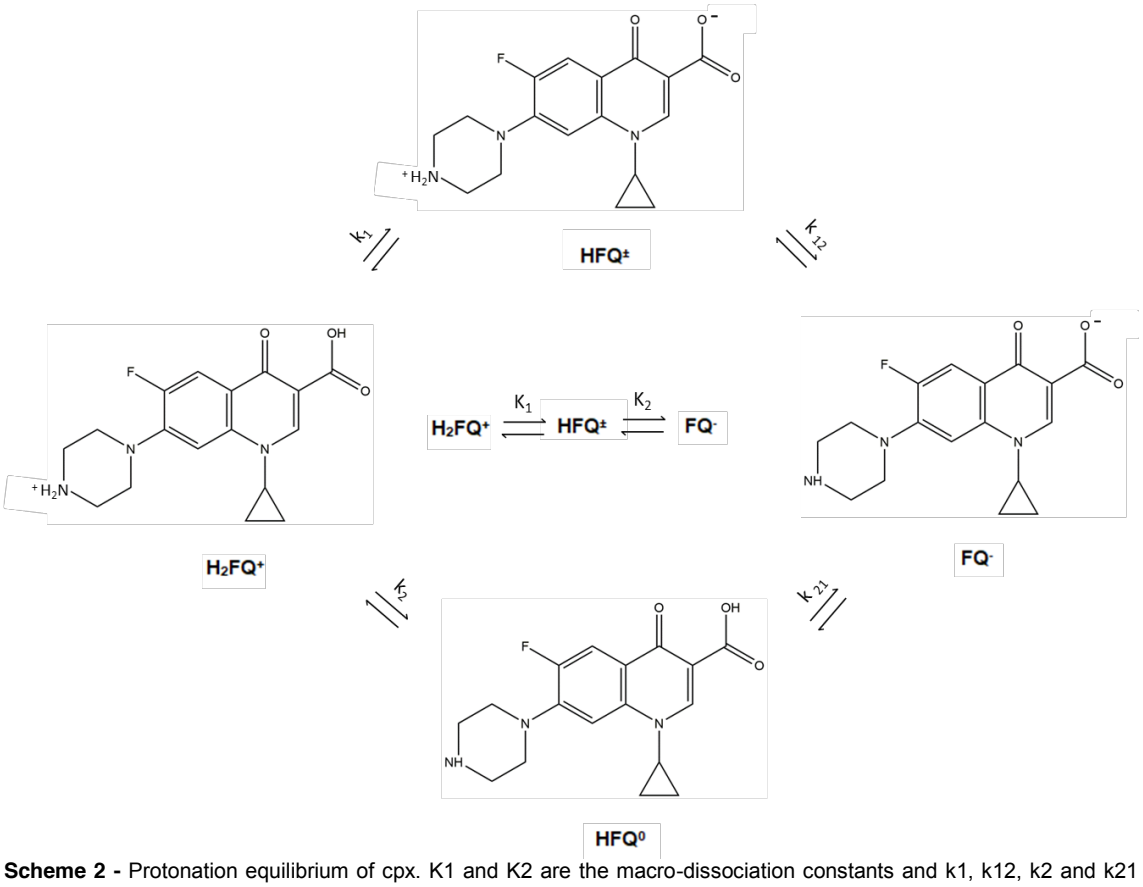

Scheme 2 - Protonation equilibrium of cpx. K1 and K2 are the macro-dissociation constants and k1, k12, k2 and k21 refer to the micro-dissociation constants of the individual functional group. The species are represented in four different forms: H_2FQ^+ (cationic form), $HFQ^{\pm}$ (zwitterionic form), HFQ^0 (neutral form) and FQ^- (anionic form), adapted from [105,106].

At physiological pH (7.4), the carboxylic acid of FQs is deprotonated (pH > pK_{a1}) and the amino group is commonly protonated (pH < pK_{a2}), which means that FQs exist mainly in a mixture of neutral (HFQ^0) and zwitterionic forms ($HFQ^{\pm}$) (Table 9).

Table 9 - Speciation of FQs under physiological conditions (pH 7.4, 0.1 mol dm^{-3} NaCl), determined using the micro and macro-dissociation constants.

Antibiotic	% $HFQ^{\pm}$ and HFQ^0	% FQ^-	log[$HFQ^{\pm}$]/[HFQ^0]
cpx	92.0	2.6	2.8
erx	65.0	31.1	1.6
lvx	82.0	14.6	2.1
mxfx	92.9	0.8	3.3
spx	50.3	47.0	1.3

Concentrations in the same range of those used in the partition studies.

Zwitterionic and neutral forms differ in terms of polarity: the zwitterion forms is a dipole, while the neutral form behaves as an apolar molecule.[176] Moreover, as the charge of a molecule is correlated to its lipophilicity, it was expected that these two forms are more lipophilic compared to the cationic and the aniconic forms. Nevertheless, some authors report reduced lipophilicity for some zwitterions in comparison to its neutral form.[106,182] This assumption corroborates the idea that the neutral form is the one that easily diffuses into the membrane, explaining the higher values of K_p for molecules with greater percentage of neutral forms.[176,177] Therefore, the calculation of the ratio zwitterionic/neutral forms, using the micro and macro-dissociation constants, is extremely important to evaluate the partition of the molecules. In some cases, the pK_{a2} has a value really close to 7.4, resulting in the presence of a substantial percentage of the anionic form (FQ^-), as observed for erx and spx (Table 9).

For the metalloantibiotics, the predominant species present in solution, at physiological pH, are cationic. The speciation studies performed for CuFQPhen complexes show that, at physiological pH, there is a mixture of mono- ($[Cu(FQ)phen]^+$) and di-cationic ($[Cu(HFQ)phen]^{2+}$) forms (Table 10).

Table 10 - Speciation of CuFQphen under physiological conditions (pH 7.4, 0.1 mol dm^{-3} NaCl).

CuFQphen	% $[Cu(HFQ)phen]^{2+}$	% $[Cu(FQ)phen]^{+}$
cpx	97.0	3.0
erx	42.7	50.1
lvx	38.5	57.0
mxfx	82.7	16.1
spx	52.6	38.1

Concentrations in the same range of those used in the partition studies.

As previously mentioned, the interaction of the drugs with the membranes is usually evaluated through the partition coefficient, which is largely dependent on the physicochemical properties of the drugs and of the membrane systems. Due to the structural and physicochemical differences between FQs and metalloantibiotics, it is expected a different ability to partition on the membrane.

The partition of a drug in the membrane consists in its ability to penetrate the membrane, remaining in a superficial part of the membrane (near the polar headgroups) or diffusing to a deeper region of hydrophobic (close to the tails of the phospholipids).[32] During several decades, the octanol/water system was the main reference model used for the determination of the K_p. However, octanol is an isotropic organic solvent, while phospholipid bilayers are anisotropic. Besides that, octanol/water system lacks the amphiphilic characteristics of membrane bilayers. For this reason and due to its structural similarity with biological membranes, liposomes are considered as privileged membrane model systems. Consequently, the determination of the K_p is commonly performed using liposomes instead of the traditional octanol/water method.[32,183]

Partition studies can be performed by several methods. Commonly, spectroscopic techniques (without phase separation) are simple and effective in terms of readiness and execution, in contrary to chromatographic techniques (with phase separation). Spectroscopic techniques include nuclear magnetic resonance (NMR), derivative spectrophotometry and fluorescence spectroscopy, being the last one the most sensitive.[135]

During the last years, the K_p values of several FQs and metalloantibiotics were determined in numerous membrane model systems of eukaryotes and prokaryotes. Concerning the prokaryotes, *E. coli* liposomes are generally used as a bacterial model system of excellence. The K_p values of the FQs and metalloantibiotics used in this work, determined in *E. coli* liposomes by fluorescence spectroscopy, are presented in Table 11.

Table 11 - Values for the partition coefficients (K_p) of FQs and metalloantibiotics in *E. coli* total lipid extract liposomes (prepared in HEPES 10 mmol dm^{-3}, pH 7.4, NaCl 0.1 mol dm^{-3}) obtained by fluorescence spectroscopy, from [123-125].

	log K_p	
Antibiotic	**FQ**	**CuFQphen**
cpx	4.21 ± 0.03 [123]	5.32 ± 0.09 [123]
erx	3.9 ± 0.2 [125]	4.85 ± 0.02 [125]
lvx	4.55 ± 0.01[a]	5.21 ± 0.09 [a]
mxfx	4.15 ± 0.02 [124]	5.38 ± 0.05 [a]
spx	4.61 ± 0.01 [73]	5.24 ± 0.01

[a] Data not published.

The K_p values clearly demonstrate a difference between the partition of the pure FQs and metalloantibiotics. With no exception, the K_p of the metalloantibiotics is greater than the one of the FQs in the bacterial model membranes, what was expected due to the negative charge (mean zeta potential - 36.8 mV) of the *E. coli* total extract liposomes.[73] For the same reason, it would be expected higher K_p values for FQs whose amount of the anionic species (FQ^-) is lower, as mxfx and cpx (Table 9). However, K_p (spx) > K_p (lvx) > K_p (cpx) > K_p (mxfx) > K_p (erx), what shows that the presence of higher content of neutral species (HFQ^0) results in a higher partition, even existing a large content of anionic species (FQ^-) in solution, as previously correlated.[177] This relationship (the lower log [$HFQ^{\pm}$] / [HFQ^0] value, the higher K_p value) is observed for spx, lvx, cpx, and mxfx but not for erx, probably due to the presence of the ethyl group that has direct implications in the hydrophilic and lipophilic properties of this FQ.[103,125]

Concerning the metalloantibiotics, similar K_p values are described for all complexes, K_p (Cumxfxphen) ≈ K_p (Cucpxphen) ≥ K_p (Cuspxphen) ≈ K_p (Culvxphen) > K_p (Cuerxphen), with exception of Cuerxphen, whose partition is significantly lower. These results are in agreement with the speciation data of the metalloantibiotics (Table 10), showing higher partition for the complexes with higher percentage of the di-cationic ([Cu(HFQ)phen] $^{2+}$) form, whose positive charges privilege the electrostatic interactions with the negative surface of the liposomes. In turn, the mono-cationic form ([Cu(FQ)phen] $^{+}$) acts as a pseudo neutral form, as the copper charge is masked by the coordination with the phen and the FQ. For this reason, the mono-cationic form behaves as a lipophilic species, possibly favouring the diffusion across the membrane. Once again, the behaviour of the complex of erx is different from what was expected, possibly due to the structural characteristic previously mentioned for the pure FQ.

Besides the differences observed between K_p values, opposite trends are observed in the fluorescence emission spectra of the FQs and metalloantibiotics in the presence of increasing amounts of liposomes. The emission spectra of the FQs show a decrease of the fluorescence intensity with the increase of the liposome concentration, in contrary to CuFQphen whose fluorescence intensity increases.[123-125] These divergences are attributed to different changes of the dipole moments of the molecules during the electronic transitions, due to distinct interactions between the solvent and the solute that interfere with the non-radiative and radiative coupling between ground and excited states. These results prove that the partition of FQs and CuFQphen rely on

different interactions, suggesting that metalloantibiotics may adopt a different influx mechanism to enter into the bacterial cell.[124,125]

3.1.2. Location studies of the FQs and metalloantibiotics in the mimetic membrane systems

Besides the partition, the assessment of the location in the membrane provides useful information to infer about the influx route of a drug. The location of the drugs is usually estimated through the study of its interaction with probes with known location in the membrane or by the use of quenchers with known preferential environments.

This part of the work comprised location studies of FQs and metalloantibiotics performed through i) the quenching of *n*-AS probes by the compounds, by steady-state and time-resolved florescence; ii) anisotropy studies using DPH and TMA-DPH probes, in the absence and presence of the compounds; and iii) the quenching of the compounds by iodide, using time-resolved fluorescence.

3.1.2.1. Quenching of *n*-AS probes by FQs and metalloantibiotics

The location studies performed with *n*-AS probes encompassed the 2-AS and 12-AS probes, incorporated in *E. coli* total extract liposomes. The quenching of the probes by free FQs and metalloantibiotics was determined for three different liposome concentrations (265, 427 and 635 μmol dm^{-3}), by steady-state and time-resolved fluorescence.[73,142] These studies did not include the non-fluorescent molecules, since the quenching studies of 2-AS and 12-AS by Cuspxphen and spx, previously performed, provided the K_p of these compounds.[73]

The spectral characterization of all compounds and fluorescent probes was carried out prior to the quenching studies (Table 12). These studies revealed spectral overlapping of the emission fluorescence of the probes (maximum emission wavelength: λ_{em} 2-AS = 458 nm; λ_{em} 12-AS = 455 nm) and lvx, mxfx, Culvxphen and Cumxfxphen. For this reason, the studies proceeded with cpx, erx, Cucpxphen and Cuerxphen.

Table 12 - Fluorescence maximum emission wavelength of FQ and metalloantibiotic solutions (prepared in HEPES 10 mmol dm^{-3}, pH 7.4, NaCl 0.1 mol dm^{-3}), determined by steady-state fluorescence spectroscopy.

	λ_{em} max / nm	
Antibiotic	**FQ**	**CuFQphen**
cpx	415	415
erx	413	412
lvx	460	460
mxfx	460	460

The steady-state data showed a quenching of the fluorescence intensity of the probes in the presence of increasing amounts of Cucpxphen and Cuerxphen (Figure 16). In turn, the time-resolved experiments revealed a decreasing of the lifetime of the probes in the presence of both metalloantibiotics, being the drastic reduction observed in the shorter lifetime component (τ_1), associated to the intermolecular hydrogen-bonded state.[178]

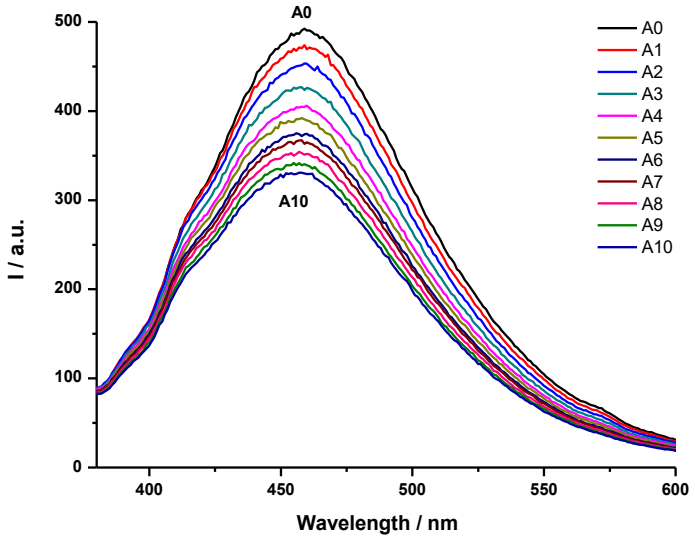

Figure 16 - Emission fluorescence spectra (*I*) of 2-AS probe incorporated in *E. coli* total lipid extract liposomes (635 µmol dm^{-3} prepared in HEPES 10 mmol dm^{-3}, pH 7.4, NaCl 0.1 mol dm^{-3}), in the absence (A0) and presence (A1-10) of Cucpxphen solution (A1: 2.9 µmol dm^{-3}; A2: 5.8 µmol dm^{-3}; A3: 8.6 µmol dm^{-3}; A4: 11.5 µmol dm^{-3}; A5: 14.4 µmol dm^{-3}; A6: 17.2 µmol dm^{-3}; A7: 20.1 µmol dm^{-3}; A8: 23.0 µmol dm^{-3}; A9: 25.9 µmol dm^{-3}; A10: 28.7 µmol dm^{-3}), with excitation wavelength of 363 nm. Each spectrum is a mean of five measurements.

The quenching extension was assessed by the determination of the Stern-Volmer constants (K_D) with the steady-state - fitting of Eq. (16) - and time-resolved data - fitting of Eq. (17) - as presented in Figure 17 and Table 13. The effective concentration of the metaloantibiotics in the membrane ([metalloantibiotic]$_m$) was determined with Eq. (15).

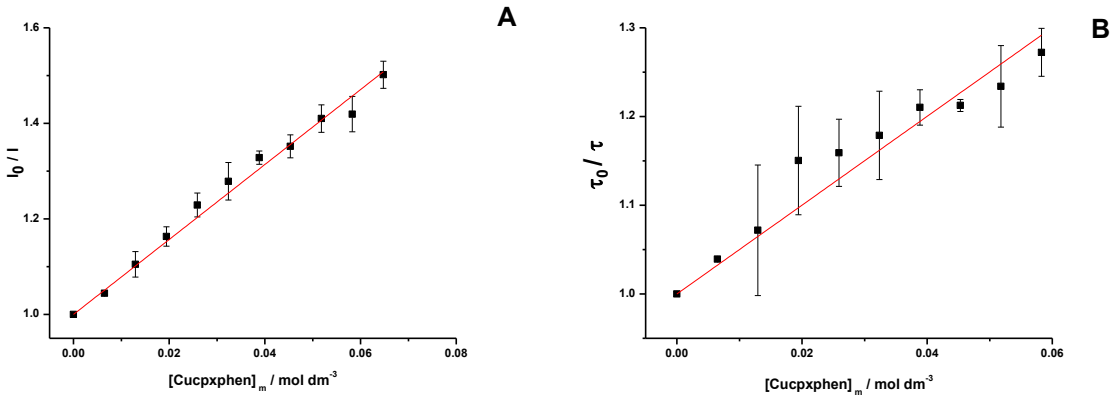

Figure 17 - Plots of I_0/I vs effective concentration of Cucpxphen in the membrane ([Cucpxphen]$_m$) (A) and of τ_0/τ vs [Cucpxphen]$_m$ (B), determined for the 2-AS probe incorporated in *E. coli* total lipid extract liposomes (635 μmol dm^{-3} prepared in HEPES 10 mmol dm^{-3}, pH 7.4, NaCl 0.1 mol dm^{-3}), with excitation and emission wavelengths of 363 and 458 nm, respectively. Eq. (16) was fitted to the steady-state experimental data (A) and Eq. (17) was fitted to the time-resolved experimental data (B). Data points are the mean of, at least, three independent experiments.

The obtained results (Table 13) show a general enhancement of the quenching with the increasing of the liposome concentration, within each experimental condition. These results demonstrate greater partition of the metalloantibiotics for increased concentrations of liposome, due to the enlargement of the amount of lipid available for the partition. Exceptionally, few K_D values obtained by time-resolved data deviate from the observed trend, possibly due to limitations of the technique related to the resolution threshold of the equipment. Analysing the data obtained for both Cucpxphen and Cuerxphen, the values of K_D calculated for 2-AS and 12-AS were comparable within each experimental condition and fluorescent technique, within experimental error. Taking all together, the results demonstrate a random distribution of Cucpxphen and Cuerxphen in the membrane.

Table 13 - Values for the Stern-Volmer constants (K_D) determined for the quenching of the probes 2-AS and 12-AS, incorporated in *E. coli* total extract liposomes (265, 427 and 635 μmol dm^{-3} prepared in HEPES 10 mmol dm^{-3}, pH 7.4, NaCl 0.1 mol dm^{-3}) in the presence of Cucpxphen and Cuerxphen, by steady-state (SS) and time-resolved (TR) fluorescence, through the fitting of Eq. (16) and Eq. (17) to the experimental data. The presented values are the mean of, at least, three independent measurements.

Compound	[liposome] / μmol dm^{-3}	K_D / mol^{-1} dm^3			
		2-AS probe		12-AS probe	
		SS [a]	TR [b]	SS [a]	TR [b]
Cucpxphen	265	3.92 ± 0.11	4.38 ± 0.32	3.11 ± 0.03	4.33 ± 0.27
	427	6.05 ± 0.13	3.80 ± 0.12	5.02 ± 0.06	5.17 ± 0.33
	635	7.84 ± 0.15	5.00 ± 0.23	5.78 ± 0.08	6.56 ± 0.41
Cuerxphen	265	2.84 ± 0.07	2.37 ± 0.17	3.21 ± 0.07	3.40 ± 0.04
	427	4.69 ± 0.13	4.58 ± 0.30	4.07 ± 0.10	3.26 ± 0.20
	635	6.88 ± 0.15	8.40 ± 0.34	5.81 ± 0.11	5.25 ± 0.33

[a] K_D calculated using Eq. (16).

[b] K_D calculated using Eq. (17).

Concerning the pure FQs, an overlapping of the emission fluorescence spectra of the drugs and the probes was observed. Consequently, although the fluorescence maximum emission wavelength of cpx and erx is distant from the one of 2-AS and 12-AS, it was not possible to perform quenching studies with these two FQs.

In summary, the similarity between the results obtained for the quenching of the two fluorescent probes with Cucpxphen and Cuerxphen points out for a random distribution of these two metalloantibiotics in the membrane. The spectral overlapping of the emission fluorescence of *n*-AS probes and most of the compounds resulted in spectroscopic limitations. Therefore, alternative strategies to assess the membrane location of all pure FQs and metalloantibiotics are required.

3.1.2.2. Steady-state anisotropy measurements

As previously mentioned, the permeability and fluidity of the membrane bilayers is dependent on its phase transition temperature (T_m). For more complex systems there may be several transition temperatures (T), which represents the switch-over between different thermotropic lipid phases.[4,27,29] Any perturbation of the membrane bilayer, including fluctuations of temperature and pressure or interactions with drugs, may result in changes of the thermotropic lipid phase of the system. For this reason, the study of the influence of a drug in the thermotropic lipid phase transitions may provide information about its location. This characterization is usually performed by different techniques as differential scanning calorimetry (DSC), Fourier transform-infrared (FT-IR) spectroscopy, DLS, NMR or fluorescence anisotropy.[31,184,185]

This work encompassed steady-state fluorescence anisotropy experiments with two fluorescent probes, DPH and TMA-DPH, incorporated in *E. coli* total lipid extract liposomes (2 mmol dm^{-3}, prepared with a lipid:probe ratio of 300:1).[31] TMA-DPH is a derivative of DPH, exhibiting a cationic trimethylammonium substitute anchored to the *para* position of one of the phenyl rings of DPH (Figure 18). The anisotropic profile of these two fluorescent probes, located around 7.8 Å (DPH) and 10.9 Å (TMA-DPH) [5] from the centre of the bilayer [186], was evaluated in the absence and presence (10 µmol dm^{-3}) of pure FQs and metalloantibiotics, in order to infer about the location of the compounds. The different location of the two probes provides information about distinct regions of the membrane, as DPH is positioned more deeply, near the acyl chains of the phospholipids, and TMA-DPH is located near the surface, close to the phospholipid headgroups.[31,186]

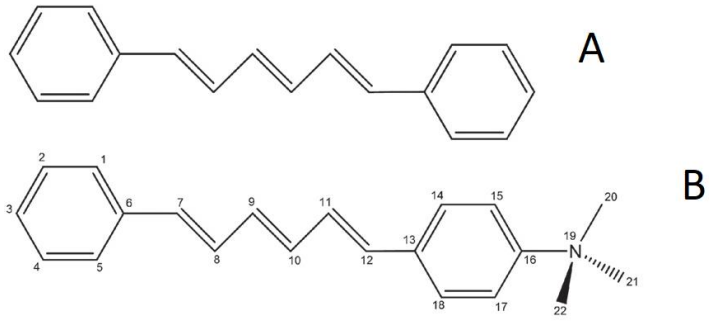

Figure 18 - Chemical structures of DPH (A) and TMA-DPH (B), adapted from [187].

[5] Values referenced for1,2-diacyl-s*n*-glycero-3-phosphocholine (PC) vesicles at pH 7.

Due to its heterogeneous composition, *E. coli* total lipid extract liposomes exhibit four T, representing different domains (Tables 14 and 15). The first one (T_1) is related to PE/CL interactions [188,189], the second (T_2) associated to PE/PG enriched domains and the last two (T_3 and T_4) linked to PE/CL interactions, being the T_4 illustrative of the presence of a wide variety of CLs in this extract.[31] The T are calculated through the fitting of Eq. (19) to the anisotropic profile of the *E. coli* total extract liposomes, obtained using DPH or TMA-DPH, as presented in Figure 19.

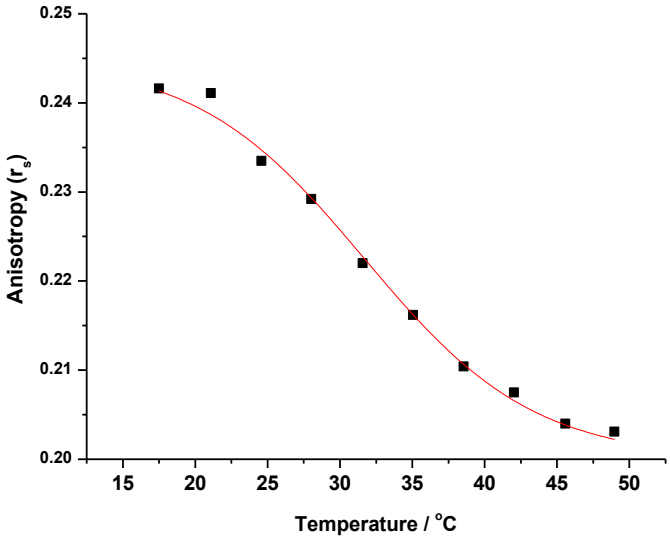

Figure 19 - Fitting of Eq. (19) to the anisotropic profile of *E. coli* total extract lipid liposomes (prepared in HEPES 10 mmol dm^{-3}, pH 7.4, NaCl 0.1 mol dm^{-3}), obtained using TMA-DPH, in the presence of Cumxfxphen solution (10 µmol dm^{-3}), by steady-state fluorescence anisotropy, for the calculation of the transition temperature 2 (T_2).

The results obtained using DPH demonstrate marked differences between the pure FQs (with exception of spx) and metalloantibiotics. In the presence of pure cpx, erx, lvx and mxfx, there is a marked decreasing of the steady-state fluorescence anisotropy (r_s) values, especially for the higher temperature ranges (Figure 20). Analysing the transitions characteristic of this system, it is possible to observe that, in the presence of these four pure FQs, the T_1 decreases about 3˚C, the T_2 value increases (and seems to merge the common T_2 and T_3) and T_3 and T_4 are not detectable (with exception to mxfx profile which exhibits a T_3), as shown in Table 14.

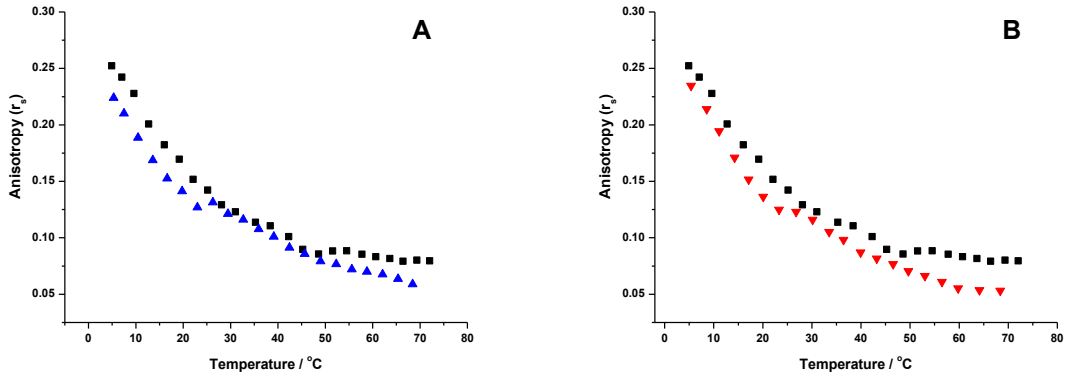

Figure 20 - Steady-state fluorescence anisotropy (r_s) of *E. coli* total lipid extract liposomes (prepared in HEPES 10 mmol dm^{-3}, pH 7.4, NaCl 0.1 mol dm^{-3}), obtained using DPH, in the absence (■) and presence of (A) cpx (▲) and (B) mxfx (▼) solutions (10 μmol dm^{-3}). A similar anisotropic profile was obtained in the presence of free cpx, erx and lvx solutions.

Table 14 - Transition temperatures (T / ˚C) of *E. coli* total extract liposomes (prepared in HEPES 10 mmol dm^{-3}, pH 7.4, NaCl 0.1 mol dm^{-3}), obtained using DPH, in the absence [31] and in the presence of pure FQs, by steady-state fluorescence anisotropy, through the fitting of Eq. (19) to the experimental data. The presented values are the mean of, at least, three independent experiments.

***E. coli* total lipid extract**	**Transition temperature / ˚C**			
	T_1	**T_2**	**T_3**	**T_4**
DPH [a] liposomes [31]	13.4 ± 0.6	28.5 ± 0.7	42.1 ± 1.2	62.5 ± 1.4
Presence of antibiotic				
cpx	≤ 10.8 ± 0.5	37.8 ± 0.4	___	___
erx	≤ 10.1 ± 0.1	34.2 ± 1.2	___	___
lvx	≤ 9.9 ± 0.9	35.0 ± 1.7	___	___
mxfx	≤ 11.3 ± 1.1	35.6 ± 1.0	50.5 ± 0.2	___

[a] DPH probe is located 7.8 Å from the centre of the bilayer in 1,2-diacyl-s*n*-glycero-3-phosphocholine (PC) vesicles.[186]

In contrast, the presence of free spx and all metalloantibiotics results in particular changes in the anisotropic profile. In these cases, although there were no drastic changes of the r_s values, the profiles lose the common outlines characteristic of the four T, showing a broadening of all the transitions and making impossible their calculation (Figure 21). These results point out for a deeper location of spx and all metalloantibiotics in the membrane bilayer, resulting in a marked change of the anisotropic profile of *E. coli* total liposome obtained with DPH, a consequence of the presence of the compounds.

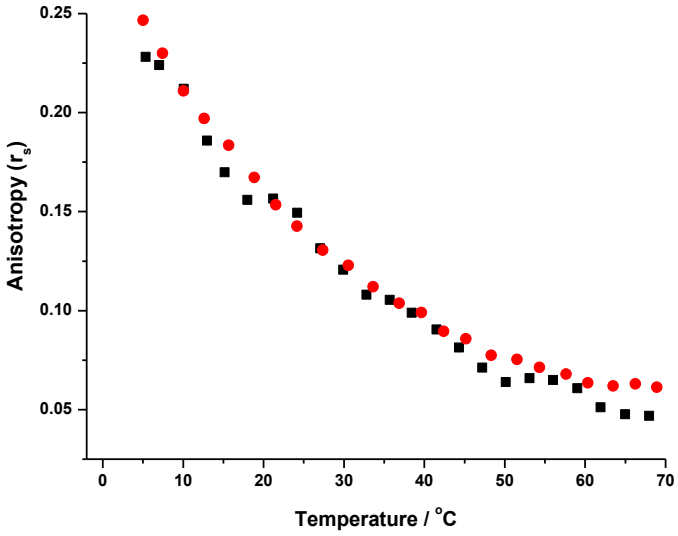

Figure 21 - Steady-state fluorescence anisotropy (r_s) of *E. coli* total lipid extract liposomes (prepared in HEPES 10 mmol dm^{-3}, pH 7.4, NaCl 0.1 mol dm^{-3}), obtained using DPH, in the absence (■) and presence (●) of Culvxphen solution (10 µmol dm^{-3}). A similar anisotropic profile was obtained in the presence of free spx, Cucpxphen, Cuerxphen, Cumxfxphen and Cuspxphen solutions.

The results obtained using TMA-DPH (Table 15 and Figure 22) show a decreasing of the r_s values resultant from the presence of the pure FQs till the T_2 (around 25 - 30˚C). In the presence of the pure erx, lvx and spx it is only possible to calculate T_1 and T_2. The first transition (T_1) is decreased (around 3˚C), while T_2 preserves its value (in the presence of spx) or seems to combine the T_2 and T_3 characteristics of this system (in the presence of erx and lvx). In turn, the presence of free cpx and mxfx allows the determination of three T, showing a decreased T_1 value, the conservation of the T_2 and a third transition (T_3), whose value mixture the T_3 and T_4 usually observed for *E. coli* total lipid extract liposomes. These results, together with the non-detection of

T_4, suggest that pure FQs are located near the CL enriched domains. Furthermore, the free antibiotics seem to have a random distribution in the membrane bilayer, with exception of spx that evidenced a deeper location due to the results previously obtained with DPH.

Table 15 - Transition temperatures (T / ˚C) of *E. coli* total extract liposomes (prepared in HEPES 10 mmol dm^{-3}, pH 7.4, NaCl 0.1 mol dm^{-3}), obtained using TMA-DPH, in the absence [31] and in the presence of free FQs and of metalloantibiotics, by steady-state fluorescence anisotropy, through the fitting of Eq. (19) to the experimental data. The presented values are the mean of, at least, three independent experiments.

***E. coli* total lipid extract**	**Transition temperature /** ˚C			
	T_1	**T_2**	**T_3**	**T_4**
TMA-DPH [a] liposomes [31]	11.1 ± 1.6	25.0 ± 1.0	43.2 ± 1.9	63.0 ± 0.8
Presence of compounds				
cpx	≤ 9.0 ± 1.3	27.5 ± 5.3	46.7 ± 3.7	___
erx	≤ 9.4 ± 0.4	37.1 ± 4.3	___	___
lvx	≤ 8.1 ± 0.7	34.8 ± 4.7	___	___
mxfx	≤ 7.8 ± 1.6	30.6 ± 4.8	53.7 ± 2.7	___
spx	≤ 7.4 ± 0.5	28.6 ± 0.7	___	___
Cuerxphen	≤ 9.0 ± 0.9	32.6 ± 1.9	53.4 ± 0.2	___
Cumxfxphen	≤ 7.8 ± 1.2	33.0 ± 1.3	52.8 ± 0.7	___
Cuspxphen	≤ 6.0 ± 0.3	36.3 ± 3.0	___	___

[a] TMA-DPH probe is located 10.9 Å from the centre of the bilayer in 1,2-diacyl-sn-glycero-3-phosphocholine (PC) vesicles.[186]

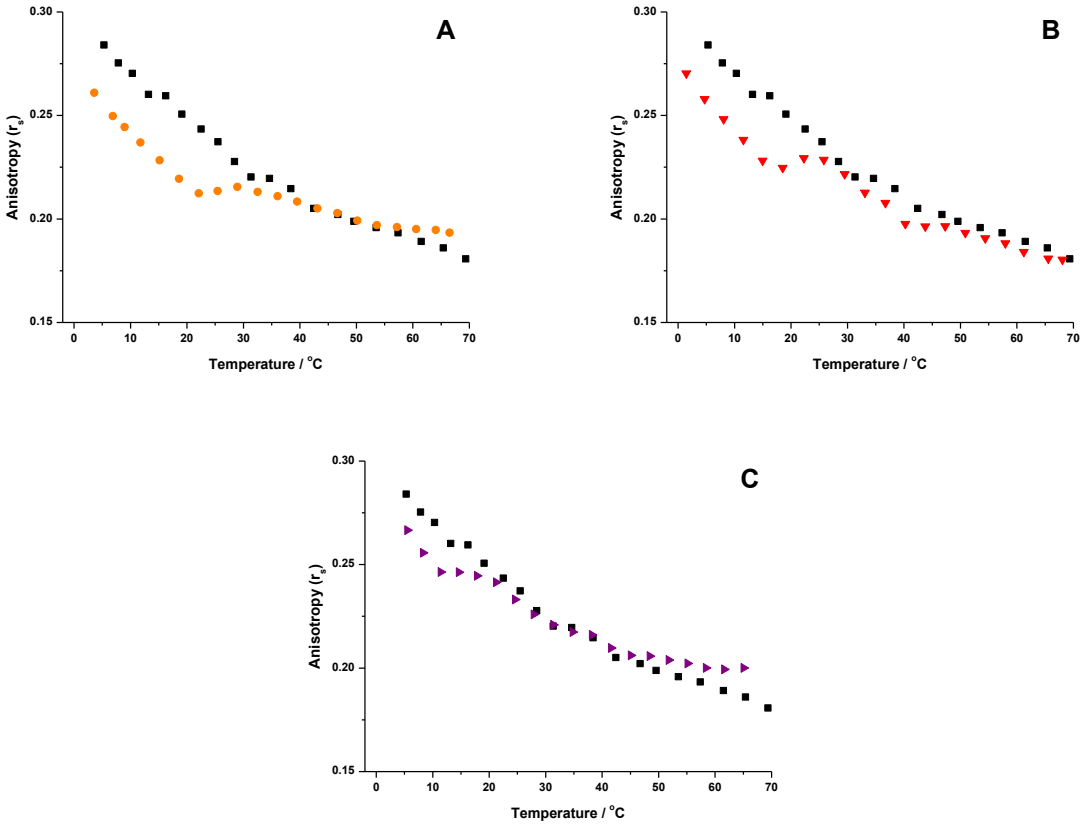

Figure 22 - Steady-state fluorescence anisotropy (r_s) of *E. coli* total lipid extract liposomes (prepared in HEPES 10 mmol dm^{-3}, pH 7.4, NaCl 0.1 mol dm^{-3}), obtained using TMA-DPH, in the absence (■) and presence of (A) erx (●), (B) mxfx (▼) and (C) spx (▶) solutions (10 μmol dm^{-3}). A similar anisotropic profile was obtained in the presence of free erx and lvx and of free cpx and mxfx solutions.

Concerning the presence of the metalloantibiotics, the results obtained using TMA-DPH (Table 15 and Figure 23) demonstrate a drastic change in the anisotropic profile in the presence of Cucpxphen and Culvxphen. Although the presence of these two metalloantibiotics did not change significantly the r_s values, it broadens all the profile, making impossible the calculation of any T. In these cases, the results are very analogous to the anisotropic profiles obtained using DPH in the presence of all metalloantibiotics. Together with the previous results, it is possible to state a random distribution of Cucpxphen and Culvxphen in the membrane bilayer, evidenced by the markedly alteration of the anisotropic profiles obtained with both DPH and TMA-DPH.

In contrary, the presence of Cuerxphen, Cumxfxphen and Cuspxphen reduces the r_s values (about 3˚C) till the T_2 (25 - 30˚C). Above this temperature, the r_s values are similar to those of the *E. coli* total lipid extract liposomes but the outlines characteristic of T_2, T_3 and T_4 are barely perceptible. For this reason, it is only possible to calculate three T in the presence of Cuerxphen and Cumxfxphen and two T in the presence of

Cuspxphen. The first T (T_1) value is meaningfully reduced (between 2 and 5˚C), while T_2 and T_3 are increased. These results along with the non-detection of T_4 point out for the presence of the compounds near the CL enriched domains.

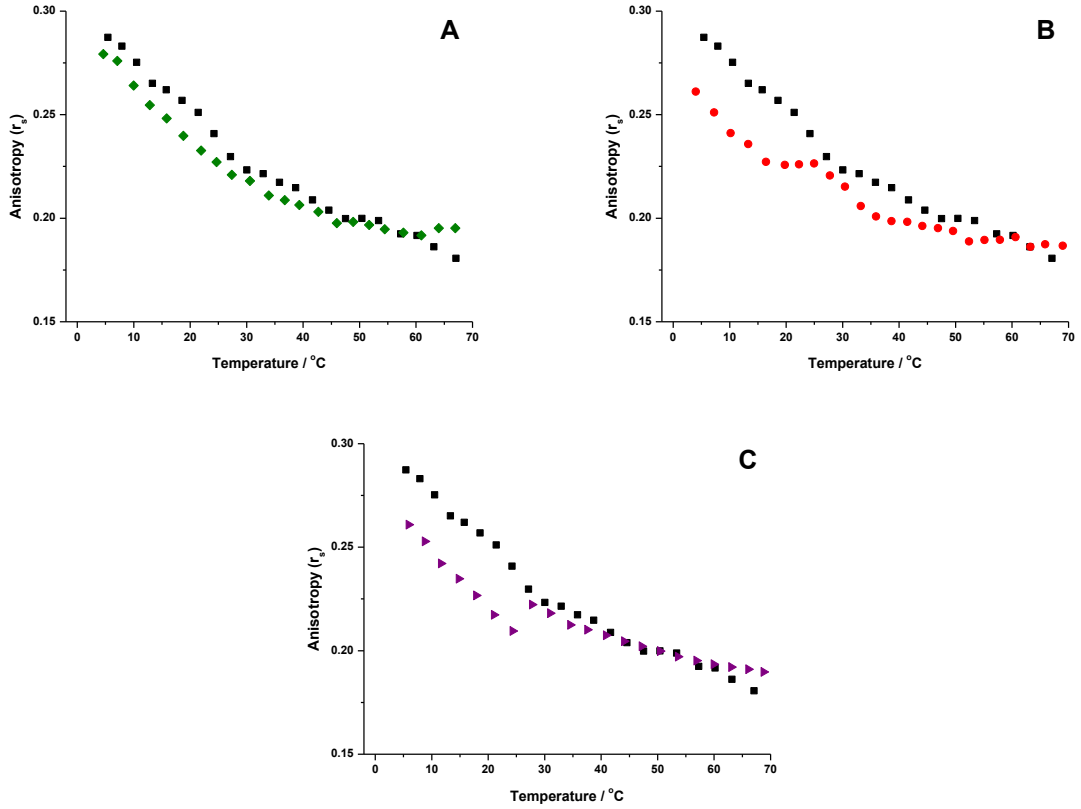

Figure 23 - Steady-state fluorescence anisotropy (r_s) of *E. coli* total lipid extract liposomes (prepared in HEPES 10 mmol dm^{-3}, pH 7.4, NaCl 0.1 mol dm^{-3}), obtained using TMA-DPH, in the absence (■) and presence of (A) Culvxphen (♦), (B) Cumxfxphen (▼) and (C) Cuspxphen (►) solutions (10 μmol dm^{-3}). A similar anisotropic profile was obtained in the presence of Cucpxphen and Culvxphen and of Cuerxphen and Cumxfxphen.

The accentuated decreasing of the T_1 value, observed in the presence of several compounds, with DPH and TMA-PH, is only indicative (reason for the use of the ≤ symbol) since it is not possible to measure r_s values below 0˚C in aqueous solutions.

When comparing the results obtained using DPH and TMA-DPH, the decreasing of the r_s values is more accentuated for higher temperatures in the DPH anisotropic profiles. These results are explained by the fact that the freedom of movement of the hydrophobic tails is greater than the one of the phospholipid headgroups (due to the interactions between the trimethylammonium group and the lipid atoms). For this

reason, the r_s range is more wide for DPH profiles (r_s values vary between 0.05 and 0.25) than for TMA profiles (r_s range between 0.17 and 0.30) of the same system.[187]

In conclusion, our results demonstrate that both free FQs and metalloantibiotics must be preferentially located near the CL enriched domains, since the presence of the compounds makes impossible the detection of the last two T (T_3 and T_4), reported for CL enriched domains.[31] Furthermore, all metalloantibiotics and the free spx are positioned in a deeper region of the membrane bilayer, as observed in the results obtained using DPH. This similar behaviour of the free spx with the metalloantibiotics was previously described and corroborates a hydrophobic pathway proposed for the translocation of this FQ.[70,73] Among all compounds, Cucpxphen and Culvxphen seem to have a random distribution in the membrane bilayer, as their presence is able to drastically change the anisotropic profile of both DPH and TMA-DPH. Taking together all results, it is possible to conclude that the free spx and all metalloantibiotics are positioned in a more embedded region of the membrane, which may favour a hydrophobic pathway for their influx.

3.1.2.3. Location studies with iodide

The location of the drugs can also be assessed through the fluorescence quenching by iodide. Due to its water-solubility, iodide quenches fluorophores in hydrophilic environments.[126,145,146] For this reason, the presence of this quencher is not sensed by the fluorophores embedded in the membrane but only affects the drugs present in aqueous environment. As this quenching occurs by a dynamic mechanism, time-resolved experiments were performed.[126]

This work comprised quenching studies of the four fluorescent metalloantibiotics (Cucpxphen, Cuerxphen, Culvxphen and Cumxfxphen) by iodide, in the absence and presence of increasing concentrations of *E. coli* total extract liposomes (250, 500 and 750 μmol dm^{-3}), in order to evaluate its location. The experiments were performed with an iodide solution concentration range from 0 to 0.5 mol dm^{-3}.

The studies started with the assessment of the fluorescence lifetimes of the metalloantibiotics in solution and in the membrane (Table 16), using Eq. (10) and Eq. (11). Although slightly smaller, the values obtained for the Cucpxphen complex are in agreement with the data available in the literature ($\tau_{Cucpxphen}$ = 1.7 ± 0.1 ns in solution and $\tau_{Cucpxphen}$ = 4.2 ns in the presence of 1 mmol dm^{-3} of *E. coli* total extract

liposomes).[123] For the rest of the metalloantibiotics there are no published values for comparison.

Table 16 - Fluorescence lifetimes of metalloantibiotics determined in HEPES (10 mmol dm^{-3}, pH 7.4, NaCl 0.1 mol dm^{-3}) and in the presence of *E. coli* total extract liposomes (500 μmol dm^{-3} prepared in HEPES). The presented values are the mean of, at least, three independent measures.

Compound	Medium	α_1	τ_1 (ns)	α_2	τ_2 (ns)	$\langle\tau\rangle$ (ns) [c]	$\bar{\tau}$ (ns) [d]
Cucpxphen	HEPES [a]		1.37			1.37 ± 0.03	1.37 ± 0.02
	Liposomes [b]	0.99	1.30	0.01	9.40	1.33 ± 0.01	1.55± 0.01
Cuerxphen	HEPES [a]		1.21			1.21 ± 0.02	1.21 ± 0.02
	Liposomes [b]	0.99	1.23	0.01	9.00	1.27 ± 0.01	1.69 ± 0.01
Culvxphen	HEPES [a]		5.93			5.93 ± 0.01	5.93 ± 0.01
	Liposomes [b]	0.81	6.43	0.19	1.60	5.54± 0.01	6.17± 0.01
Cumxfxphen	HEPES [a]		2.93			2.93 ± 0.05	2.93 ± 0.04
	Liposomes [b]	0.92	2.62	0.08	5.34	2.88 ± 0.09	3.07 ± 0.11

[a] HEPES (10 mmol dm^{-3}, pH 7.4, NaCl 0.1 mol dm^{-3}).

[b] *E. coli* total extract liposomes (500 μmol dm^{-3}) prepared in HEPES (10 mmol dm^{-3}, pH 7.4, NaCl 0.1 mol dm^{-3}).

[c] The amplitude-weighted lifetime, $\langle\tau\rangle$, calculated using Eq. (10).

[d] The average lifetime, $\bar{\tau}$, calculated using Eq. (11).

As observed for Cucpxphen, the lifetime of the majority of the metalloantibiotics has a reduced value in solution. In the presence of liposome suspension, the average lifetime of the complexes increases, as part of the molecules are embedded into the membrane bilayer, penetrating in an environment with reduced polarity.[131] For this reason, in the presence of liposome suspension, it is possible to calculate two different fluorescence lifetime components for each drug, one corresponding to the lifetime in solution (lifetime of lower value but higher pre-exponential factor) and the other to the lifetime in the membrane (lifetime of higher value but lower pre-exponential factor).

The results obtained for Culvxphen diverge from the rest of the metalloantibiotics. Although the average lifetime increases in the presence of liposome suspension, the second component (regarding the molecules partitioned in the membrane) exhibits a reduced value compared to the one obtained in solution. These values may be related to the structural differences of the lvx molecule, which has a methoxy group (at 8th position) connected to a ring-opened cyclopropyl group (at 1st position).

The average fluorescence lifetimes of the pure FQs were also determined in HEPES (Table 17), to further comparison to the respective metalloantibiotic.

Table 17 - Fluorescence lifetimes of FQs determined in HEPES (10 mmol dm^{-3}, pH 7.4, NaCl 0.1 mol dm^{-3}), with λ_{ex} = 290 nm and λ_{em} = maximum emission wavelength of each FQ (415 nm for cpx, 413 nm for erx and 460 nm for lvx and mxfx), calculated with Eq. (11). The presented values are the mean of, at least, three independent measures.

	Antibiotic			
	cpx	**erx**	**lvx**	**mxfx**
$\bar{\tau}$ **(ns)**	1.35 ± 0.01	1.24 ± 0.01	5.95 ± 0.05	2.97 ± 0.02

The results obtained show a similarity of the average lifetime values among each pure FQ and its respective metalloantibiotic. In addition, the value obtained for cpx is in agreement with the lifetime values previously reported in the literature (τ_{cpx} = 1.5 ± 0.1 ns in solution).[123,190]

The second part of the work included the determination of the Stern-Volmer constants (K_D) for the quenching of the metalloantibiotics by iodide, in the absence and presence of increasing concentrations of liposome suspension (Figure 24). The K_D values determined using Eq. (4) are presented in Table 18.

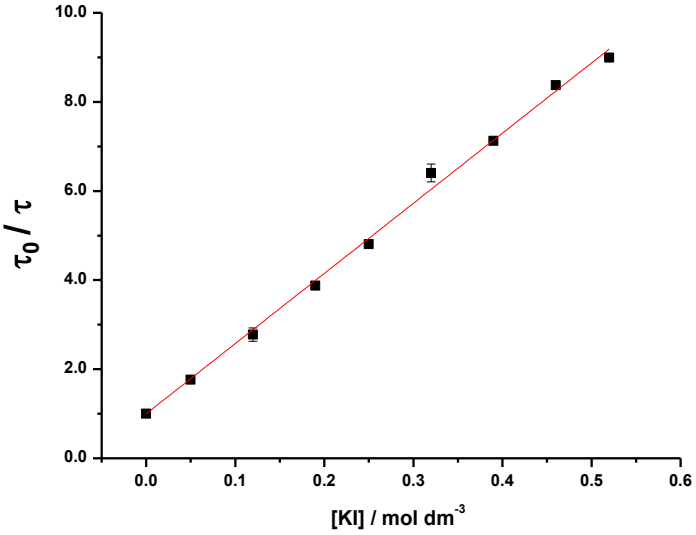

Figure 24 - Plot of τ_0/τ vs iodide concentration ([KI]), determined for Cumxfxphen in HEPES (10 mmol dm^{-3}, pH 7.4, NaCl 0.1 mol dm^{-3}). Eq. (4) was fitted to the experimental data. Data points are the mean of, at least, three independent experiments.

Table 18 - Values for the Stern-Volmer constants (K_D) determined for the quenching of the metalloantibiotics by iodide, in the absence (in HEPES 10 mmol dm^{-3}, pH 7.4, NaCl 0.1 mol dm^{-3}) and in the presence of increasing concentrations of *E. coli* total extract liposomes (250, 500 and 750 µmol dm^{-3} prepared in HEPES), by time-resolved fluorescence, through the fitting of Eq. (4) to the data. The presented values are the mean of, at least, three independent experiments.

Compound	K_D / mol^{-1} dm^3			
	[liposome] / µmol dm^{-3}			
	Absent	**250**	**500**	**750**
Cucpxphen	14.17 ± 0.27	13.63 ± 0.09	11.56 ± 0.17	10.83 ± 0.12
Cuerxphen	14.79 ± 0.17	12.92 ± 0.04	9.18 ± 0.22	8.44 ± 0.39
Culvxphen	41.32 ± 0.17	38.58 ± 0.20	38.58 ± 0.31	37.45 ± 0.41
Cumxfxphen	16.16 ± 0.12	15.77 ± 0.12	15.87 ± 0.12	15.93 ± 0.04

With the exception of Cumxfxphen, the K_D values clearly show a reduction of the quenching constants with increasing concentrations of the liposome suspension, which means that fewer molecules are accessible to iodide. These results prove that part of

the metalloantibiotic molecules are inserted into the membrane bilayer, being inaccessible to a quencher that only acts on fluorophores present in hydrophilic environments. Regarding the results of Cumxfxphen, the K_D values obtained in the absence and presence of liposome suspension are very similar. These results are explained by the similarity between the average lifetimes determined for this metalloantibiotic in solution and in the presence of liposome suspension (Table 16). Although the lifetime component referring to the molecules present in the membrane has an increased value, the difference is not pronounced enough to be detected in the average lifetime, which explains the similar K_D values.

Therefore, the location studies performed with iodide corroborate the results of the previous location studies, which demonstrate a higher partition of the metalloantibiotics within the membrane bilayer. Once again, the ability of the metalloantibiotics to penetrate the membrane supports the hydrophobic translocation route proposed for these compounds.

3.1.3. Drug-protein interaction

As described in the beginning of the chapter, the influx of FQs in *E. coli* has a porin-mediated pathway that is extremely associated to OmpF channel.[11,149] Therefore, the study of the drug-porin interaction is important to try to clarify the translocation of these drugs. On the other hand, since CuFQphen complexes have been studied as promising alternatives to pure FQs, possibly due to an alternative translocation pathway [70,71,103,123], it is also crucial to evaluate the role of this porin in the influx of the metalloantibiotics.

E. coli, considered a well-characterized Gram-negative bacterial model, has two main porins responsible for the translocation of FQs, OmpF and OmpC, two general β-barrel proteins.[16,23] Among these two porins, OmpF has proved to be the major channel implicated in the transport of several FQs in *E. coli*. For this reason, mutations in OmpF related to resistance bacterial mechanisms are widely described in literature.[22,23]

OmpF is a homotrimeric protein whose monomers comprise two Trp residues (Trp^{214} – W214 and Trp^{61} – W61) each. These aromatic residues are located in different regions of the channel: W214 is positioned close to the phospholipid headgroups, in the lipid-protein interface, in contrary to W61 that is found in the centre

of the channel (Figure 25).[22,149] Although with different location, both Trp are enclosed in hydrophobic environments, with hydrophobicity being highest surrounding W61.[149,151]

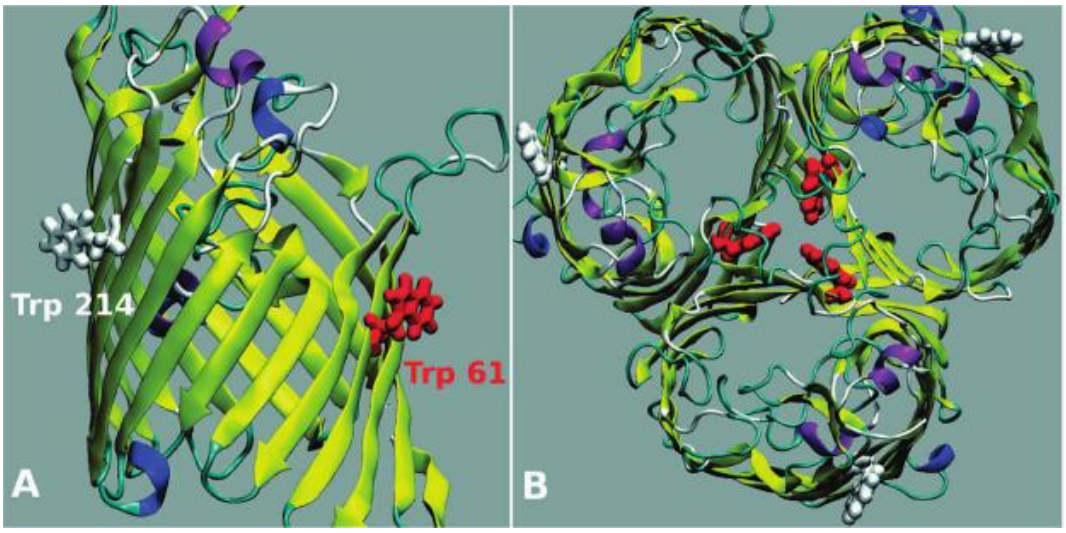

Figure 25 - The OmpF porin: a monomer side view (A) and the homotrimer top view (B). The two Trp residues of the monomers of the porin are represented in red (Trp^{61}) and in white (Trp^{214}), from [149].

The presence of fluorescent residues in the structure of OmpF confers intrinsic fluorescence to this porin, allowing the use of fluorescence spectroscopy techniques to characterize the interactions between the compounds and the porin. In addition, the use of specific quenchers that act in particular regions of the membrane also contributes to these studies and may give information about the location of the compounds. Acrylamide and iodide are two quenchers widely used in the studies performed with the OmpF channel, as it is known that acrylamide quenches W61 while iodide has preference for W214.[22,149,151] Acrylamide is a small polar molecule able to quench fluorophores independently of the polarity of the surrounding environment, with the exception of fluorophores embedded in the membrane. In contrary, iodide is a water-soluble molecule that acts in the hydrophobic regions of the membranes, having preference for residues located in the lipid-protein interface.[126]

Besides the Trp residues, the fluorescence of the proteins may also be due to other fluorescent amino acids as Tyr or Phe, especially if the absorption of the proteins occurs around 280 nm.[126] For this reason, the experiments were performed with an excitation wavelength of 290 nm, to assure that the observed fluorescence was only provided by the Trp residues.

The compound-OmpF association was studied through the evaluation of the fluorescence of the Trp residues of the protein in the absence and presence of

increasing amounts of FQs and metalloantibiotics (Figure 26), through steady-state fluorescence. The experiments were performed with *E. coli* total extract proteoliposomes of OmpF native protein (OmpF WT) and of two OmpF mutants (W61F and W214F), which lack one of each Trp, substituted by Phe. The studies encompassed cpx, erx, lvx, mxfx and their metalloantibiotics. The interaction of OmpF with spx and Cuspxphen is already characterized and available in the literature: K_{ass} spx = 3.74 ± 0.07 and K_{ass} Cuspxphen = 4.15 ± 0.06, determined in OmpF WT/*E. coli* total extract proteoliposomes by SPR [191]; K_{ass} spx = 4.47 ± 0.01 and K_{ass} Cuspxphen = 4.58 ± 0.01, determined by fluorescence spectroscopy [6].

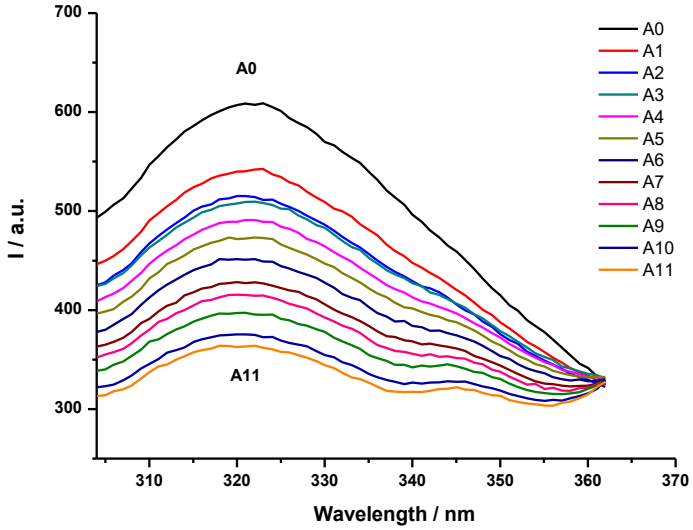

Figure 26 - Emission fluorescence spectra of OmpF WT/*E. coli* total lipid extract proteoliposomes (prepared in HEPES 10 mmol dm^{-3}, pH 7.4, NaCl 0.1 mol dm^{-3}), in the absence (A0) and presence (A1–11) of cpx solution (A1: 7.0 µmol dm^{-3}; A2: 8.1 µmol dm^{-3}; A3: 9.3 µmol dm^{-3}; A4: 10.4 µmol dm^{-3}; A5: 11.5 µmol dm^{-3}; A6: 12.6 µmol dm^{-3}; A7: 13.7 µmol dm^{-3}; A8: 14.8 µmol dm^{-3}; A9: 15.9 µmol dm^{-3}; A10: 16.9 µmol dm^{-3}; A11: 18.0 µmol dm^{-3}), with excitation wavelength of 290 nm. Each spectrum is a mean of five measurements.

As reported in previous studies, the experimental data revealed a static fluorescence quenching of the protein resultant from the presence of the antibiotics.[151,152] For this reason, and due to the linearity observed in the Stern-Volmer plot, the association constants (K_{ass}) were determined through the fitting of the Eq. (7) to the quenching data (Figure 27 and Table 19).

[6] Data not published.

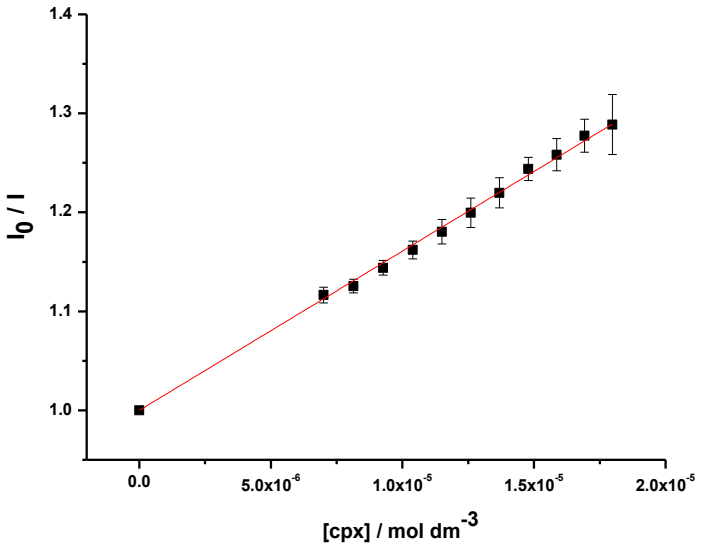

Figure 27 - Plot of I_0/ I vs cpx concentration ([cpx]), determined for OmpF WT/*E. coli* total extract proteoliposomes (prepared in HEPES 10 mmol dm^{-3}, pH 7.4, NaCl 0.1 mol dm^{-3}). Eq. (7) was fitted to the experimental data. Data points are the mean of, at least, three independent experiments.

Table 19 - Values for the association constants (K_{ass}) of OmpF-antibiotics, determined with OmpF(WT, W61F and W214F)/*E. coli* total extract proteoliposomes (prepared in HEPES 10 mmol dm^{-3}, pH 7.4, NaCl 0.1 mol dm^{-3}), by steady-state fluorescence, using Eq. (7). The presented values are the mean of, at least, three independent experiments.

Porin	Antibiotic	log K_{ass}	
		FQ	CuFQphen
OmpF WT	cpx	4.21 ± 0.01	4.56 ± 0.01
	erx	4.37 ± 0.01	4.40 ± 0.01
	lvx	4.53 ± 0.01	4.62 ± 0.01
	mxfx	4.63 ± 0.01	4.73 ± 0.01
OmpF W214F	cpx	4.24 ± 0.01	4.47 ± 0.02
OmpF W61F		4.13 ± 0.01	4.47 ± 0.01

The K_{ass} values obtained for the pure FQs have the same magnitude of the values reported in the literature (log K_{ass} cpx = 4.37 ± 0.05 and log K_{ass} mxfx = 4.65 ± 0.04, determined with the porin in oPOE by fluorescence spectroscopy [152]; log K_{ass} cpx = 3.90 ± 0.10 and log K_{ass} spx = 3.74 ± 0.07, determined in OmpF WT/*E. coli* total extract proteoliposomes by SPR [191]). In turn, the K_{ass} values determined for the metalloantibiotics are very similar to the ones of the free FQs, being even slightly higher. This same tendency was described in studies of the interaction of OmpF WT/*E. coli* total extract proteoliposomes with two metalloantibiotics ($\log K_{ass}$ cpx = 3.90 ± 0.10 and log K_{ass} Cucpxphen = 3.96 ± 0.08, and log K_{ass} spx = 3.74 ± 0.07 and log K_{ass} Cuspxphen = 4.15 ± 0.06, determined by SPR [191]; log K_{ass} spx = 4.47 ± 0.01 and log K_{ass} Cuspxphen = 4.58 ± 0.01, determined by fluorescence spectroscopy [7]).

The similarity of the values obtained for the free FQs and metalloantibiotics may be explained by the fact that fluorescence spectroscopy, as SPR, does not allow to infer about the specific region of the binding. Therefore, it is not possible to conclude if the association occurs through the amino acid residues of the constriction zone or via other residues located far from that region. Besides that, a stronger association does not implicate a greater ability to cross the channel, as the metalloantibiotics exhibit faster association and dissociation, compared to the free FQs.[191]

The work proceeded with the study of the interaction of OmpF mutants (W61F and W214F) with the compounds, to try to infer a possible location for the binding site of the compounds. Cpx and Cucpxphen were chosen for the first experiments since cpx is one of the vastly used FQs in the clinical therapy. The K_{ass} values determined are presented in Table 19.

The association of the pure cpx with the two Trp residues revealed differences. The K_{ass} determined for cpx with OmpF W214F has a greater value (log K_{ass} cpx = 4.24 ± 0.01) than the one obtained with the OmpF W61F (log K_{ass} cpx = 4.13 ± 0.01). As the mutant W214F reveals an interaction of the drug near W61 (located in the centre of the bilayer) and the mutant W61F discloses the interaction near W214 (positioned at the interface of the bilayer/protein), these results show that the interaction of cpx is stronger in the region of the centre of the channel. Previous studies, performed with erx and mxfx, also described a preferential interaction of the drugs near W61, proposing a location of the free FQs near the centre of the channel.[22,149]

[7] Data not published.

In contrast, the K_{ass} values determined with the OmpF mutant (W61F and W214F) proteoliposomes exhibit comparable values for the association of the Cucpxphen with both Trp residues. These results suggest a similar interaction of the metalloantibiotic with the residues located near the centre of the channel (W214F) or in the bilayer/protein interface (W61F).

The experimental data revealed differences in the fluorescence intensity and in the wavelength of maximum intensity of the proteoliposomes (320 nm for WT, 318 nm for W61F and 312 nm for W214F). The lower the emission wavelength of the Trp, the higher the hydrophobicity of the surrounding environment.[126] Besides the lower wavelength of maximum intensity, the mutant W214F exhibited the higher fluorescence intensity, indicative of a greater hydrophobicity of the surrounding environment of W61, as previously stated by others authors.[149,151]

The work proceeded with the study of the quenching of OmpF by iodide and acrylamide, two quenchers that provide information about different regions of the protein.

3.1.3.1. Fluorescence quenching of OmpF by iodide and acrylamide

Quenching studies of proteins are widely performed with iodide and acrylamide, as these two molecules are able to quench Trp residues. Due to their chemical differences, iodide and acrylamide act in distinct regions of the membrane.[126] Iodide is negatively charged, providing information about the Trp residues located in more hydrophilic environments, in the protein/membrane interface (W214), while the polar behaviour and the neutral charge of the acrylamide favour the quenching of the Trp residues positioned in environments with higher hydrophobicity, near the centre of the pore (W61).[22,126,149] Consequently, studies performed with these quenchers may provide information about the location of drugs according to the accessibility of the Trp residues to the quenchers.[126]

This part of the work comprised quenching studies of OmpF (WT, W61F and W214F)/*E. coli* total extract proteoliposomes by iodide and acrylamide, in the absence and presence of cpx and Cucpxphen.

The experimental data exhibited linear Stern-Volmer plots (Figure 28), with the exception of the quenching of OmpF WT/*E. coli* total extract proteoliposomes by iodide

in the presence of the metalloantibiotic (Figure 29) and of the quenching of the cpx solution by iodide (Figure 30). The linear Stern-Volmer plots suggest that all Trp residues have similar accessibility to the quencher.

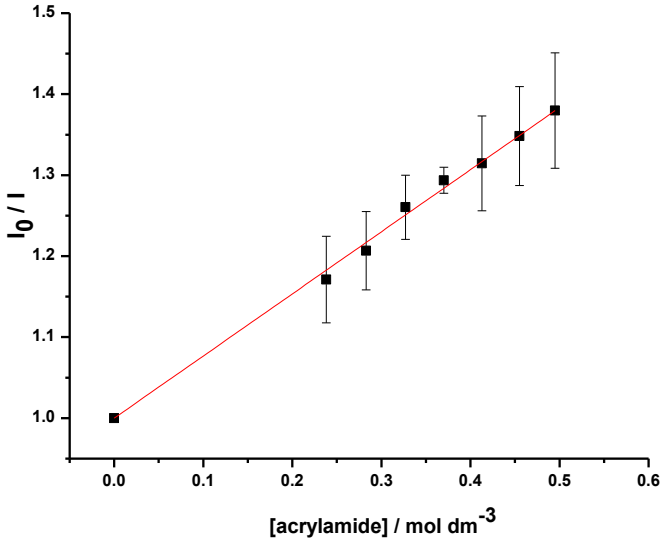

Figure 28 - Plot of I_0/I vs acrylamide concentration ([acrylamide]), determined for the quenching of OmpF WT/*E. coli* total lipid extract liposomes (prepared in HEPES 10 mmol dm^{-3}, pH 7.4, NaCl 0.1 mol dm^{-3}) by acrylamide, with excitation and emission wavelengths of 290 and 320 nm, respectively. Eq. (2) was fitted to the experimental data. Data points are the mean of, at least, three independent experiments.

The quenching constants, determined by the fitting of the Eq. (2), Eq. (22) and Eq. (26) to the experimental data, are summarized in Table 20.

The results obtained for the quenching of the proteoliposomes by acrylamide show a decrease of the Stern-Volmer constant (K_D) determined in W214F proteoliposomes in the presence of cpx. This result suggests that the presence of the drug shields the W61 from the action of the quencher, corroborating the previous results that pointed out for the location of cpx near the centre of the porin. In turn, the presence of cpx doesn't affect the quenching of the WT and W61F proteoliposomes by acrylamide, as the K_D values determined in the absence and presence of cpx are comparable. The quenching observed for the W61F by acrylamide suggests that W214 is located in a more hydrophobic environment, as acrylamide was able to quench it. For this reason, the results obtained with WT proteoliposomes may reveal the quenching of both trp by acrylamide. Taking together, these results suggest that cpx should not be found near W214. In addition, the K_D obtained for the quenching of W214F proteoliposomes by acrylamide increases in the presence of Cucpxphen. This result is indicative of the

enhancement of the exposure of W61 to the quencher, probably due to conformational changes resultant from the binding of the metalloantibiotic in other regions of the protein.

Table 20 - Values for the Stern-Volmer constants (K_D and K_a) determined for the quenching of OmpF (WT, W61F and W214F)/*E. coli* total extract proteoliposomes (prepared in HEPES 10 mmol dm^{-3}, pH 7.4, NaCl 0.1 mol dm^{-3}) by iodide and acrylamide, in the absence and in the presence of cpx and Cucpxphen solutions, by steady-state fluorescence, using Eq. (2), Eq. (22) and Eq. (26). The presented values are the mean of, at least, three independent experiments.

Porin	Compound	K_D / mol^{-1} dm^3			
		Compound absent		Compound present	
		Acrylamide	Iodide	Acrylamide	Iodide
OmpF WT	cpx	0.77 ± 0.01	N.d.	0.77 ± 0.01	N.d.
	Cucpxphen		N.d.	N.d.	K_a = 1.38 ± 0.01; fa = 0.10 [a]
OmpF W214F	cpx	0.49 ± 0.01	N.d.	0.32 ± 0.01	N.d.
	Cucpxphen		N.d.	1.43 ± 0.02	N.d.
OmpF W61F	cpx	0.54 ± 0.02	N.d.	0.57 ± 0.01	N.d.
	Cucpxphen		N.d.	N.d.	N.d.

Quenching of the compounds (porin absent)		
Compound	**Acrylamide**	**Iodide**
cpx	N.d.	K_a = 6.00 ± 0.04 [b]
Cucpxphen	N.d.	8.62 ± 0.10

[a] K_a obtained by the fitting of the Eq. (26) to the experimental data.

[b] K_a obtained by the fitting of the Eq. (22) to the experimental data .

The quenching of the proteoliposomes by iodide was only observed in WT proteoliposomes when in the presence of Cucpxphen. In this case, the Stern-Volmer plot exhibited a negative deviation from the linearity characteristic of the general Stern-Volmer plots (Figure 29). The negative deviation is indicative of the existence of two populations of residues with different accessibility to the quencher: one accessible and other not accessible. The Trp residues accessible to iodide must be turned towards the surface of the protein, to the surrounding medium.[126] Therefore, this result suggests the existence of two different populations of W214 residues, one still shielded from iodide (around 90% of the residues) and the other (about 10%) exposed to the quencher. Moreover, the fact that no quenching was observed in WT proteoliposomes (in the absence of the compounds) corroborates the idea that W214 is more embedded in the membrane than what was expected, not allowing the quenching by iodide. Taking together, these results suggest that the presence of Cucpxphen induces modifications in the conformation of the protein, increasing the exposure of W214 to iodide.

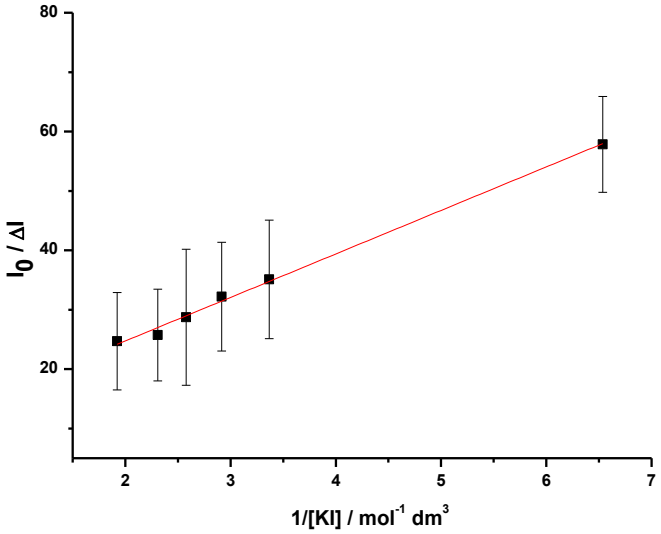

Figure 29 - Plot of $I_0/\Delta I$ vs the inverse of the iodide concentration (1/[KI]), determined for the quenching of OmpF WT/*E. coli* total lipid extract liposomes (prepared in HEPES 10 mmol dm^{-3}, pH 7.4, NaCl 0.1 mol dm^{-3}) by iodide, in the presence of Cucpxphen solution, with excitation and emission wavelengths of 290 and 320 nm, respectively. Eq. (26) was fitted to the experimental data. Data points are the mean of, at least, three independent experiments.

The quenching of cpx and Cucpxphen solutions by iodide and acrylamide was also studied. The quenching of the solutions was only observed by iodide, which is in agreement to what was expected as this quencher acts in hydrophilic environments. In

the case of the quenching of cpx, the Stern-Volmer plot exhibited an upward curvature concave toward the y-axis (Figure 30). This deviation to the linearity of the Stern-Volmer plot is indicative of a process that encompass both dynamic and static quenching or of an apparent static quenching, known as the sphere of action model. This model proposes that the quencher is in the neighbouring of the fluorophore at the moment of the excitation, there being a virtual "sphere" within which there is a high probability of contact between the quencher and the fluorophore. As the quencher concentration increases, a greater contact is expected.[126]

The magnitude of the obtained values supports a dynamic process for the quenching by iodide.

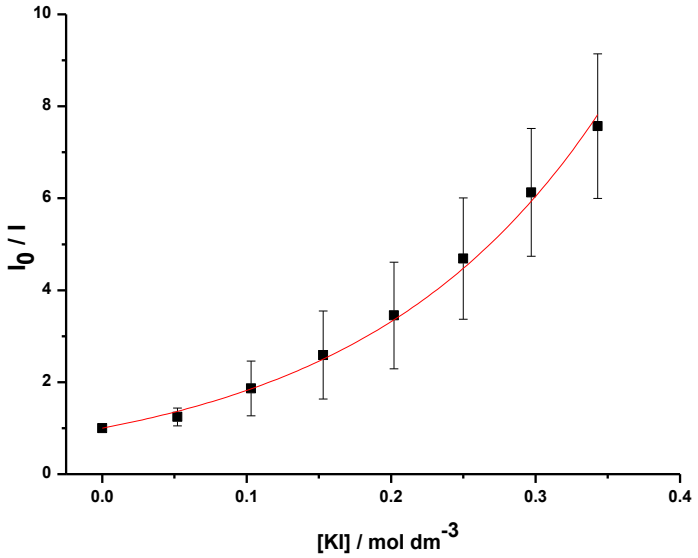

Figure 30 - Plot of I_0/I vs the iodide concentration ([KI]), determined for the quenching of cpx solution (prepared in HEPES 10 mmol dm^{-3}, pH 7.4, NaCl 0.1 mol dm^{-3}) by iodide, with excitation and emission wavelengths of 290 and 415 nm, respectively. Eq. (22) was fitted to the experimental data. Data points are the mean of, at least, three independent experiments.

In summary, it is possible to conclude that cpx has a preferential interaction with W61, located at the centre of the protein channel, which supports a hydrophilic pathway (OmpF dependent) as previously proposed for the influx of cpx. In turn, it was not possible to infer about the location of Cucpxphen, as it seems to have no preference for the interaction with either Trp. However, the presence of the metalloantibiotic increased the exposure of both Trp to the quenchers, suggesting that

Cucpxphen induced conformational changes in the channel. These results may support a hydrophobic pathway (independent of the porin or using the lipid-protein interface) for the translocation of Cucpxphen.

Everything considered, more experiments are required to better clarify the influx and infer about the role of the porins (and the residues involved in the association) of these compounds with the OmpF protein. The use of OmpF mutants with mutations in the amino acid residues of the constriction zone should be a good strategy. However, the procedure of the expression and purification of the OmpF mutants is a complex process that results in reduced amounts of the purified proteins, which is a limiting factor.

3.2. Microbiological assays

AMR became one of the major public health concerns worldwide.[41,42,44] Several deaths, resulting from such ability of microorganisms to bypass the action of numerous antimicrobial agents, are reported every year.[43-45]

FQs are one of the antibiotic families extensively used in the clinical practise.[64,65] These antimicrobial agents are bactericidal antibiotics that act directly on DNA gyrase or topoisomerase IV, inhibiting the bacterial replication.[65,68] However, as happens for most antibiotics, bacterial resistance mechanisms to FQs are commonly reported. The reduction of the intracellular concentration of the drug (via efflux pumps or through the reduced influx), chromosomal mutations or plasmid-acquired resistance genes that confer modifications of the topoisomerases are the main bacterial resistance mechanisms described against FQs.[76,78]

One of the strategies to try to circumvent the mechanisms of resistance to FQs is based on the complexation of these antibiotics with copper(II) and phen, giving rise to ternary complexes known as metalloantibiotics.[70,71,103,123-125] Previous studies performed with these metalloantibiotics evidenced antibacterial activity as well as high stability under physiological conditions.[70,71,103] Additionally, the structural differences between pure FQs and metalloantibiotics anticipate dissimilar influx mechanisms, which could be advantageous to bypass some bacterial resistance mechanisms. Although it is necessary to further characterize these ternary complexes, the mentioned findings propose that metalloantibiotics could be an alternative to pure FQs.[70,121]

This section aimed to i) infer about the role of the porins, especially OmpF and OmpC, in the translocation of FQs and metalloantibiotics in *E. coli* and to ii) determine the effectiveness of the metalloantibiotics against several MDR clinical isolates. The first part of the work encompassed the assessment of the antimicrobial activity of the compounds in susceptible *E. coli* strains and their derived porin-deficient mutants. The obtained results were complemented with some disk diffusion tests. In turn, the second part consisted in the antimicrobial susceptibility testing performed against a panel of MDR clinical isolates of Gram-negative and Gram-positive pathogens.

The studies comprised five metalloantibiotics and respective pure FQs (cpx, erx, lvx, mxfx and spx), phen, Cu(II)/phen (1:1) and $Cu(NO_3)_2.3H_2O$ salt, as these components integrate the metalloantibiotics.

The antimicrobial activity of the compounds was evaluated through the assessment of the MIC, the lowest concentration of the antimicrobial agent that completely inhibits the bacterial growth, detected by naked eye.[192]

Commonly, the MIC is presented in terms of ɣ (μg mL^{-1}).[159,169] However, the high difference between the molecular weights of pure FQs and metalloantibiotics ($MW_{Metalloantibiotics} \approx 2x\ MW_{FQs}$) may be misleading in the interpretation of the MIC results (Table 21). For this reason, all MIC results are presented in μg mL^{-1} and in μmol dm^{-3}.

Table 21 - Molecular weight of cpx, erx, lvx, mxfx, spx and respective CuFQphen complexes, expressed in g mol^{-1}. The molecular weights of metalloantibiotics were calculated based on the crystallographic data previously available.[70]

Antibiotic	Molecular weight (g mol^{-1})	
	FQ	CuFQphen
cpx	331.34	709.16 [a]
erx	359.39	674.05 [b]
lvx	361.37	721.18 [c]
mxfx	437.89	788.26 [d]
spx	392.4	770.22 [e]

[a] $[Cu(cpx)(phen)](NO_3).4H_2O$; [b] $[Cu(erx)(phen)]Cl_2$; [c] $[Cu(lvx)(phen)(H_2O)]NO_3.2H_2O$; [d] $[Cu(mxfx)(phen)]NO_3.4.5H_2O$; [e] $[Cu(spx)(phen)H_2O]NO_3.3H_2O$

The antimicrobial susceptibility testing was performed using four reference strains: *E. coli* ATCC 25922, *P. aeruginosa* ATCC 27853 (Gram-negatives), *S. aureus* ATCC 25923 and ATCC 29213 (Gram-positives). The MIC values of all compounds against the four reference strains are presented in Table 22.

The results obtained for the pure FQs are in agreement with the MIC values recommended by the CLSI, with the exception of cpx against *P. aeruginosa* ATCC 27853.[169] The MIC value of cpx against *P. aeruginosa* ATCC 27853 was 0.06 μg mL^{-1}, a lower value compared to the range recommended in the guidelines (0.25 - 1 μg mL^{-1}). This result could be due to the use of the medium MHB, whose cation content was absent. The CLSI guidelines stated that the cation content of the broth used in the antimicrobial susceptibility testing may affect the MIC results. Moreover, the guidelines suggest the supplementation of the broth with cations in some cases where lower MIC values were observed in *P. aeruginosa* ATCC 27853.[157]

Table 22 - MIC values of several FQs, CuFQphen complexes, phen, Cu(II)/phen (1:1) and $Cu(NO_3)_2.3H_2O$ salt aqainst control strains of *E. coli (E. coli* ATCC 25922*), P. aeruginosa (P. aeruginosa* ATCC 27853*)* and *S. aureus (S. aureus* ATCC 25923 *and S. aureus* ATCC 29213), expressed in μg mL^{-1} and μmol dm^{-3} for comparative purposes. The values presented were obtained from at least three independent experiments.

Antibiotic	**MIC value**							
	***E. coli* ATCC 25922**		***P. aeruginosa* ATCC 27853**		***S. aureus* ATCC 25923**		***S. aureus* ATCC 29213**	
	μg mL^{-1}	**μmol dm^{-3}**	**μg mL^{-1}**	**μmol dm^{-3}**	**μg mL^{-1}**	**μmol dm^{-3}**	**μg mL^{-1}**	**μmol dm^{-3}**
cpx	0.004	0.012	0.06	0.18	0.12 – 0.25	0.36 – 0.75	0.25 – 0.5	0.75 – 1.51
erx	0.008	0.022	1	2.78	0.12 – 0.25	0.33 – 0.70	0.12	0.33
lvx	0.008	0.022	0.5	1.38	0.12 – 0.25	0.33 – 0.69	0.12	0.33
mxfx	0.008	0.018	0.5 - 1	1.14 – 2.28	0.03 – 0.06	0.07 – 0.14	0.06	0.14
spx	0.004	0.010	0.25 – 0.5	0.64 – 1.27	0.03 – 0.06	0.08 – 0.15	0.06	0.15
Cucpxphen	0.008	0.011	0.12 – 0.25	0.17 – 0.35	0.25 – 0.5	0.35 – 0.71	1	1.41
Cuerxphen	0.015	0.022	2	2.97	0.25 – 0.5	0.37 – 0.74	0.12 – 0.25	0.18 – 0.37
Culvxphen	0.015 – 0.03	0.021 – 0.042	1	1.39	0.25 – 0.5	0.35 – 0.69	0.25	0.35
Cumxfxphen	0.015 – 0.03	0.019 – 0.038	2	2.54	0.06 – 0.12	0.08 – 0.15	0.06 – 0.12	0.08 – 0.15
Cuspxphen	0.004 – 0.008	0.005 – 0.010	0.5	0.65	0.25	0.32	0.06 – 0.12	0.08 – 0.16
phen	8	40.4	128	645.7	16 - 32	80.7 – 161.4	32	161.4
Cu(II)/phen (1:1)	32	72.8	≥ 512	≥ 1164.1	32	72.8	64	145.5
$Cu(NO_3)_2.3H_2O$	≥ 1024	≥ 4238.2	≥ 1024	≥ 4238.2	≥ 1024	≥ 4238.2	≥ 880	≥ 3642.2

On the other hand, the fact that the experimental value is lower than the recommended ones means more susceptibility of the strain to the compound being tested, excluding the hypothesis of bacterial resistance development. Besides that, Chalkley and Koornhof have also published a value of 0.016 μg mL^{-1} for cpx against this control strain, a value even lower than the one obtained in our work.[193]

The MIC values determined for metalloantibiotics were always comparable to the ones of the FQs within each reference strain. These results are in agreement with the similarity previously observed in *E. coli* ATCC 25922 by Feio *et al*.[70]

In turn, the MIC values determined for phen, Cu(II)/phen (1:1) and copper solution were always greater compared to the MIC values of FQs and metalloantibiotics (more than 10^3-fold higher), which means that in the event of metalloantibiotic dissociation, the antimicrobial activity observed would not arise from these substituents. The higher MIC value of the copper solution compared to the ones of FQs and metalloantibiotics had been previously observed by Feio *et al*.[70]

3.2.1. Antimicrobial susceptibility testing using porin-deficient *E. coli* mutants

As previously mentioned, one of the reasons that could make metalloantibiotics promising alternatives to pure FQs is their different translocation pathway. Generally, pure FQs need porins to penetrate into the bacterial cell, while little is known on the influx of the metalloantibiotics. Therefore, in order to infer about the role of the porins in the influx of the metalloantibiotics, some microbiological studies were performed using parental *E. coli* strains and their porin-deficient mutant derivatives (Tables 24 - 26). Three parental strains were used: *E. coli* JF568 (derived from K12), *E. coli* W3110 and *E. coli* B_E BL21 (DE3).

As previously reported, OmpF and OmpC are the main proteins involved in the translocation of the FQs.[16,18,19] Thus, mutants devoid of OmpF and OmpC or both porins were used: *E. coli* JF701 (devoid of OmpC); *E. coli* JF703 (devoid of OmpF); *E. coli* W3110 ΔC (devoid of OmpC); *E. coli* W3110 ΔF (devoid of OmpF); *E. coli* W3110 ΔFΔC (devoid of OmpC and OmpF); *E. coli* BL21 (DE3) omp2 (devoid of OmpF); and *E. coli* BL21 (DE3) omp8 (devoid of OmpC, OmpA and OmpF).[19,194] The description of the relevant genotype of each *E. coli* strain is summarized in Table 23.

Table 23 - Description of the *E. coli* strains used in this study, from [19,194].

Strain	Relevant genotype described	Reference
E. coli K-12		
JF568	*F⁻, lacY29, proC24, tsx-63, purE41, λ⁻ aroA357, his-53, rpsL97(strR), xyl-14, metB65, cycA1, ilv-277, cycB2*	[19]
JF701	JF568, *ompC*264	[19]
JF703	JF568, *aro*A^{+}, *ompF*254	[19]
W3110	*F⁻ λ⁻* IN(*rrnD-rrnE*)1 *rph-1*	[19]
W3110 ΔC	W3110, *ΔompC*	
W3110 ΔF	W3110, *ΔompF*	
W3110 ΔF ΔC	W3110, *ΔompF ΔompC*	[19]
E. coli B_E		
BL21 (DE3)	F, *ompT hsdS$_B$* (r_B^- m_B^-) *gal dcm* (DE3)	[194]
BL21 (DE3) omp2	BL21(DE3), *ompF*::Tn5	[194]
BL21 (DE3) omp8	BL21(DE3), *ΔlamB ompF*::Tn5 *ΔompA Δ ompC*	[194]

The MICs of antibiotics or metalloantibiotics determined against the parental strains and respective mutants of *E. coli* JF568 (Table 24) and *E. coli* W3110 (Table 25) were comparable, only differing from one well in some cases. Therefore, the use of these parental strains and respective porin-mutants did not allow to anticipate a different influx route between antibiotics and the respective metalloantibiotics.

Table 24 - MIC values of several FQs, CuFQphen complexes, phen, Cu(II)/phen (1:1) and $Cu(NO_3)_2.3H_2O$ salt against *E. coli* strains (JF568, JF701 and JF703), expressed in μg mL^{-1} and μmol dm^{-3} for comparative purposes. The values presented were obtained from at least three independent experiments.

Antibiotic	MIC value					
	JF568		JF701 (Δ OmpC)		JF703 (Δ OmpF)	
	μg mL^{-1}	μmol dm^{-3}	μg mL^{-1}	μmol dm^{-3}	μg mL^{-1}	μmol dm^{-3}
cpx	0.016	0.05	0.008 – 0.016	0.02 – 0.05	0.016 – 0.03	0.05 – 0.09
erx	0.016 – 0.03	0.04 – 0.08	0.016 – 0.03	0.04 – 0.08	0.03	0.08
lvx	0.03	0.08	0.03	0.08	0.03 – 0.06	0.08 – 0.17
mxfx	0.06	0.14	0.06	0.14	0.06	0.14
spx	0.016 – 0.03	0.04 – 0.08	0.016 – 0.03	0.04 – 0.08	0.016 – 0.03	0.04 – 0.08
Cucpxphen	0.03	0.04	0.016 – 0.03	0.02 - 0.04	0.03	0.04
Cuerxphen	0.06	0.09	0.06	0.09	0.12	0.18
Culvxphen	0.06	0.08	0.06	0.08	0.06	0.08
Cumxfxphen	0.12	0.15	0.12 – 0.25	0.15 – 0.32	0.12	0.15
Cuspxphen	0.03	0.04	0.06	0.08	0.03	0.04
phen	8	40.4	8 - 16	40.4 – 80.7	16	80.7
Cu(II)/phen (1:1)	64	145.5	64	145.5	32 - 64	72.8 – 145.5
$Cu(NO_3)_2.3H_2O$	1024	4238.2	1024	4238.2	1024	4238.2

Table 25 - MIC values of several FQs, CuFQphen complexes, phen, Cu(II)/phen (1:1) and $Cu(NO_3)_2.3H_2O$ salt against *E. coli* strains (W3110, W3110 ΔC, W3110 ΔF and W3110 ΔFΔC), expressed in μg mL^{-1} and μmol dm^{-3} for comparative purposes. The values presented were obtained from at least three independent experiments.

Antibiotic	MIC value							
	W3110		W3110 ΔC (Δ OmpC)		W3110 ΔF (Δ OmpF)		W3110 ΔFΔC (Δ OmpF and OmpC)	
	μg mL^{-1}	μmol dm^{-3}	μg mL^{-1}	μmol dm^{-3}	μg mL^{-1}	μmol dm^{-3}	μg mL^{-1}	μmol dm^{-3}
Cpx	0.016	0.05	0.016	0.05	0.03	0.09	0.03	0.09
Erx	0.03	0.08	0.03	0.08	0.06	0.17	0.03	0.08
Lvx	0.03	0.08	0.03	0.08	0.06	0.17	0.03	0.08
mxfx	0.06	0.14	0.06	0.14	0.06	0.14	0.03	0.07
Spx	0.016	0.04	0.016	0.04	0.03	0.08	0.016	0.04
Cucpxphen	0.04	0.04	0.04	0.04	0.03	0.04	0.06	0.08
Cuerxphen	0.09	0.08	0.09	0.08	0.12	0.18	0.06	0.09
Culvxphen	0.08	0.07	0.08	0.07	0.12	0.17	0.06	0.08
Cumxfxphen	0.15	0.14	0.15	0.14	0.12	0.15	0.06	0.08
Cuspxphen	0.04	0.04	0.04	0.04	0.03	0.04	0.016	0.02
Phen	16	80.7	16	80.7	16	80.7	16	80.7
Cu(II)/phen (1:1)	64	145.5	64	145.5	64	145.5	64	145.5
$Cu(NO_3)_2.3H_2O$	124	4238.2	1024	4238.2	1024	4238.2	1024	4238.2

Concerning the *E. coli* JF568 and JF701 (Δ OmpC), the MIC values obtained are in agreement with the values reported by Feio *et al.*, with exception of the Cuspxphen against *E. coli* JF568, whose MIC value was lower (~ 3-fold).[70] In turn, the results obtained in *E. coli* JF703 (Δ OmpF) were comparable or lower (3 to 4-fold in some cases) than the ones stated in literature.[70] The decreasing of the MIC value leads us to anticipate that this mutant may have suffered genotypic changes, possibly a reverse mutation on the *ompF* gene. This strain, JF703, has a mutation called *ompF*254, which could have been reverted throughout time. The ability of mutant genes to revert suggests that mutation, at least in some cases, is not a permanent, irreversible process. To prove true this supposition, it would be advisable to do a quantitative PCR, for instance, directed to the detection and quantification of the *ompF* gene. This could not be done within this thesis work, but it is an aim worth to be further pursued. On the other hand, as described by Feio *et al.*[70], the expression of alternative porins with similar functionality to the mutated ones may also occur.

Regarding the *E. coli* W3110 strain and respective mutants, there are no published MIC values in literature to compare. The analysis of the obtained results does not allow to understand if porins are a requirement for the translocation of the compounds, as previously pointed out by Feio *et al.*[70]

Nonetheless, the MIC values determined against some strains of the *E. coli* BL21 (DE3) Omp collection (Table 26) evidenced clear differences between the presence – in *E. coli* BL21 (DE3) - and the absence – in *E. coli* BL21 (DE3) omp2 and *E. coli* BL21 (DE3) omp8 - of the porins.

Concerning the pure FQs, the MIC values obtained against *E. coli* BL21 (DE3) omp2 (devoid of OmpF) are comparable to those against the parental strain, *E. coli* BL21 (DE3), with the exception of cpx, whose MIC increases 3 to 6-fold in the absence of OmpF. In *E. coli* BL21 (DE3) omp8, the absence of OmpC, OmpA and OmpF does not change the MIC values of mxfx and spx but there are evident increases for cpx (6 to 12-fold), erx (4-fold) and lvx (4-fold). The higher MIC value is indicative of the active role of the porin in the influx, meaning that the drug uses this protein for its translocation.

Table 26 - MIC values of several FQs, CuFQphen complexes, phen, Cu(II)/phen (1:1) and $Cu(NO_3)_2.3H_2O$ salt against *E. coli* strains (B_E BL21 (DE3), BL21 (DE3) omp2 and BL21 (DE3) omp8), expressed in μg mL^{-1} and μmol dm^{-3} for comparative purposes. The values presented were obtained from at least three independent experiments.

Antibiotic	MIC value					
	B_E BL21 (DE3)		BL21 (DE3) omp2 (Δ OmpF)		BL21 (DE3) omp8 (Δ OmpC, OmpA and OmpF)	
	μg mL^{-1}	μmol dm^{-3}	μg mL^{-1}	μmol dm^{-3}	μg mL^{-1}	μmol dm^{-3}
cpx	0.0005	0.002	0.002 – 0.004	0.006 – 0.012	0.004 – 0.008	0.012 – 0.024
erx	0.001	0.003	0.002	0.006	0.004	0.011
lvx	0.002	0.006	0.004	0.011	0.008	0.022
mxfx	0.002 – 0.004	0.005 – 0.009	0.002 – 0.004	0.005 – 0.009	0.004 – 0.008	0.009 – 0.018
spx	0.0005 – 0.001	0.001 – 0.003	0.0005 – 0.001	0.001 – 0.003	0.002	0.005
Cucpxphen	0.001	0.001	0.004	0.006	0.008 – 0.016	0.011 – 0.023
Cuerxphen	0.004 – 0.008	0.006 – 0.012	0.008	0.012	0.008	0.012
Culvxphen	0.004	0.006	0.008 – 0.016	0.011 – 0.022	0.016	0.022
Cumxfxphen	0.008	0.010	0.008	0.010	0.016	0.020
Cuspxphen	0.001	0.001	0.001	0.001	0.002	0.003
phen	8	40.4	8	40.4	8 - 16	40.4 - 80.7
Cu(II)/phen (1:1)	16 - 32	36.4 – 72.8	16 - 32	36.4 – 72.8	16	36.4
$Cu(NO_3)_2.3H_2O$	512	2119.1	1024	4238.2	1024	4238.2

The metalloantibiotics showed comparable MIC values between the parental strain and *E. coli* BL21 (DE3) omp2 and *E. coli* BL21 (DE3) omp8 for Cuerxphen, Cumxfxphen and Cuspxphen. The MIC values of Cucpxphen were greater against *E. coli* BL21 (DE3) omp2 (4-fold) and *E. coli* BL21 (DE3) omp8 (8 to 16-fold) than against the parental strain. For Culvxphen, although not so pronounced, there was an increasing of the MIC value in the absence of porins, especially against *E. coli* BL21 (DE3) omp8 (4-fold). These results indicate that the translocation of Cuerxphen, Cumxfxphen and Cuspxphen is independent of porins, while Cucpxphen and Culvxphen need them for their influx.

Generally, the experimental MIC values were in agreement with previous reports [70], with some fluctuations for cpx and Cuerxphen against *E. coli* BL21(DE3) and for mxfx and Cucpxphen against *E. coli* BL21(DE3)omp8.

The MIC values determined for phen, Cu(II)/phen (1:1) and copper solution against all parental strains and respective mutants were comparable to the ones previously obtained against the reference strains (Table 22). Once again, these values reinforce that complex dissociation is not happening and allow to attribute antimicrobial activity to the metalloantibiotics.

Taking all together, the results suggest that the permeation of mxfx and spx is independent of the porins, while cpx, erx and lvx use those proteins for their influx. In turn, Cuerxphen, Cumxfxphen and Cuspxphen seem to cross the membrane bilayer by a porin-independent way, while Cucpxphen and Culvxphen use the porins to penetrate into the bacterial cell.

Our results are in agreement with previous studies that point out for an OmpF-dependent translocation of cpx, erx and lvx, a porin-independent pathway of mxfx, spx, Cuerxphen, Cumxfxphen and Cuspxphen and a partially OmpF-dependent influx of Cucpxphen and Culvxphen.[70,73,191]

3.2.1.1. Disk diffusion test

Due to the inexistence of differences in the MIC values obtained for the antibiotics and metalloantibiotics against *E. coli* JF568 and *E. coli* W3110 strains (between parental and mutants), the disk diffusion test was performed as a complement method. The agar disk-diffusion testing is widely used in clinical microbiology as it is simple to perform, inexpensive, valid for numerous microorganisms and the obtained results are easily interpreted. The method consists in the inoculation of microorganisms in the surface of agar plates, where disks containing the antimicrobial agents are then placed. After incubation, the drugs penetrate into the agar and the inhibition of the bacterial growth is measured through the diameter of the zone of inhibition visible around the disk.[192]

The study encompassed *E. coli* JF568, JF701 (devoid of OmpC) and JF703 (devoid of OmpF). Cpx was adopted as the drug control and *E. coli* ATCC 25922 as the reference strain. The test was performed with blank paper disks impregnated with solutions of several compounds (FQs, metalloantibiotics, phen, Cu(II)/phen (1:1) and $Cu(NO_3)_2.3H_2O$ salt) and the drug control was also tested using commercial disks.

The obtained results (Table 27 and Figure 31) show similar growth inhibition zones for each compound against the three *E. coli* strains used, corroborating the results inferred by the MIC values.

Table 27 - Results from the disk diffusion test obtained for several FQs, CuFQphen complexes, phen, Cu(II)/phen (1:1) and $Cu(NO_3)_2.3H_2O$ salt against *E. coli* strains (*E. coli* ATCC 25922, JF568, JF701 and JF703). The diameter of the zones of growth inhibition is presented and expressed in mm. The values presented were obtained from at least two independent experiments. The disk diffusion tests were performed using 5 µg of each compound/disk.

Antibiotic	**Zone diameter (mm)**			
	***E. coli* ATCC 25922**	**JF568**	**JF701 (Δ OmpC)**	**JF703 (Δ OmpF)**
Commercial cpx disk [1]	37 – 40	35	35	35
cpx	37 - 41	36	38	37 – 38
erx	N. d.	34 – 35	37	35 – 36
lvx	N. d.	34 – 35	37	36 – 38
mxfx	N. d.	33 – 34	30	34
spx	N. d.	37 – 39	35	37 – 38
Cucpxphen	N. d.	36	36	35
Cuerxphen	N. d.	33 – 38	35	32 – 34
Culvxphen	N. d.	33 – 37	33	33
Cumxfxphen	N. d.	30 – 32	29	30 – 32
Cuspxphen	N. d.	35	33	36
phen	N. d.	0	0	0
Cu(II)/phen (1:1)	N. d.	0	0	0
$Cu(NO_3)_2.3H_2O$	N. d.	0	0	0

[1] Oxoid ciprofloxacin antimicrobial susceptibility disks.

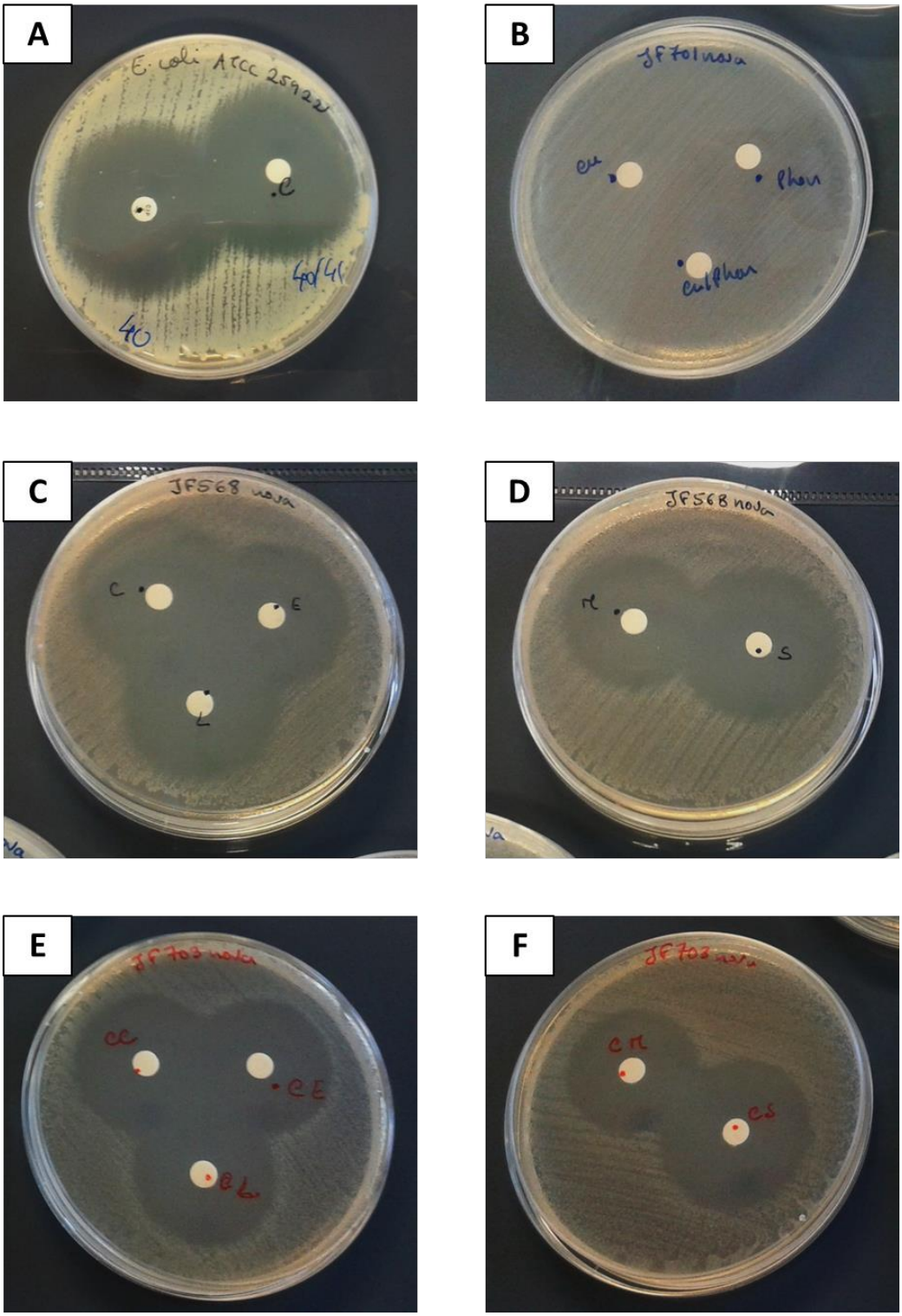

Figure 31 - Growth inhibition zones obtained by the disk diffusion test for (A) *E. coli* ATCC 25922 in the presence of cpx (5 µg) - commercial disk (left side) and solution (right side); (B) *E. coli* JF701 (Δ OmpC) in the presence of phen, Cu(II)/phen (1:1) and copper solution (Cu); (C and D) *E. coli* JF568 in the presence of cpx (C), erx (E), lvx (L), mxfx (M) and spx (S); (E and F) *E. coli* JF703 (Δ OmpF) in the presence of Cucpxphen (CC), Cuerxphen (CE), Culvxphen (CL), Cumxfxphen (CM) and Cuspxphen (CS). The disk diffusion tests were performed using 5 µg of each compound/disk. Similar results were obtained for *E. coli* JF568, JF701 (Δ OmpC) and JF703 (Δ OmpF).

Thus, the absence of considerable differences within the three *E. coli* strains, parental and mutants, does not provide information about the function of the porins in the translocation of the compounds. In turn, the presence of phen, Cu(II)/phen (1:1) and copper solution revealed, again, the poor antimicrobial activity of these substituents, as they cause no growth inhibition zones.

The diameter of the growth inhibition zones obtained for the reference strain were in agreement with the CLSI and EUCAST guidelines.[169,170]

Since the results obtained by the disk diffusion test did not provide additional information, conclusions on the role of the porins in the influx of the compounds were drawn using the MIC results previously obtained against some strains of the *E. coli* BL21 (DE3) Omp collection.

The test was not extended to the *E. coli* W3110 parental strain and respective mutants since the disk diffusion test did not seem to give any new additional information. These results were likely to be dependent on the strains and not on the method used, due to the presumable alteration of the strains, as previously proposed.

3.2.2. Antimicrobial susceptibility testing against multidrug-resistant clinical isolates

Concerning the MDR isolates (whose antibiotic resistance profiles are presented in the Supplementary data), the results obtained from Gram-negative bacteria were visibly different from those obtained from Gram-positive bacteria (Tables 28 – 30).

MIC values of all compounds were obtained, within the range of concentrations tested, against MDR isolates of Gram-negative bacteria (Tables 28 and 29), with the exception of copper solution (MIC ≥ 4238.2 μmol dm^{-3}). The MIC values of phen and Cu(II)/phen (1:1) were generally similar or higher than the MIC values of FQs and metalloantibiotics. Within the twelve MDR isolates tested, all strains revealed to be resistant to the tested FQs, according to EUCAST guidelines.[171]

Analysing the results from MDR *E. coli* isolates (Table 28), the MIC values of the metalloantibiotics were comparable to those of the respective pure FQ, indicating that metalloantibiotics are not able to bypass the bacterial resistance mechanisms of these resistant isolates. However, the antibacterial activity of Cucpxphen is considerably higher than the one observed for cpx against the isolates HSJ Ec002 (4-fold higher) and HSJ Ec003 (2 to 4-fold higher).

Table 28 - MIC values of several FQs, CuFQphen complexes, phen, Cu(II)/phen (1:1) and $Cu(NO_3)_2.3H_2O$ salt against eight multidrug-resistant (MDR) isolates of *E. coli* (Ec1-SA1, Ec2-SA1, Ec3-SA1, Ec4-SA1, HSJ Ec001, HSJ Ec002, HSJ Ec003 and HSJ Ec004), expressed in μg mL^{-1} and μmol dm^{-3} for comparative purposes. The values presented were obtained from at least three independent experiments.

Antibiotic	MIC value							
	Ec1-SA1		Ec2-SA1		Ec3-SA1		Ec4-SA1	
	μg mL^{-1}	μmol dm^{-3}	μg mL^{-1}	μmol dm^{-3}	μg mL^{-1}	μmol dm^{-3}	μg mL^{-1}	μmol dm^{-3}
cpx	1	3.0	64	193.2	4	12.1	16	48.3
erx	0.5 – 1	1.4 – 2.8	32	89.0	8	22.3	32 – 64	89.0 – 178.1
lvx	0.5	1.4	8 - 16	22.1 – 44.3	4	11.1	8	22.1
mxfx	0.5 – 1	1.1 – 2.3	8	18.3	4	9.1	8 – 16	18.3 – 36.5
spx	4	10.2	32 - 64	81.6 – 163.1	8	20.4	32	81.6
Cucpxphen	2	2.8	64	90.3	8	11.3	64	90.3
Cuerxphen	2 - 4	3.0 – 5.9	64	95.0	16	23.7	64	95.0
Culvxphen	1 - 2	1.4 – 2.8	64 - 128	88.7 – 177.5	8	11.1	16 – 32	22.2 – 44.4
Cumxfxphen	1 – 2	1.3 – 2.5	32 - 64	40.6 – 81.2	8	10.2	16 – 32	20.3 – 40.6
Cuspxphen	4	5.2	64 - 128	83.1 – 166.2	16	20.8	64	83.1
phen	8 – 16	40.4 – 80.7	8	40.4	8	40.4	8	40.4
Cu(II)/phen (1:1)	32 – 64	72.8 – 145.5	32	72.8	32 – 64	72.8 – 145.5	32	72.8
$Cu(NO_3)_2.3H_2O$	> 1024	> 4238.2	≥ 1024	≥ 4238.2	≥ 1024	≥ 4238.2	≥ 1024	≥ 4238.2

Table 28 – Continued.

Antibiotic	MIC value							
	HSJ Ec001		HSJ Ec002		HSJ Ec003		HSJ Ec004	
	μg mL^{-1}	μmol dm^{-3}	μg mL^{-1}	μmol dm^{-3}	μg mL^{-1}	μmol dm^{-3}	μg mL^{-1}	μmol dm^{-3}
cpx	16	48.3	128	386.3	64	193.2	8	24.1
erx	16	44.5	64	178.1	64	178.1	8	22.3
lvx	8	22.1	8	22.1	32	88.6	4	11.1
mxfx	4	9.1	8	18.3	8	18.3	2	4.6
spx	8	20.4	16	40.8	32	81.6	4	10.2
Cucpxphen	64	90.3	64	93.0	32 – 64	45.1 – 90.3	16	22.6
Cuerxphen	64	95.0	64	95.0	64	95.0	16	23.7
Culvxphen	16	22.2	32	44.4	32 – 64	44.4 – 88.7	8	11.1
Cumxfxphen	8	10.2	16	20.3	32	40.6	4	5.1
Cuspxphen	32	41.6	32	41.6	64	83.1	8	10.4
phen	8	40.4	16	80.7	8	40.4	8	40.4
Cu(II)/phen (1:1)	32	72.8	64	145.5	32	72.8	32	72.8
$Cu(NO_3)_2.3H_2O$	> 1024	> 4238.2	> 1024	> 4238.2	≥ 1024	≥ 4238.2	≥ 1024	≥ 4238.2

Table 29 - MIC values of several FQs, CuFQphen complexes, phen, Cu(II)/phen (1:1) and $Cu(NO_3)_2.3H_2O$ salt against four multidrug-resistant (MDR) isolates of *P. aeruginosa* (Pa1-SA2, Pa2-SA2, Pa3-SA2 and Pa4-SA2), expressed in μg mL^{-1} and μmol dm^{-3} for comparative purposes. The values presented were obtained from at least three independent experiments.

Antibiotic	MIC value							
	Pa1-SA2		Pa2-SA2		Pa3-SA2		Pa4-SA2	
	μg mL^{-1}	μmol dm^{-3}	μg mL^{-1}	μmol dm^{-3}	μg mL^{-1}	μmol dm^{-3}	μg mL^{-1}	μmol dm^{-3}
cpx	0.5	1.5	2 - 4	6.0 – 12.1	8	24.1	8 – 16	24.1 – 48.3
erx	4	11.1	8	22.3	32	89.0	32 – 64	89.0 – 178.1
lvx	2	5.5	4	11.1	8	22.1	32	88.6
mxfx	4	9.1	8	18.3	16	36.5	16	36.5
spx	4 - 8	10.2 – 20.4	8	20.4	32	81.6	16 - 32	40.8 – 81.6
Cucpxphen	1 - 2	1.4 – 2.8	4 - 8	5.6 – 11.3	16 - 32	22.6 – 45.1	16 – 32	22.6 – 45.1
Cuerxphen	8	11.9	32	47.5	128 - 256	189.9 – 379.8	256	379.8
Culvxphen	4	5.6	8	11.1	32	44.4	32	44.4
Cumxfxphen	8	10.2	32	40.6	64	81.2	32	40.6
Cuspxphen	8	10.4	16 - 32	20.8 – 41.6	128	166.2	16 – 32	20.8 – 41.6
phen	16	80.7	64	322.9	64	322.9	32 – 64	161.4 – 322.9
Cu(II)/phen (1:1)	64 - 128	145.5 – 291.0	256	582.0	> 512	> 1164.1	256	582.0
$Cu(NO_3)_2.3H_2O$	1024	4238.2	1024	4238.2	1024	4238.2	1024	4238.2

The obtained results reinforce the importance of choosing the suitable units to compare the antimicrobial activity of compounds with relatively different molecular weights. In this particular case, the analysis of the results in the conventional units (μg mL^{-1}) suggests a difference of a single well, 2-fold, (128 μg mL^{-1} for cpx and 64 μg mL^{-1} for Cucpxphen), while the comparison of the results in μmol dm^{-3} reveals a difference of 4-fold (386.3 μmol dm^{-3} for cpx and 93.0 μmol dm^{-3} for Cucpxphen). Nevertheless, despite the improved antibacterial activity of Cucpxphen, the MIC value is quite high, meaning that the bacterial isolate is also probably resistant to the metalloantibiotic.

Furthermore, generally, the MIC values of metalloantibiotics and respective pure FQs were similar against MDR *P. aeruginosa* isolates (Table 29). The exceptions were observed for Cuerxphen, whose MICs revealed a weak antimicrobial activity compared to erx against two out of the four tested isolates (Pa3-SA2 and Pa4-SA2).

Besides that, the results obtained from the clinical isolates of *P. aeruginosa* revealed to be more difficult to replicate. This phenomenon could be attributed to the ability of this species to easily acquire resistance to drugs. Mulcahy *et al.* have previously reported the presence of drug-tolerant persistent cells in clinical isolates of *P. aeruginosa* that could account for the 2-fold discrepancy obtained from the repeated experiments.[195]

Together with the results obtained from the *E. coli* isolates, it can be assumed that the metalloantibiotics may not be a good alternative to pure FQs in Gram-negative bacteria. For this reason, the antimicrobial assays proceeded using Gram-positive isolates, concretely 18 MRSA clinical isolates (Table 30).

Nowadays, FQs are no longer used in clinical therapy for infections caused by MRSA due to the bacterial resistance mechanisms developed against these antibiotics.[196] Thus, if metalloantibiotics prove to be more effective than FQs against MRSA isolates, it may be a promising choice for the treatment of infections caused by *S. aureus*. In fact, and contrarily to what was observed for the Gram-negative bacteria, the results were encouraging for several metalloantibiotics in numerous MRSA isolates.

In 15 out of the 18 MRSA tested, metalloantibiotics evidenced improved antibacterial activity in comparison to the respective pure FQs. Only in three isolates (Sa4-SA3, 38/13 bis and 16/01), pure FQs and the respective metalloantibiotics exhibited similar MIC values.

Table 30 - MIC values of several FQs, CuFQphen complexes, phen, Cu(II)/phen (1:1) and $Cu(NO_3)_2.3H_2O$ salt against 18 methicillin-resistant *S. aureus* (Sa1-SA3, Sa2-SA3, Sa3-SA3, Sa4-SA3, 17/05, 17/08, 37/3, 38/13 bis, 59/57, 27/17, 5/41, 58/01, 6/16 bis, 3/146, 7/21 bis, 19/35, 26/01 and 16/01), expressed in μg mL^{-1} and μmol dm^{-3} for comparative purposes. The values presented were obtained from at least three independent experiments.

Antibiotic	MIC value							
	Sa1-SA3		Sa2-SA3		Sa3-SA3		Sa4-SA3	
	μg mL^{-1}	μmol dm^{-3}	μg mL^{-1}	μmol dm^{-3}	μg mL^{-1}	μmol dm^{-3}	μg mL^{-1}	μmol dm^{-3}
cpx	128	386.3	128	386.3	128 – 256	386.3 – 772.6	8	24.1
erx	8	22.3	128	356.2	16 - 32	44.5 – 89.0	4	11.1
lvx	256	708.4	64	177.1	16	44.3	4	11.1
mxfx	8	18.3	16	36.5	128	292.3	2	4.6
spx	256	652.4	128	326.2	8	20.4	4	10.2
Cucpxphen	64	90.3	32 – 64	45.1 – 90.3	64	90.3	16	22.6
Cuerxphen	64	95.0	32 – 64	47.5 – 95.0	64	95.0	8	11.9
Culvxphen	64	88.7	64	88.7	64 – 128	88.7 – 177.5	8	11.1
Cumxfxphen	8	10.2	16	20.3	8	10.2	8	10.2
Cuspxphen	64 – 128	83.1 – 166.2	32 – 64	41.6 – 83.1	32	41.6	16	20.8
phen	512	2582.9	32	161.4	128	645.7	128	645.7
Cu(II)/phen (1:1)	32	72.8	32	72.8	32	72.8	32	72.8
$Cu(NO_3)_2.3H_2O$	≥ 1024	≥ 4238.2	1024	4238.2	≥ 1024	≥ 4238.2	≥ 1024	≥ 4238.2

Table 30 – Continued.

Antibiotic	MIC value							
	17/05		17/08		37/3		38/13 bis	
	μg mL^{-1}	**μmol dm^{-3}**	**μg mL^{-1}**	**μmol dm^{-3}**	**μg mL^{-1}**	**μmol dm^{-3}**	**μg mL^{-1}**	**μmol dm^{-3}**
cpx	≥ 256	772.6	32 – 64	96.6 – 193.2	≥ 512	≥ 1545.2	128 - 512	386.3 – 1545.2
erx	4 – 8	11.1 - 22.3	8 – 16	22.3 – 44.5	32	89.0	8	22.3
lvx	16	44.3	8 – 16	22.1 – 44.3	64	177.1	8 – 16	22.1
mxfx	4	9.1	2	4.6	8	18.3	2	4.6
spx	16	40.8	32	81.6	16 - 32	40.8 – 81.6	16 – 32	40.8
Cucpxphen	128	180.5	64 – 128	90.3 – 180.5	128	180.5	128	180.5
Cuerxphen	8 – 16	11.9 – 23.7	16	23.7	64	95.0	16	23.7
Culvxphen	8 – 32	11.1 – 44.4	16	22.2	64	88.7	32	44.4
Cumxfxphen	4 – 8	5.1 – 10.2	4	5.1	16	20.3	4 – 8	5.1 – 10.2
Cuspxphen	32	41.6	16	20.8	16	20.8	16 - 32	20.8 - 41.6
phen	256 – 512	1291.4 – 2582.9	32	16.4	64 - 128	322.9 – 645.7	64	322.9
Cu(II)/phen (1:1)	64	145.5	64 – 128	145.5 – 291.0	64	145.5	64	145.5
$Cu(NO_3)_2.3H_2O$	≥ 880	≥ 3642.2	≥ 880	≥ 3642.2	≥ 880	≥ 3642.2	≥ 880	≥ 3642.2

Table 30 – Continued.

Antibiotic	MIC value							
	59/57		27/17		5/41		58/01	
	μg mL^{-1}	**μmol dm^{-3}**	**μg mL^{-1}**	**μmol dm^{-3}**	**μg mL^{-1}**	**μmol dm^{-3}**	**μg mL^{-1}**	**μmol dm^{-3}**
cpx	≥ 1024	≥ 3090.5	≥ 1024	≥ 3090.5	64	193.2	32	96.6
erx	32	89.0	64	178.1	64 - 128	178.1 – 356.2	8 – 16	22.3 – 44.5
lvx	32	88.6	64 – 128	177.1 – 354.2	32	88.6	8 - 16	22.1 – 44.3
mxfx	4	9.1	4 - 8	9.1 – 18.3	8	18.3	8	18.3
spx	32	81.6	16 – 32	40.8 – 81.6	64	163.1	32	81.6
Cucpxphen	128	180.5	128	180.5	128	180.5	64	90.3
Cuerxphen	64	95.0	64	95.0	64	95.0	16	23.7
Culvxphen	64	88.7	64	88.7	64	88.7	16	22.2
Cumxfxphen	8	10.2	16	20.3	16	20.3	4	5.1
Cuspxphen	32	41.6	16 – 32	20.8 - 41.6	32	41.6	16	20.8
phen	128	645.7	64	322.9	128	645.7	256	1291.4
Cu(II)/phen (1:1)	32 - 64	72.8 – 145.5	64	145.5	64	145.5	64	145.5
$Cu(NO_3)_2.3H_2O$	≥ 880	≥ 3642.2	≥ 880	≥ 3642.2	≥ 880	≥ 3642.2	≥ 880	≥ 3642.2

Table 30 – Continued.

Antibiotic	MIC value							
	6/16 bis		3/146		7/21 bis		19/35	
	μg mL^{-1}	μmol dm^{-3}	μg mL^{-1}	μmol dm^{-3}	μg mL^{-1}	μmol dm^{-3}	μg mL^{-1}	μmol dm^{-3}
cpx	32 – 64	96.6 – 193.2	64 – 128	193.2 – 386.3	256	772.6	≥ 1024	≥ 3090.5
erx	16	44.5	8	22.3	8	22.3	64	178.1
lvx	16	44.3	16 – 32	44.3 – 88.6	32	88.6	64	177.1
mxfx	2	4.6	4	9.1	4	9.1	8	18.3
spx	32	81.6	16 – 32	40.8 – 81.6	32	81.6	64	163.1
Cucpxphen	64	90.3	64 – 128	90.3 – 180.5	128	180.5	128	180.5
Cuerxphen	16	23.7	16	23.7	16	23.7	64	95.0
Culvxphen	16	22.2	32	44.4	32	44.4	64	88.7
Cumxfxphen	4	5.1	8	10.2	8	10.2	16	20.3
Cuspxphen	16	20.8	16	20.8	16	20.8	32	41.6
phen	128	645.7	32	161.4	32	161.4	64	322.9
Cu(II)/phen (1:1)	64	145.5	32 - 64	72.8 – 145.5	64	145.5	64	145.5
$Cu(NO_3)_2.3H_2O$	≥ 880	≥ 3642.2	≥ 880	≥ 3642.2	≥ 880	≥ 3642.2	≥ 880	≥ 3642.2

Table 30 – Continued.

Antibiotic	MIC value			
	26/01		16/01	
	μg mL^{-1}	μmol dm^{-3}	μg mL^{-1}	μmol dm^{-3}
cpx	512	1545.2	16	48.3
erx	256	712.3	2 – 8	5.6 – 22.3
lvx	512	1416.8	4 – 8	11.1 – 22.1
mxfx	32	73.1	2	4.6
spx	256	652.4	4 – 8	10.2 – 20.4
Cucpxphen	128	180.5	64	90.3
Cuerxphen	64	95.0	8	11.9
Culvxphen	64	88.7	8 – 16	11.1 – 22.2
Cumxfxphen	32	40.6	4	5.1
Cuspxphen	64	83.1	8 – 16	10.4 – 20.8
phen	64 - 128	322.9 – 645.7	32	161.4
Cu(II)/phen (1:1)	64	145.5	64	145.5
$Cu(NO_3)_2.3H_2O$	≥ 880	≥ 3642.2	≥ 880	≥ 3642.2

Cucpxphen and Cuspxphen showed to be more effective in a greater number of isolates. The results obtained for Cucpxphen demonstrated that this metalloantibiotic is about 4-fold more effective against three isolates (Sa1-SA3,17/05 and 7/21 bis), 4 to 8-fold against four isolates (Sa2-SA3, Sa3-SA3, 37/3 and 26/01) and more than 16-fold against three isolates (59/57, 27/17 and 19/35). Moreover, Cuspxphen have revealed an inferior MIC to spx of 4-fold against nine isolates (Sa1-SA3,17/08, 37/3, 5/41, 58/01, 6/16 bis, 3/146, 7/21 bis and 19/35) and 4 to 8-fold against two isolates (Sa2-SA3 and 26/01).

Cuerxphen showed improved effectiveness against three isolates: 4-fold more effective agaisnt Sa2-SA3 and 5/41 isolates and 7-fold against 26/01 isolate. The MIC values obtained for Culvxphen were 4-fold lower than lvx against Sa1-SA3 and 27/17 isolates and 15-fold lower against 26/01 isolate. Finally, the antimicrobial activity of

Cumxfxphen has proved to be advantageous against two isolates: 58/01 (4-fold) and Sa3-SA3 (28-fold).

Once again, the MIC values determined for phen and Cu(II)/phen (1:1) were comparable or greater than the MIC values of FQs and metalloantibiotics and no antimicrobial activity could be attributed to the copper solution, since the MIC was ≥ 3642.2 μmol dm^{-3}.

For this reason, metalloantibiotics seem promising against MRSA strains. Their improved antimicrobial activity could be possibly due to an alternative translocation pathway, as previously explained. The absence of porins in the Gram-positive bacterial membrane together with the structural and physicochemical properties of the metalloantibiotics support the assumption of an influx route independent of proteins and based on the passive diffusion of the molecules.

However, although the MIC values of the metalloantibiotics are greatly decreased compared to pure FQs, the absolute value of the MIC can still be considered clinically rather high.

3.3. Activity and toxicity assays

This work finishes by i) studying the mechanism of action of the compounds, performed through enzymatic inhibitory activity assays against DNA gyrase and topoisomerase IV of *E. coli* and *S. aureus,* and ii) performing preliminary toxicological tests, comprising cytotoxicity and hemolytic assays.

3.3.1. Enzymatic inhibitory activity assays

The mechanism of action of FQs is well known, being the type II topoisomerases (DNA gyrase and topoisomerase IV) the main targets of quinolones.[172] These two enzymes play a crucial role in the bacterial replication. DNA gyrase is implicated in the introduction of the negative supercoils in the DNA strand, while topoisomerase IV separates the DNA molecules to finish the replication process.[67,74]

During the bacterial replication, FQs bind to the enzyme-DNA complex, forming a ternary complex (drug, enzyme, and DNA) that blocks the progression of the replication.[51,68,75] Taking into account the nuclease activity and the high affinity to intercalate into the DNA described for metalloantibiotics, it is expected a similar mechanism of action in the bacterial cell.[70,117] However, more studies around the mechanism of action of these complexes are required.

For this reason, the enzymatic inhibitory activity of the metalloantibiotics was assessed against topoisomerases II of both *E. coli* and *S. aureus*.

The study comprised two metalloantibiotics, Cucpxphen and Cuspxphen, and cpx was adopted as the drug control. The experiments were performed using DNA gyrase supercoiling assay kits and topoisomerase IV relaxation assay kits of *S. aureus* and *E. coli*, from Inspiralis. Three controls were used: a negative control, lacking the enzyme (containing a mixture of the plasmid, water, assay buffer and dilution buffer) and two positive controls containing the enzyme and differing only in the solvent (water or HEPES buffer). The enzymatic activity of the drug control was always evaluated using two different concentrations (one able and other incapable to inhibit the enzyme).

The experiments started by determining the activity of the four enzymes. The results obtained (Table 31 and Figures 32 and 33) allowed to define the concentration of enzyme necessary to perform each enzymatic inhibitory activity assay.

Table 31 - DNA gyrase and topoisomerase IV concentrations (of *E. coli* and *S. aureus*) used in each DNA gyrase supercoiling inhibition assays and topoisomerase IV relaxation assays. Each experiment was performed using 0.5 µL of pBR322 plasmid (relaxed in the case of gyrases and supercoiled in the case of topoisomerases IV).

Assay	Bacterial enzyme	Enzyme concentration (U)
Gyrase supercoiling inhibition assay	*E. coli* DNA gyrase	1
	S. aureus DNA gyrase	1
Topoisomerase IV relaxation assay	*E. coli* topoisomerase IV	1.5
	S. aureus topoisomerase IV	2

The concentration of the stock of enzyme supplied in each kit was 10 Units/µL (10U/µL). In the case of DNA gyrases, the concentration of the enzyme corresponds to the units required to completely supercoil the relaxed plasmids (Figure 32). In turn, the concentration of enzyme assessed for the topoisomerases reveals the amount of enzyme necessary to totally relax the supercoiled plasmids (Figure 33).

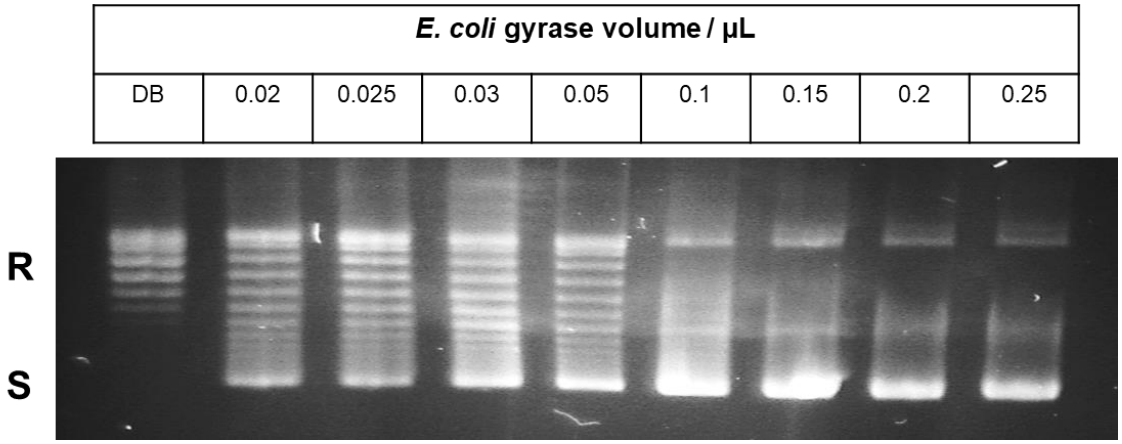

Figure 32 - Activity of *E. coli* DNA gyrase in a supercoiling assay performed with 0.5 µL of relaxed pBR322 plasmid, determined in a 1% (w/v) agarose gel in TAE buffer. DB is dilution buffer, and the respective band is the negative control, containing the relaxed plasmid in the absence of the enzyme. The experiment was also performed with the *S. aureus* DNA gyrase supercoiling assay kit. R and S are the relaxed and supercoiled DNA bands, respectively.

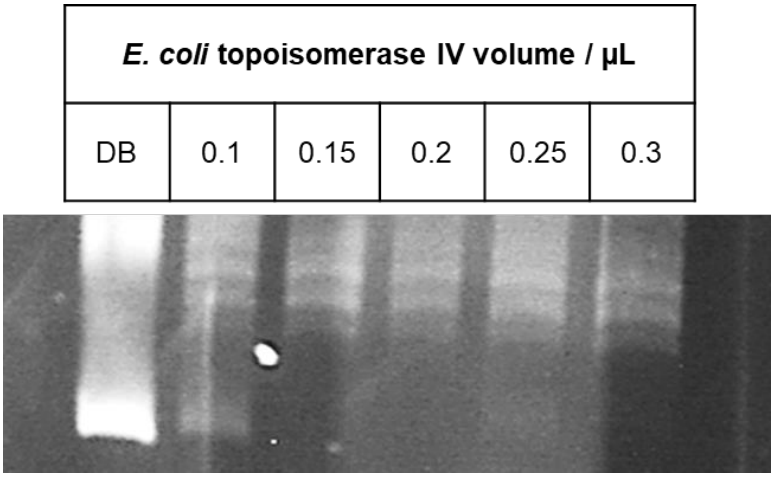

Figure 33 - Activity of *E. coli* topoisomerase IV in a relaxation assay performed with 0.5 µL of supercoiled pBR322 plasmid, determined in a 1% (w/v) agarose gel in TAE buffer. DB is dilution buffer, and the respective band is the negative control, containing the supercoiled plasmid in the absence of the enzyme. The experiment was also performed with the *S. aureus* topoisomerase IV relaxation assay kit.

The results revealed that DNA gyrases are more active than the topoisomerases IV, as for the same amount of plasmid, 1 unit of DNA gyrase is able to completely supercoil it, while 1.5 or 2 units of topoisomerase IV are required to totally relax it.

The results of the inhibitory enzymatic activity experiments, performed with cpx and the two studied metalloantibiotics (Cucpxphen and Cuspxphen), are presented in Table 32 and Figures 34 and 35. Cpx was used as the drug control due to its known inhibitory enzymatic activity. The results revealed inhibitory enzymatic activity for both metalloantibiotics, suggesting the same mechanism of action of the FQs. The results obtained for the two metalloantibiotics were comparable within each assay.

Analysing the results obtained in the DNA gyrase supercoiling inhibition assays (Table 32 and Figure 34), the results obtained for cpx were similar to the ones determined for the metalloantibiotics within each assay. Thus, it is possible to conclude that metalloantibiotics seem to inhibit the DNA gyrases in a comparable way as cpx. Comparing the results obtained for *E. coli* and *S. aureus*, it could be observed that it is necessary a higher concentration of compound to inhibit the same amount of enzyme in the case of the Gram-positive bacteria. These results show that all tested compounds, pure FQ or metalloantibiotic, are more active against the DNA gyrase of the Gram-negative bacteria.

Table 32 - Concentrations of cpx, Cucpxphen and Cuspxphen able to inhibit the enzymatic activity of DNA gyrase and topoisomerase IV of *E. coli* and *S. aureus*. The values presented were obtained from at least three independent experiments.

Assay	Bacterial enzyme	Concentration of compound able to inhibit the enzyme / μmol dm^{-3}		
		cpx	Cucpxphen	Cuspxphen
DNA gyrase supercoiling inhibition assay	*E. coli* DNA gyrase	5	5	5
	S. aureus DNA gyrase	50	50	50
Topoisomerase IV relaxation assay	*E. coli* topoisomerase IV	10	5 - 10	5 - 10
	S. aureus topoisomerase IV	10	5	5

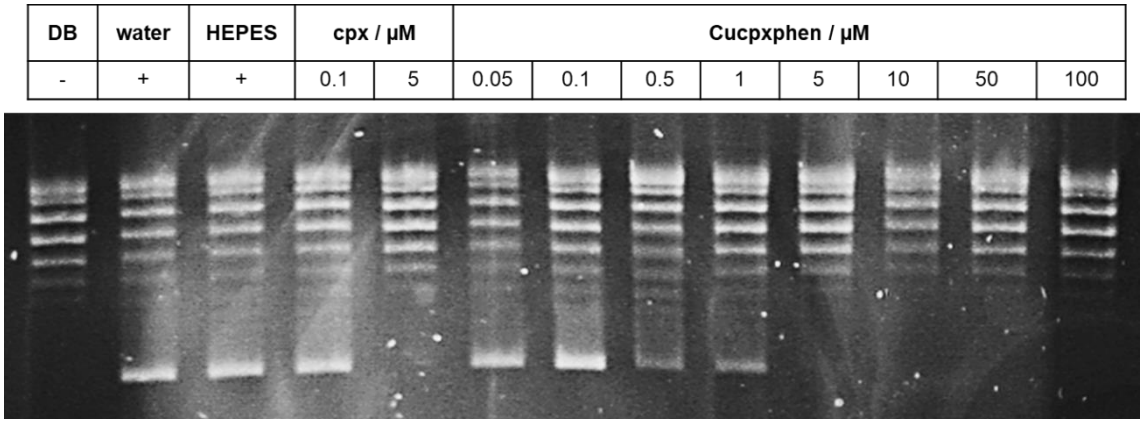

Figure 34 - DNA gyrase supercoiling inhibition assay obtained for Cucpxphen as enzymatic inhibitor of the *E. coli* DNA gyrase, performed with 0.5 μL of relaxed pBR322 plasmid, determined in a 1% (w/v) agarose gel in TAE buffer. DB is dilution buffer, and the respective band is the negative control, containing the relaxed plasmid in the absence of the enzyme. Water and HEPES are the positive control bands containing the enzyme and the plasmid. The cpx bands represent the drug control. μM means μmol dm^{-3} and refers to the concentration of the compound. The experiment was also performed with the *S. aureus* DNA gyrase supercoiling inhibition assay kit. The enzymatic inhibitory activity of Cucpxphen and Cuspxphen was evaluated in both kits.

In turn, the results of the topoisomerase IV relaxation assays (Table 32 and Figure 35) reveal differences between cpx and the metalloantibiotics. The concentration of the metalloantibiotics required to inhibit the topoisomerases IV was always reduced compared to the one of cpx. This difference was more evident in the case of the topoisomerase IV of the *S. aureus*, showing that metalloantibiotics are more effective against topoisomerase IV of Gram-positive bacteria. The inhibitory activity of each compound was comparable for Gram-positive and Gram-negative bacteria.

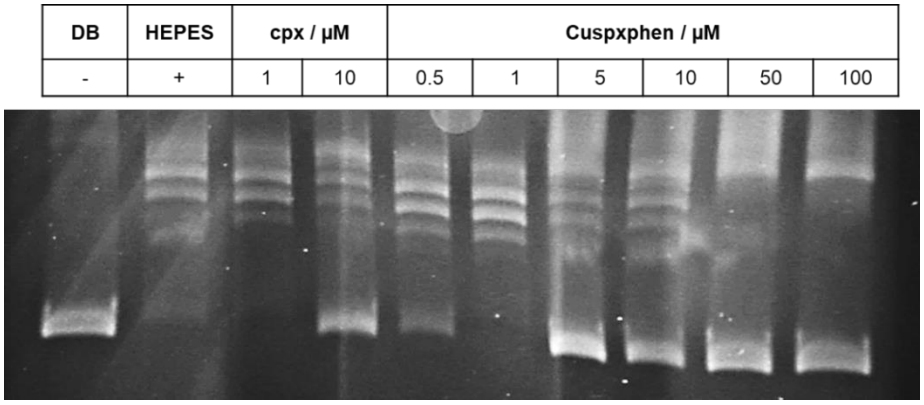

Figure 35 - Topoisomerase IV relaxation assay obtained for Cuspxphen as enzymatic inhibitor of the *S. aureus* topoisomerase IV, performed with 0.5 µL of supercoiled pBR322 plasmid, determined in a 1% (w/v) agarose gel in TAE buffer. DB is dilution buffer, and the respective band is the negative control, containing the relaxed plasmid in the absence of the enzyme. HEPES is the positive control containing the enzyme and the plasmid. The cpx bands represent the drug control. µM means µmol dm^{-3} and refers to the concentration of the compound. The experiment was also performed with the *E. coli* topoisomerase IV relaxation assay kit. The enzymatic inhibitory activity of Cucpxphen and Cuspxphen was evaluated in both kits.

Taking all together, is seems that FQs and metalloantibiotics easily target the DNA gyrase of *E. coli* and topoisomerases IV of *E. coli* and *S. aureus*. In turn, the DNA gyrase of *S. aureus* revealed to be less susceptible to the action of both compounds. Thus, it is possible to expect that these compounds easily act against both topoisomerases in Gram-negative bacteria, while could have preference for topoisomerase IV in the case of Gram-positive bacteria. These results are in agreement with several authors that describe DNA gyrase as the principal target in Gram-negative bacteria and topoisomerase IV as the major target in Gram-positive bacteria. However, exceptions may occur in some bacterial species, depending on the FQ used.[76-78]

Metalloantibiotics are more active against topoisomerase IV in comparison to pure FQs and seem more effective in Gram-positive bacteria, corroborating the greater antimicrobial activity previously obtained in several MRSA strains.

3.3.2. Cytotoxicity assay

The evaluation of the toxicity is a mandatory requirement for the characterization of any compound candidate to be a novel drug. Therefore, and due to the scarce and controversial knowledge, the toxicological safety of the metalloantibiotics was studied.[70,122]

The cytotoxic activity of the compounds - FQs, metalloantibiotics, phen, cation copper and complex Cu(II):phen (1:1) - was assessed through the MTT assay. The dose-dependent effect of the compounds was determined taking into account the cell viability of an immortalized human fibroblasts cell line (HFF-1, ATCC number SCRC-1041), after 24 hours of drug exposure. The concentration range for each compound tested was chosen based on the MIC values obtained against MDR strains. The amount of purple formazan crystals, formed by the metabolically active cells, was measured and compared to the controls (cells not exposed to the compounds).

The results obtained for the pure FQs (Figure 36) showed high cell viability (~ 100%) under drug exposure. The cell viability remained higher for all the six studied concentrations, only being reduced to 80% in the presence of 25.0 μmol dm^{-3} (maximum concentration studied) of cpx or erx. The results were comparable for all studied FQs. Therefore, in the subsequent tests, cpx was chosen as the control drug.

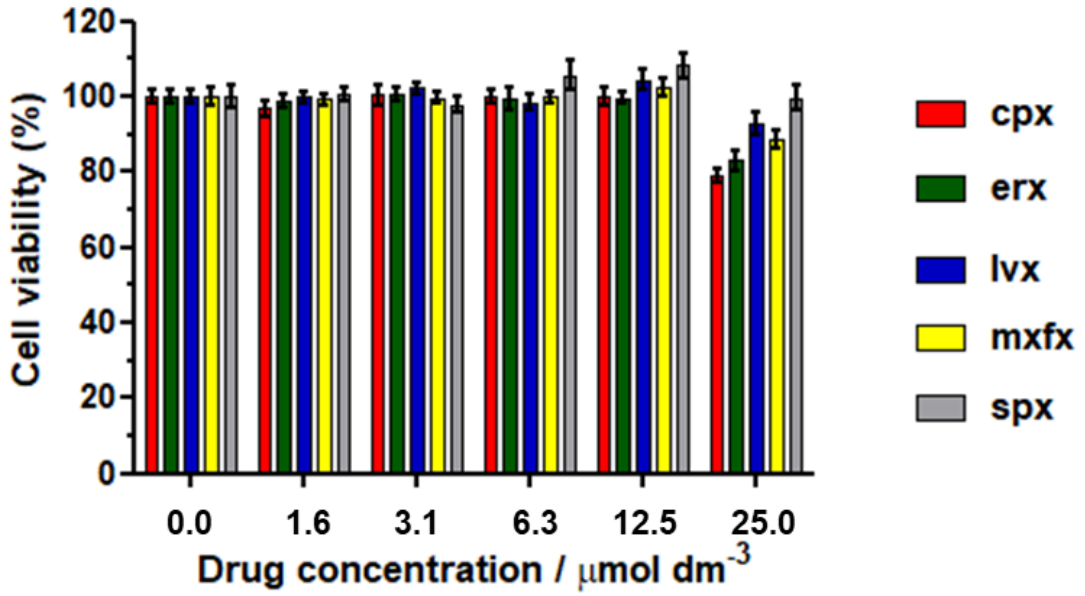

Figure 36 - Dose-dependent cytotoxicity of pure FQs (cpx, erx, lvx, mxfx and spx) on human fibroblasts cell line (HFF-1, ATCC number SCRC 1041) over a 24 hours period of drug exposure, using the MTT assay. The results are expressed as the mean ± SEM of three independent experiments, each performed in six replicates. The cell viability was calculated in comparison to the control (cells not exposed to compounds), which was considered as 100%.

Metalloantibiotics (Figures 37 and 38) showed high cellular metabolic activity till a concentration of compound of 6.3 μmol dm^{-3}, above which there is a drastic reduction of the cell viability (to 60%). The graph of Figure 37 displays statistical significance in cells treated with 12.5 μmol dm^{-3} and 25.0 μmol dm^{-3} of complex concentration. These results were obtained for all studied metalloantibiotics. Therefore, the experimental data demonstrated that metalloantibiotics induced cell cytotoxicity for concentrations ≥ 12.5 μmol dm^{-3}, being more cytotoxic than the pure FQs.

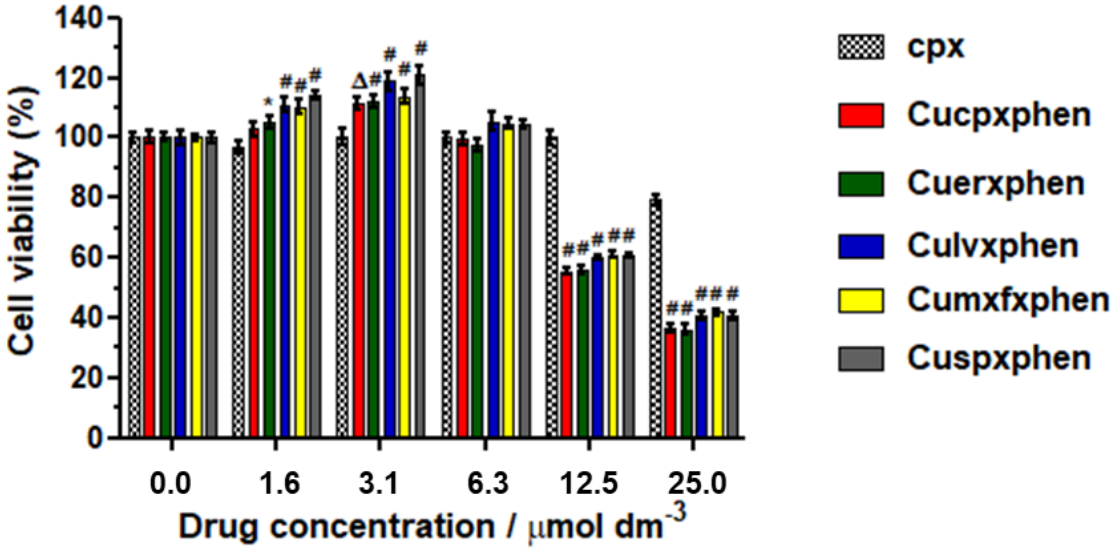

Figure 37 - Dose-dependent cytotoxicity of metalloantibiotics (Cucpxphen, Cuerxphen, Culvxphen, Cumxfxphen and Cuspxphen) and cpx (drug control) on human fibroblasts cell line (HFF-1, ATCC number SCRC 1041) over a 24 hours period of compound exposure, using the MTT assay. The results are expressed as the mean ± SEM of three independent experiments, each performed in six replicates. The cell viability was calculated in comparison to the control (cells not exposed to compounds), which was considered as 100%. * $p < 0.05$; Δ $p < 0.01$; # $p < 0.001$ in comparison with drug control (Bonferroni multiple comparison post-test).

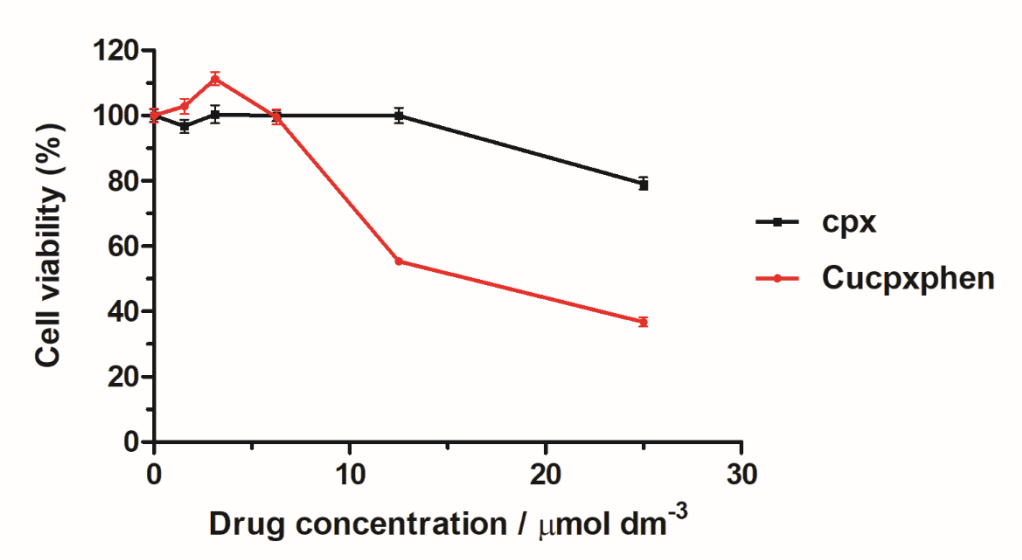

Figure 38 - Dose-dependent cell viability curves obtained for cpx and Cucpxphen on human fibroblasts cell line (HFF-1, ATCC number SCRC 1041) over a 24 hours period of compound exposure, using the MTT assay. Each data point represents the mean ± SEM of three independent experiments, each performed in six replicates. The cell viability was calculated in comparison to the control (cells not exposed to compounds), which was considered as 100%.

Concerning phen (Figure 39), the experimental data revealed that this ligand was innocuous under the studied conditions since the cell viability remained unaltered under exposure to this compound.

In turn, the copper solution (Figure 39) proved to be slightly toxic at a concentration of 25.0 μmol dm^{-3}, reducing the cell viability to 80%. Therefore, there is a comparable cytotoxic effect between the copper solution and the pure FQs. However, besides the absolute values of the cell viability obtained in the presence of copper and cpx seem comparable, differences were statistically significant for concentrations of 3.1 μmol dm^{-3}, 6.3 μmol dm^{-3} and 12.5 μmol dm^{-3}.

Contrarily to phen and copper solutions, the solution of the binary complex of Cu(II):phen (1:1) affected the cell viability at a concentration of 12.5 μmol dm^{-3}, resulting in a reduction on the cell viability of 40% (Figure 39). Therefore, the higher cytotoxic activity of the metalloantibiotics may arise from the presence of the moiety Cu(II):phen. Although the cytotoxic activity of the metalloantibiotics is comparable to the one of the binary complex Cu(II):phen (1:1), the speciation diagrams of the metalloantibiotics clearly demonstrate that the binary complex does not exist free in ternary complexes solution, at physiological pH.[70]

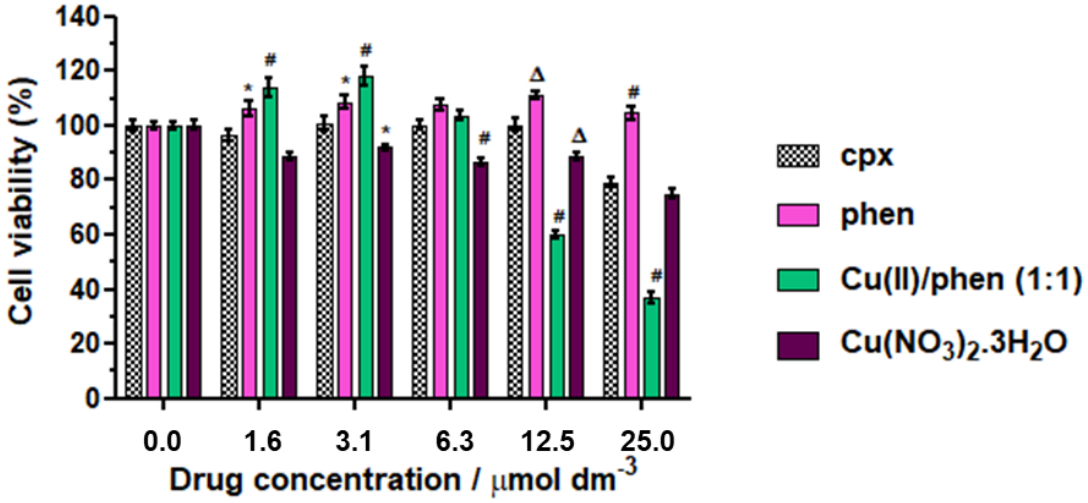

Figure 39 - Dose-dependent cytotoxicity of phen, Cu(II):phen (1:1), $Cu(NO_3)_2.3H_2O$ and cpx (drug control) on human fibroblasts cell line (HFF-1, ATCC number SCRC 1041) over a 24 hours period of compound exposure, using the MTT assay. The results are expressed as the mean ± SEM of three independent experiments, each performed in six replicates. The cell viability was calculated in comparison to the control (cells not exposed to compounds), which was considered as 100%. * $p < 0.05$; Δ $p < 0.01$; # $p < 0.001$ in comparison with drug control (Bonferroni multiple comparison post-test).

The half maximal inhibitory concentration (IC_{50}) of a drug is a factor widely used to illustrate the toxicological activity of a compound. Thus the IC_{50} of all compounds was evaluated through the analysis of the logarithmic dose dependent cell viability curves (Figure 40).

The IC_{50} values calculated for all pure FQs varied from 26 to 32 μmol dm^{-3}, with the exception of spx whose IC_{50} was not determined due to the absence of curvature in the dose-dependent cell viability curve. In turn, the value of IC_{50} assessed for all metalloantibiotics and for a solution of the binary complex of Cu(II):phen (1:1) was 10 μmol dm^{-3}. These results reinforce the enhanced cell cytotoxicity of the metalloantibiotics compared to the pure FQs. Lastly, the IC_{50} obtained for the copper solution had a value of 40 μmol dm^{-3}, showing that this cation is less cytotoxic than the pure FQs for the fibroblasts cells. The values reported in the literature concerning the cytotoxicity of copper solutions against normal cell lines (after 24h of exposure) are widely variable: Cao *et al.* state a median lethal dose (LD_{50}) of 29 μmol dm^{-3} against mouse fibroblast cells [197], while Bunetel *et al.* report values of cytotoxic doses (CD_{50}) of 178 μmol dm^{-3} (23.97 mg L^{-1}) against human osteoblast cells and of 232 μmol dm^{-3} (31.18 mg L^{-1}) against human endothelial cells [198]. Besides the characteristics of the cell lines, this variability may also arise from the properties of the metal salt solution

(both metal and counterions). Bongers *et al.* demonstrated that the toxicity of a metal salt solution depend on the metal but it is also affected by the counterion present in solution.[199] Our results are in agreement with the data reported by Cao *et al.*.[197]

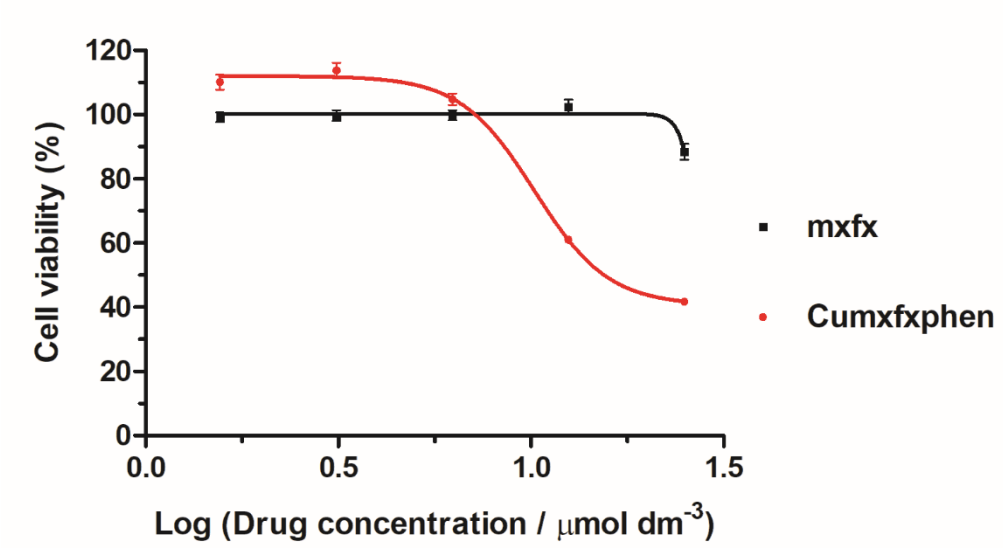

Figure 40 - Logarithmic dose-dependent cell viability curves obtained for mxfx and Cumxfxphen on human fibroblasts cell line (HFF-1, ATCC number SCRC 1041) over a 24 hours period of compound exposure, using the MTT assay. The results are expressed as the mean ± SEM of three independent experiments, each performed in six replicates. The cell viability was calculated in comparison to the control (cells not exposed to compounds), which was considered as 100%.

In brief, metalloantibiotics are more cytotoxic than the pure FQs. Furthermore, it is presumed that the presence of the Cu(II)/phen moiety can confer the higher cytotoxicity of the metalloantibiotics . The phen solution and the copper solution proved to be safe to the fibroblasts cells. These preliminary results should be complemented with cytotoxic assays performed in other cell lines, such as hepatocytes, in order to clarify the cytotoxic effect of the metalloantibiotics in different organs.

3.3.3. Hemolytic activity assay

Additionally, the evaluation of the toxicity of the compounds against human red blood cells (RBCs), through a hemolytic assay, was performed The experiments were performed using two pure FQs (cpx and spx), their metalloantibiotics (Cucpxphen and Cuspxphen), phen, Cu(II):phen (1:1) and a copper solution. The compound

concentrations tested were the same used in the MTT assay. The percentage of hemolysis was determined for each sample, after 1 hour of exposure to the tested compounds.

The results of the hemolytic activity assay (Figure 41) showed no significant hemolytic activity for all the tested compounds. The percentage of the hemolysis, calculated using Eq. (27), was always lower than 1%. The erythrocyte lysis was only observed in the positive control, considered as the experimental condition resulting in the hemolysis of 100% of the RBCs, due to the presence of Triton X-100.

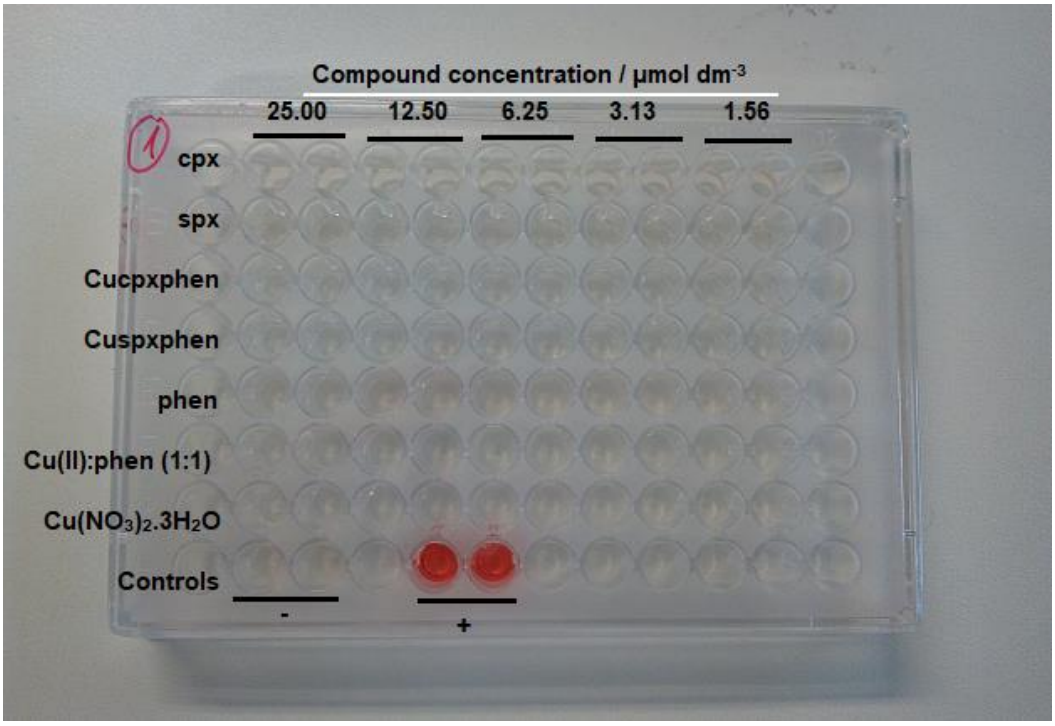

Figure 41 - Hemolytic activity assay results obtained for cpx, spx, Cucpxphen, Cuspxphen, phen, Cu(II):phen (1:1) and $Cu(NO_3)_2.3H_2O$ against human red blood cells (RBCs), after 1 hour of exposure to the compounds. The negative control (-) consists of RBCs in PBS buffer and the positive control (+) contains RBCs suspended in Triton X-100. Each condition was studied in duplicate and two independent experiments were performed.

The weak hemolytic activity of the FQs was previously described by Yamamoto *et al.*, being proposed that these drugs induce erythrocyte lysis in concentrations above 100 μg/ml (corresponding to ~ 280 μmol dm^{-3} of FQs and 140 μmol dm^{-3} of metalloantibiotics). [90]

As a final remark, it is important to state that the comparable hemolytic activity of the metalloantibiotics and FQs is a very positive input for future perspectives.

Final Remarks

4

Antimicrobial resistance (AMR) is on the top of the major public health concerns of the 21st century due to the great plasticity of bacteria to bypass the action of antimicrobial agents. During the last decades, a prompt spreading of several bacterial resistance mechanisms has been observed.

Fluoroquinolones (FQs) are a family of antibiotics extensively used in the clinical practise. However, such as reported for other antimicrobial agents, different AMR mechanisms are described against FQs. One of the strategies adopted to circumvent this problematic is the complexation of these drugs with divalent metal ions and phenanthroline (phen), which forms stable complexes entitled as metalloantibiotics.

The purpose of this work was to elucidate the translocation pathways of fluoroquinolones and respective Cu(II)/FQ/phen metalloantibiotics. The work encompassed 10 compounds, five FQs and respective metalloantibiotics, and was carried out through biophysical, microbiological, biochemical and toxicological approaches.

The biophysical work was focused on the influx of the compounds in *E. coli*. As the membrane of the Gram-negative bacteria is a complex structure, the interactions that govern the permeation may depend on the phospholipidic content and/or on the porins. The results obtained in the partition studies, performed with the non-fluorescent compounds (spx and Cuspxphen), are in agreement with the data previously reported in literature for the other compounds used in this work. A comprehensive comparison of the partition coefficients (K_p) and physicochemical properties of the 10 studied compounds was performed. The results clearly demonstrate greater K_p values for the metalloantibiotics compared to FQs. Furthermore, the different interactions that govern the partition of FQs and metalloantibiotics, dependent on the species present in solution, support the different influx routes.

The work proceeded with location studies, whose results pointed out for a deeper location of all metalloantibiotics and pure spx, in comparison to the rest of the pure FQs. Among all metalloantibiotics, Cumxfxphen and Cuspxphen proved to be more embedded in the membrane, while Cucpxphen, Cuerxphen and Culvxphen were positioned both near the polar heads of lipids as well as close to the hydrophobic tails of lipids. In general, both FQs and metalloantibiotics seemed to prefer regions of the membrane enriched by cardiolipin.

The study of the interaction of the compounds with the major porin involved in the uptake of FQs in *E. coli* (OmpF) was also assessed. The association constants determined for FQs and metalloantibiotics with OmpF wild-type were very similar. In turn, the experiments carried out with mutants of the porin revealed differences for the

pure FQ cpx and the metalloantibiotic Cucpxphen. The cpx-OmpF interaction is stronger in the centre of the channel, while Cucpxphen-OmpF is similar in the centre and in the periphery of the protein.

In summary, the biophysical results evidenced a greater partition for all metalloantibiotics and a deeper location of pure spx and metalloantibiotics in the membrane, especially Cumxfxphen and Cuspxphen. These results may support a hydrophobic pathway for metalloantibiotics and pure spx, independent on the need of porins. In addition, the uptake of cpx seems to occur via a hydrophilic pathway (dependent on OmpF), while Cucxphen might adopt a hydrophobic route to enter into the bacterial cell, using the porin. The implementation of different fluorescent methodologies proved to be useful to provide complementary information.

The work proceeded with the microbiological section, whose initial goal was to elucidate the role of the porins in the influx of the compounds. The microbiological results obtained with porin-deficient *E. coli* mutants disclosed that OmpF plays an active role in the influx of cpx, erx and lvx. In turn, the uptake of mxfx, spx, Cuerxphen, Cumxfxphen and Cuspxphen in *E. coli* seems independent on the porins. Concerning Cucpxphen and Culvxphen, the absence of porins affected their uptake, showing that these compounds may need Omp channels for their influx.

Taking together the biophysical and microbiological results, it is possible to expect different translocation pathways for FQs and metalloantibiotics, dependent on distinct interactions. The permeation of cpx erx and lvx into the bacterial cell is based on a hydrophilic-pathway (dependent on porins), while the translocation of mxfx, spx, Cuerxphen, Cumxfxphen and Cuspxphen occurs through a hydrophobic route (independent on porins). Cucpxphen and Culvxphen may adopt an influx route mediated by the porins. These results suggest that metalloantibiotics could be a promising alternative to FQs against Gram-negative bacteria, possibly overcoming the AMR mechanism based on the decreasing of the expression of porins. The biophysical and microbiological approaches, used to study the influx of the compounds, proved to reach similar results, which reinforces the importance of complementary biophysical/microbiological studies.

The second aim of the microbiological studies was to evaluate the antimicrobial activity of the compounds against a panel of MDR clinical isolates. The minimum inhibitory concentration (MIC) was determined for all compounds against several MDR isolates of Gram-negative (*E. coli* and *P. aeruginosa*) and Gram-positive (methicillin-resistant *S. aureus* - MRSA) bacteria. The obtained results showed comparable MIC values for FQs and metalloantibiotics against the Gram-negative

strains. In turn, the metalloantibiotics exhibited a greater antimicrobial activity against the majority of the MRSA isolates, which suggests that these compounds may be a promising alternative to FQs against *S. aureus*. Among all metalloantibiotics, Cucpxphen and Cuspxphen evidenced improved activity against a greater number of MRSA strains. These results triggered the need to clarify the mechanism of action and the safety of these compounds.

The work proceeded with a biochemical section, whose purpose was to clarify the mechanism of action of the metalloantibiotics in Gram-negative and Gram-positive bacteria. The obtained results evidenced enzymatic inhibitory activity for the metalloantibiotics against DNA gyrase and topoisomerase IV, the bacterial targets of FQs. Thus, it is expected a similar mechanism of action for FQs and metalloantibiotics. Among the four tested enzymes, DNA gyrase of *E. coli* and topoisomerases IV of *E. coli* and *S. aureus* seem to be the preferential targets of both FQs and metalloantibiotics. These results are in agreement with data previous reported in literature for FQs. Furthermore, the inhibitory activity of metalloantibiotics proved to be greater against the Gram-positive enzymes. These results reinforce the microbiological outcomes previously achieved, showing greater effectiveness against strains of *S. aureus*.

The work could not finish without the assessment of preliminary toxicity tests, in order to evaluate the safety of the metalloantibiotics. The cytotoxicity tests performed with fibroblasts cells evidenced that metalloantibiotics are more cytotoxic than FQs. It was also proposed that the cytotoxicity of the metalloantibiotics may arise from the Cu(II):phen moiety present in their structure. On the other hand, the hemolytic activity of the metalloantibiotics proved to be irrelevant, evidencing no erythrocyte lysis in the presence of the compounds.

This work was enriched by the combination of the multidisciplinary approaches, whose results provide complementary information. The main goals of our work were achieved, suggesting that metalloantibiotics could be a promising alternative to pure FQs due to its different translocation pathway and improved antimicrobial activity. The alternative influx route is especially relevant for Gram-negative bacteria, possibly overcoming one of the mechanisms of the bacterial resistance to FQs based on alterations on the permeability of the bacterial membrane. In turn, the improved activity observed against MRSA strains has particular interest for Gram-positive bacteria.

As future perspectives, the performance of biophysical studies focused on the interaction of the compounds with amino acid residues specific of the constriction zone should be a good strategy to better understand the permeation of the compounds.

Concerning the microbiological studies, it would be of interest to further explore the metalloantibiotics in combination with several families of antibiotics. Due to their improved antimicrobial activity, metalloantibiotics could be a promising alternative to pure FQs also in combined therapy, as a possible synergistic compound, which would decrease the cytotoxic effect by itself.

References

5

1 Fernández, L. & Hancock, R. E. W. Adaptive and Mutational Resistance: Role of Porins and Efflux Pumps in Drug Resistance. Clinical Microbiology Reviews 25, 661-681, doi:10.1128/cmr.00043-12 (2012).

2 Graef, F. et al. The bacterial cell envelope as delimiter of anti-infective bioavailability – An in vitro permeation model of the Gram-negative bacterial inner membrane. Journal of Controlled Release 243, 214-224, doi:http://dx.doi.org/10.1016/j.jconrel.2016.10.018 (2016).

3 Epand, R. M. & Epand, R. F. Lipid domains in bacterial membranes and the action of antimicrobial agents. Biochimica et Biophysica Acta (BBA) - Biomembranes 1788, 289-294, doi:https://doi.org/10.1016/j.bbamem.2008.08.023 (2009).

4 Strahl, H. & Errington, J. Bacterial Membranes: Structure, Domains, and Function. Annual Review of Microbiology 71, 519-538, doi:10.1146/annurev-micro-102215-095630 (2017).

5 Brown, L., Wolf, J. M., Prados-Rosales, R. & Casadevall, A. Through the wall: extracellular vesicles in Gram-positive bacteria, mycobacteria and fungi. Nat Rev Micro 13, 620-630, doi:10.1038/nrmicro3480 (2015).

6 Willey, J. M., Sherwood, L. M. & Woolverton, C. J. Prescott, Harley, and Klein's Microbiology. (McGraw-Hill Higher Education, 2008).

7 Silhavy, T. J., Kahne, D. & Walker, S. The Bacterial Cell Envelope. Cold Spring Harbor Perspectives in Biology 2, a000414, doi:10.1101/cshperspect.a000414 (2010).

8 Epand, R. M., Walker, C., Epand, R. F. & Magarvey, N. A. Molecular mechanisms of membrane targeting antibiotics. Biochimica et Biophysica Acta (BBA) - Biomembranes 1858, 980-987, doi:https://doi.org/10.1016/j.bbamem.2015.10.018 (2016).

9 Epand, R. F., Savage, P. B. & Epand, R. M. Bacterial lipid composition and the antimicrobial efficacy of cationic steroid compounds (Ceragenins). Biochimica et Biophysica Acta (BBA) - Biomembranes 1768, 2500-2509, doi:https://doi.org/10.1016/j.bbamem.2007.05.023 (2007).

10 Nadesalingam, J., Dodds, A. W., Reid, K. B. M. & Palaniyar, N. Mannose-Binding Lectin Recognizes Peptidoglycan via the N-Acetyl Glucosamine Moiety, and Inhibits Ligand-Induced Proinflammatory Effect and Promotes Chemokine Production by Macrophages. The Journal of Immunology 175, 1785-1794, doi:10.4049/jimmunol.175.3.1785 (2005).

11 Delcour, A. H. Outer Membrane Permeability and Antibiotic Resistance. Biochimica et biophysica acta 1794, 808-816, doi:10.1016/j.bbapap.2008.11.005 (2009).

12 Koebnik, R., Locher, K. P. & Van Gelder, P. Structure and function of bacterial outer membrane proteins: barrels in a nutshell. Molecular Microbiology 37, 239-253, doi:10.1046/j.1365-2958.2000.01983.x (2000).

13 Masi, M. & Pagès, J.-M. Structure, Function and Regulation of Outer Membrane Proteins Involved in Drug Transport in Enterobactericeae: the OmpF/C – TolC

Case. The Open Microbiology Journal 7, 22-33, doi:10.2174/1874285801307010022 (2013).

14 Rollauer, S. E., Sooreshjani, M. A., Noinaj, N. & Buchanan, S. K. Outer membrane protein biogenesis in Gram-negative bacteria. Philosophical Transactions of the Royal Society B: Biological Sciences 370, doi:10.1098/rstb.2015.0023 (2015).

15 Galdiero, S. et al. Microbe-Host Interactions: Structure and Role of Gram-Negative Bacterial Porins. Current Protein & Peptide Science 13, 843-854, doi:10.2174/138920312804871120 (2012).

16 Ziervogel, Brigitte K. & Roux, B. The Binding of Antibiotics in OmpF Porin. Structure 21, 76-87, doi:https://doi.org/10.1016/j.str.2012.10.014 (2013).

17 Mahendran, K. R., Kreir, M., Weingart, H., Fertig, N. & Winterhalter, M. Permeation of Antibiotics through Escherichia coli OmpF and OmpC Porins. Journal of Biomolecular Screening 15, 302-307, doi:doi:10.1177/1087057109357791 (2010).

18 Schulz, G. E. The structure of bacterial outer membrane proteins. Biochimica et Biophysica Acta (BBA) - Biomembranes 1565, 308-317, doi:http://dx.doi.org/10.1016/S0005-2736(02)00577-1 (2002).

19 Saraiva, R. G., Lopes, J. A., Machado, J., Gameiro, P. & Feio, M. J. Discrimination of single-porin Escherichia (E.) coli mutants by ATR and transmission mode FTIR spectroscopy. Journal of Biophotonics 7, 392-400, doi:10.1002/jbio.201200131 (2014).

20 Masi, M., Réfregiers, M., Pos, K. M. & Pagès, J.-M. Mechanisms of envelope permeability and antibiotic influx and efflux in Gram-negative bacteria. 2, 17001, doi:10.1038/nmicrobiol.2017.1 (2017).

21 Nikaido, H. Molecular Basis of Bacterial Outer Membrane Permeability Revisited. Microbiology and Molecular Biology Reviews 67, 593-656, doi:http://dx.doi.org/10.1128/MMBR.67.4.593-656.2003 (2003).

22 Mahendran, K. R. et al. Molecular Basis of Enrofloxacin Translocation through OmpF, an Outer Membrane Channel of Escherichia coli - When Binding Does Not Imply Translocation. The Journal of Physical Chemistry B 114, 5170-5179, doi:10.1021/jp911485k (2010).

23 Lou, H. et al. Altered Antibiotic Transport in OmpC Mutants Isolated from a Series of Clinical Strains of Multi-Drug Resistant E. coli. PLoS ONE 6, e25825, doi:10.1371/journal.pone.0025825 (2011).

24 Kojima, S. & Nikaido, H. High Salt Concentrations Increase Permeability through OmpC Channels of Escherichia coli. Journal of Biological Chemistry 289, 26464-26473, doi:10.1074/jbc.M114.585869 (2014).

25 Yoshida, T., Qin, L., Egger, L. A. & Inouye, M. Transcription Regulation of ompF and ompC by a Single Transcription Factor, OmpR. Journal of Biological Chemistry 281, 17114-17123, doi:10.1074/jbc.M602112200 (2006).

26 Li, J. et al. A review on phospholipids and their main applications in drug delivery systems. Asian Journal of Pharmaceutical Sciences 10, 81-98, doi:https://doi.org/10.1016/j.ajps.2014.09.004 (2015).

27 Jouhet, J. Importance of the hexagonal lipid phase in biological membrane organization. Frontiers in Plant Science 4, 494, doi:10.3389/fpls.2013.00494 (2013).

28 Akbarzadeh, A. et al. Liposome: classification, preparation, and applications. Nanoscale Research Letters 8, 102-102, doi:10.1186/1556-276x-8-102 (2013).

29 Eze, M. O. Phase transitions in phospholipid bilayers: Lateral phase separations play vital roles in biomembranes. Biochemical Education 19, 204-208, doi:10.1016/0307-4412(91)90103-f (1991).

30 Avanti Polar Lipids, I., http://www.avantilipids.com/, accessed on february 2019.

31 Lopes, S., Neves, C. S., Eaton, P. & Gameiro, P. Cardiolipin, a key component to mimic the E. coli bacterial membrane in model systems revealed by dynamic light scattering and steady-state fluorescence anisotropy. Analytical and Bioanalytical Chemistry 398, 1357-1366, doi:10.1007/s00216-010-4028-6 (2010).

32 Matos, C., Moutinho, C. & Lobão, P. Liposomes as a Model for the Biological Membrane: Studies on Daunorubicin Bilayer Interaction. The Journal of Membrane Biology 245, 69-75, doi:10.1007/s00232-011-9414-2 (2012).

33 Czogalla, A., Grzybek, M., Jones, W. & Coskun, Ü. Validity and applicability of membrane model systems for studying interactions of peripheral membrane proteins with lipids. Biochimica et Biophysica Acta (BBA) - Molecular and Cell Biology of Lipids 1841, 1049-1059, doi:https://doi.org/10.1016/j.bbalip.2013.12.012 (2014).

34 Rigaud, J. L. Membrane proteins: functional and structural studies using reconstituted proteoliposomes and 2-D crystals. Braz J Med Biol Res 35, 753-766 (2002).

35 Sejwal, K. et al. in Nanotechnology Reviews Vol. 6 57 (2017).

36 Alavi, M., Karimi, N. & Safaei, M. Application of Various Types of Liposomes in Drug Delivery Systems. Advanced Pharmaceutical Bulletin 7, 3-9, doi:10.15171/apb.2017.002 (2017).

37 Sercombe, L. et al. Advances and Challenges of Liposome Assisted Drug Delivery. Frontiers in Pharmacology 6, doi:10.3389/fphar.2015.00286 (2015).

38 White, G. F., Racher, K. I., Lipski, A., Hallett, F. R. & Wood, J. M. Physical properties of liposomes and proteoliposomes prepared from Escherichia coli polar lipids. Biochimica et Biophysica Acta (BBA) - Biomembranes 1468, 175-186, doi:https://doi.org/10.1016/S0005-2736(00)00255-8 (2000).

39 Pandit, K. R. & Klauda, J. B. Membrane models of E. coli containing cyclic moieties in the aliphatic lipid chain. Biochimica et Biophysica Acta (BBA) - Biomembranes 1818, 1205-1210, doi:https://doi.org/10.1016/j.bbamem.2012.01.009 (2012).

40 Lopes, S. C., Ferreira, M., Sousa, C. F. & Gameiro, P. A fast way to track functional OmpF reconstitution in liposomes: Escherichia coli total lipid extract. Analytical Biochemistry 479, 54-59, doi:https://doi.org/10.1016/j.ab.2015.03.026 (2015).

41 Global priority list of antibiotic-resistant bacteria to guide research, discovery, and development of new antibiotics. (World Health Organization, 2017).

42 von Wintersdorff, C. J. H. et al. Dissemination of Antimicrobial Resistance in Microbial Ecosystems through Horizontal Gene Transfer. Frontiers in Microbiology 7, doi:10.3389/fmicb.2016.00173 (2016).

43 Blair, J. M. A., Webber, M. A., Baylay, A. J., Ogbolu, D. O. & Piddock, L. J. V. Molecular mechanisms of antibiotic resistance. Nat Rev Micro 13, 42-51, doi:10.1038/nrmicro3380 (2015).

44 Antimicrobial resistance surveillance in Europe 2015. Annual Report of the European Antimicrobial Resistance Surveillance Network (EARS-Net). (European Centre for Disease Prevention and Control, Stockholm: ECDC, 2017).

45 Ferri, M., Ranucci, E., Romagnoli, P. & Giaccone, V. Antimicrobial resistance: A global emerging threat to public health systems. Critical Reviews in Food Science and Nutrition 57, 2857-2876, doi:10.1080/10408398.2015.1077192 (2017).

46 Davies, J. & Davies, D. Origins and Evolution of Antibiotic Resistance. Microbiology and Molecular Biology Reviews : MMBR 74, 417-433, doi:10.1128/mmbr.00016-10 (2010).

47 Lin, J. et al. Mechanisms of antibiotic resistance. Frontiers in Microbiology 6, doi:10.3389/fmicb.2015.00034 (2015).

48 Worldwide country situation analysis: response to antimicrobial resistance., (World Health Organization (WHO), Geneva, 2015).

49 Randall, C. P., Mariner, K. R., Chopra, I. & O'Neill, A. J. The Target of Daptomycin Is Absent from Escherichia coli and Other Gram-Negative Pathogens. Antimicrobial Agents and Chemotherapy 57, 637-639, doi:10.1128/aac.02005-12 (2013).

50 Berger-Bächi, B. Resistance mechanisms of Gram-positive bacteria. International Journal of Medical Microbiology 292, 27-35, doi:https://doi.org/10.1078/1438-4221-00185 (2002).

51 Tenover, F. C. Mechanisms of antimicrobial resistance in bacteria. American Journal of Infection Control 34, S3-S10, doi:https://doi.org/10.1016/j.ajic.2006.05.219 (2006).

52 Lewis, K. Platforms for antibiotic discovery. Nat Rev Drug Discov 12, 371-387, doi:10.1038/nrd3975 (2013).

53 Wright, G. D. Molecular mechanisms of antibiotic resistance. Chemical Communications 47, 4055-4061, doi:10.1039/c0cc05111j (2011).

54 Munita, J. M. & Arias, C. A. Mechanisms of Antibiotic Resistance. Microbiology spectrum 4, 10.1128/microbiolspec.VMBF-0016-2015, doi:10.1128/microbiolspec.VMBF-0016-2015 (2016).

55 Talan, D. A. et al. Fluoroquinolone-Resistant and Extended-Spectrum β-Lactamase–Producing Escherichia coli Infections in Patients with

Pyelonephritis, United States. Emerging Infectious Diseases 22, 1594-1603, doi:10.3201/eid2209.160148 (2016).

56 Bush, K. Bench-to-bedside review: The role of beta-lactamases in antibiotic-resistant Gram-negative infections. Critical care (London, England) 14, 224-224, doi:10.1186/cc8892 (2010).

57 Fernández-Cuenca, F. et al. Relationship between β-lactamase production, outer membrane protein and penicillin-binding protein profiles on the activity of carbapenems against clinical isolates of Acinetobacter baumannii. Journal of Antimicrobial Chemotherapy 51, 565-574, doi:10.1093/jac/dkg097 (2003).

58 Kim, J.-Y. et al. Resistance to Fluoroquinolone by a Combination of Efflux and Target Site Mutations in Enteroaggregative Escherichia coli Isolated in Korea. Osong Public Health and Research Perspectives 3, 239-244, doi:10.1016/j.phrp.2012.11.002 (2012).

59 Sivagurunathan, N. et al. Synergy of gatifloxacin with cefoperazone and cefoperazone–sulbactam against resistant strains of Pseudomonas aeruginosa. Journal of Medical Microbiology 57, 1514-1517, doi:doi:10.1099/jmm.0.2008/001636-0 (2008).

60 Lister, P. D., Wolter, D. J. & Hanson, N. D. Antibacterial-Resistant Pseudomonas aeruginosa: Clinical Impact and Complex Regulation of Chromosomally Encoded Resistance Mechanisms. Clinical Microbiology Reviews 22, 582-610, doi:10.1128/cmr.00040-09 (2009).

61 Yayan, J., Ghebremedhin, B. & Rasche, K. Antibiotic Resistance of Pseudomonas aeruginosa in Pneumonia at a Single University Hospital Center in Germany over a 10-Year Period. PLoS ONE 10, e0139836, doi:10.1371/journal.pone.0139836 (2015).

62 Tong, S. Y. C., Davis, J. S., Eichenberger, E., Holland, T. L. & Fowler, V. G. Staphylococcus aureus Infections: Epidemiology, Pathophysiology, Clinical Manifestations, and Management. Clinical Microbiology Reviews 28, 603-661, doi:10.1128/cmr.00134-14 (2015).

63 Campanile, F. et al. Epidemiology of Staphylococcus aureus in Italy: First nationwide survey, 2012. Journal of Global Antimicrobial Resistance 3, 247-254, doi:https://doi.org/10.1016/j.jgar.2015.06.006 (2015).

64 Andersson, M. I. & MacGowan, A. P. Development of the quinolones. Journal of Antimicrobial Chemotherapy 51, 1-11, doi:10.1093/jac/dkg212 (2003).

65 Appelbaum, P. C. & Hunter, P. A. The fluoroquinolone antibacterials: past, present and future perspectives. International Journal of Antimicrobial Agents 16, 5-15, doi:http://dx.doi.org/10.1016/S0924-8579(00)00192-8 (2000).

66 Emmerson, A. M. & Jones, A. M. The quinolones: decades of development and use. Journal of Antimicrobial Chemotherapy 51, 13-20, doi:http://dx.doi.org/10.1093/jac/dkg208 (2003).

67 Andriole, V. T. The Quinolones: Past, Present, and Future. Clinical Infectious Diseases 41, S113-S119, doi:10.1086/428051 (2005).

68 Oliphant, C. M. & Green, G. M. Quinolones: a comprehensive review. American Family Physician 65, 455-464 (2002).

69 Martinez, M., McDermott, P. & Walker, R. Pharmacology of the fluoroquinolones: A perspective for the use in domestic animals. The Veterinary Journal 172, 10-28, doi:http://dx.doi.org/10.1016/j.tvjl.2005.07.010 (2006).

70 Feio, M. J. et al. Fluoroquinolone–metal complexes: A route to counteract bacterial resistance? Journal of Inorganic Biochemistry 138, 129-143, doi:http://dx.doi.org/10.1016/j.jinorgbio.2014.05.007 (2014).

71 Sousa, I. et al. Synthesis, characterization and antibacterial studies of a copper(II) levofloxacin ternary complex. Journal of Inorganic Biochemistry 110, 64-71, doi:http://dx.doi.org/10.1016/j.jinorgbio.2012.02.003 (2012).

72 Naqvi, S. A. R. & Drlica, K. Fluoroquinolones as imaging agents for bacterial infection. Dalton Transactions 46, 14452-14460, doi:10.1039/c7dt01189j (2017).

73 Sousa, C. F., Ferreira, M., Abreu, B., Medforth, C. J. & Gameiro, P. Interactions of a non-fluorescent fluoroquinolone with biological membrane models: A multi-technique approach. International Journal of Pharmaceutics 495, 761-770, doi:http://dx.doi.org/10.1016/j.ijpharm.2015.09.037 (2015).

74 Gould, K. A., Pan, X.-S., Kerns, R. J. & Fisher, L. M. Ciprofloxacin Dimers Target Gyrase in Streptococcus pneumoniae. Antimicrobial Agents and Chemotherapy 48, 2108-2115, doi:10.1128/aac.48.6.2108-2115.2004 (2004).

75 Mustaev, A. et al. Fluoroquinolone-Gyrase-DNA Complexes: Two Modes of Drug Binding. Journal of Biological Chemistry, doi:10.1074/jbc.M113.529164 (2014).

76 Fàbrega, A., Madurga, S., Giralt, E. & Vila, J. Mechanism of action of and resistance to quinolones. Microbial biotechnology 2, 40-61, doi:10.1111/j.1751-7915.2008.00063.x (2009).

77 Redgrave, L. S., Sutton, S. B., Webber, M. A. & Piddock, L. J. V. Fluoroquinolone resistance: mechanisms, impact on bacteria, and role in evolutionary success. Trends in Microbiology 22, 438-445, doi:https://doi.org/10.1016/j.tim.2014.04.007 (2014).

78 Aldred, K. J., Kerns, R. J. & Osheroff, N. Mechanism of Quinolone Action and Resistance. Biochemistry 53, 1565-1574, doi:10.1021/bi5000564 (2014).

79 Hooper, D. C. & Jacoby, G. A. Topoisomerase Inhibitors: Fluoroquinolone Mechanisms of Action and Resistance. Cold Spring Harbor Perspectives in Medicine 6, doi:10.1101/cshperspect.a025320 (2016).

80 Antibacterial agents in clinical development: an analysis of the antibacterial clinical development pipeline, including tuberculosis., (World Health Organization, Geneva, 2017 (WHO/EMP/IAU/2017.12)).

81 Wohlkonig, A. et al. Structural basis of quinolone inhibition of type IIA topoisomerases and target-mediated resistance. Nature Structural &Amp; Molecular Biology 17, 1152, doi:10.1038/nsmb.1892 (2010).

82 Scholar, E. M. Fluoroquinolines: Past, Present and Future of a Novel Group of Antibacterial Agents. American Journal of Pharmaceutical Education 66, 164-172 (2003).

83 Schentag, J. J. Clinical Pharmacology of the Fluoroquinolones: Studies in Human Dynamic/Kinetic Models. Clinical Infectious Diseases 31, S40-S44, doi:10.1086/314059 (2000).

84 Bergogne-Bérézin, E. Clinical Role of Protein Binding of Quinolones. Clinical Pharmacokinetics 41, 741-750, doi:10.2165/00003088-200241100-00004 (2002).

85 Wright, D. H., Brown, G. H., Peterson, M. L. & Rotschafer, J. C. Application of fluoroquinolone pharmacodynamics. Journal of Antimicrobial Chemotherapy 46, 669-683, doi:10.1093/jac/46.5.669 (2000).

86 Fish, D. N., Choi, M. K. & Jung, R. Synergic activity of cephalosporins plus fluoroquinolones against Pseudomonas aeruginosa with resistance to one or both drugs. Journal of Antimicrobial Chemotherapy 50, 1045-1049, doi:10.1093/jac/dkf211 (2002).

87 Drago, L. et al. Comparative evaluation of synergy of combinations of β-lactams with fluoroquinolones or a macrolide in Streptococcus pneumoniae. Journal of Antimicrobial Chemotherapy 66, 845-849, doi:10.1093/jac/dkr016 (2011).

88 Louie, A. et al. Combination Treatment With Meropenem Plus Levofloxacin Is Synergistic Against Pseudomonas aeruginosa Infection in a Murine Model of Pneumonia. The Journal of Infectious Diseases 211, 1326-1333, doi:10.1093/infdis/jiu603 (2015).

89 Stergiopoulou, T. et al. Comparative pharmacodynamic interaction analysis between ciprofloxacin, moxifloxacin and levofloxacin and antifungal agents against Candida albicans and Aspergillus fumigatus. Journal of Antimicrobial Chemotherapy 63, 343-348, doi:10.1093/jac/dkn473 (2009).

90 Yamamoto, T., Tsurumaki, Y., Takei, M., Hosaka, M. & Oomori, Y. In vitro method for prediction of the phototoxic potentials of fluoroquinolones. Toxicology in Vitro 15, 721-727, doi:https://doi.org/10.1016/S0887-2333(01)00089-3 (2001).

91 Hayashi, N., Nakata, Y. & Yazaki, A. New Findings on the Structure-Phototoxicity Relationship and Photostability of Fluoroquinolones with Various Substituents at Position 1. Antimicrobial Agents and Chemotherapy 48, 799-803 (2004).

92 Stahlmann, R. Clinical toxicological aspects of fluoroquinolones. Toxicology Letters 127, 269-277, doi:http://dx.doi.org/10.1016/S0378-4274(01)00509-4 (2002).

93 Seto, Y. et al. Combined Use of In Vitro Phototoxic Assessments and Cassette Dosing Pharmacokinetic Study for Phototoxicity Characterization of Fluoroquinolones. AAPS J 13, 482-492, doi:10.1208/s12248-011-9292-7 (2011).

94 Oliveira, H. S., Gonçalo, M. & Figueiredo, A. C. Photosensitivity to lomefloxacin. A clinical and photobiological study. Photodermatology, Photoimmunology & Photomedicine 16, 116-120, doi:10.1111/j.1600-0781.2000.160303.x (2000).

95 Fernandes, P. et al. Synthesis, characterization and antibacterial studies of a copper(II) lomefloxacin ternary complex. Journal of Inorganic Biochemistry 131, 21-29, doi:https://doi.org/10.1016/j.jinorgbio.2013.10.013 (2014).

96 Kim, E. S. & Hooper, D. C. Clinical Importance and Epidemiology of Quinolone Resistance. Infection & Chemotherapy 46, 226-238, doi:10.3947/ic.2014.46.4.226 (2014).

97 Bansal, S. & Tandon, V. Contribution of mutations in DNA gyrase and topoisomerase IV genes to ciprofloxacin resistance in Escherichia coli clinical isolates. International Journal of Antimicrobial Agents 37, 253-255, doi:https://doi.org/10.1016/j.ijantimicag.2010.11.022 (2011).

98 Jung, C. M., Heinze, T. M., Strakosha, R., Elkins, C. A. & Sutherland, J. B. Acetylation of fluoroquinolone antimicrobial agents by an Escherichia coli strain isolated from a municipal wastewater treatment plant. Journal of Applied Microbiology 106, 564-571, doi:10.1111/j.1365-2672.2008.04026.x (2009).

99 Watanabe, R. & Doukyu, N. Contributions of mutations in acrR and marR genes to organic solvent tolerance in Escherichia coli. AMB Express 2, 58-58, doi:10.1186/2191-0855-2-58 (2012).

100 Aeschlimann, J. R. The Role of Multidrug Efflux Pumps in the Antibiotic Resistance of Pseudomonas aeruginosa and Other Gram-Negative Bacteria. Pharmacotherapy: The Journal of Human Pharmacology and Drug Therapy 23, 916-924, doi:10.1592/phco.23.7.916.32722 (2003).

101 Costa, S. S., Viveiros, M., Amaral, L. & Couto, I. Multidrug Efflux Pumps in Staphylococcus aureus: an Update. The Open Microbiology Journal 7, 59-71, doi:10.2174/1874285801307010059 (2013).

102 Adabi, M. et al. Spread of Efflux Pump Overexpressing-Mediated Fluoroquinolone Resistance and Multidrug Resistance in Pseudomonas aeruginosa by using an Efflux Pump Inhibitor. Infect Chemother 47, 98-104 (2015).

103 Saraiva, R. et al. Solution and biological behaviour of enrofloxacin metalloantibiotics: A route to counteract bacterial resistance? Journal of Inorganic Biochemistry 104, 843-850, doi:http://dx.doi.org/10.1016/j.jinorgbio.2010.03.017 (2010).

104 Gameiro, P., Rodrigues, C., Baptista, T., Sousa, I. & de Castro, B. Solution studies on binary and ternary complexes of copper(II) with some fluoroquinolones and 1,10-phenanthroline: Antimicrobial activity of ternary metalloantibiotics. International Journal of Pharmaceutics 334, 129-136, doi:http://dx.doi.org/10.1016/j.ijpharm.2006.10.035 (2007).

105 Luis Vázquez, J. et al. Determination by Fluorimetric Titration of the Ionization Constants of Ciprofloxacin in Solution and in the Presence of Liposomes¶. Photochemistry and Photobiology 73, 14-19, doi:10.1562/0031-8655(2001)0730014dbftot2.0.co2 (2001).

106 Sun, J. et al. Determination of lipophilicity of two quinolone antibacterials, ciprofloxacin and grepafloxacin, in the protonation equilibrium. European Journal of Pharmaceutics and Biopharmaceutics 54, 51-58, doi:https://doi.org/10.1016/S0939-6411(02)00018-8 (2002).

107 Turel, I. The interactions of metal ions with quinolone antibacterial agents. Coordination Chemistry Reviews 232, 27-47, doi:https://doi.org/10.1016/S0010-8545(02)00027-9 (2002).

108 Hernández-Gil, J. et al. Synthesis, structure and biological properties of several binary and ternary complexes of copper(II) with ciprofloxacin and 1,10 phenanthroline. Polyhedron 28, 138-144, doi:http://dx.doi.org/10.1016/j.poly.2008.09.018 (2009).

109 Osredkar, J. & Sustar, N. Copper and Zinc, Biological Role and Significance of Copper/Zinc Imbalance. Journal of Clinical Toxicology, doi:10.4172/2161-0495.S3-001 (2011).

110 Gaetke, L. M., Chow-Johnson, H. S. & Chow, C. K. Copper: Toxicological relevance and mechanisms. Archives of toxicology 88, 1929-1938, doi:10.1007/s00204-014-1355-y (2014).

111 Cobine, P. A., Pierrel, F. & Winge, D. R. Copper trafficking to the mitochondrion and assembly of copper metalloenzymes. Biochimica et Biophysica Acta (BBA) - Molecular Cell Research 1763, 759-772, doi:https://doi.org/10.1016/j.bbamcr.2006.03.002 (2006).

112 Samanovic, M. I., Ding, C., Thiele, D. J. & Darwin, K. H. Copper in microbial pathogenesis: meddling with the metal. Cell host & microbe 11, 106-115, doi:10.1016/j.chom.2012.01.009 (2012).

113 Palmer, L. D. & Skaar, E. P. Transition Metals and Virulence in Bacteria. Annual review of genetics 50, 67-91, doi:10.1146/annurev-genet-120215-035146 (2016).

114 Sigman, D. S., Graham, D. R., D'Aurora, V. & Stern, A. M. Oxygen-dependent cleavage of DNA by the 1,10-phenanthroline . cuprous complex. Inhibition of Escherichia coli DNA polymerase I. Journal of Biological Chemistry 254, 12269-12272 (1979).

115 Chen, C.-h. B., Milne, L., Landgraf, R., Perrin, D. M. & Sigman, D. S. Artificial Nucleases. CHEMBIOCHEM 2, 735-740 (2001).

116 Chen, C. H. & Sigman, D. S. Nuclease activity of 1,10-phenanthroline-copper: sequence-specific targeting. Proceedings of the National Academy of Sciences of the United States of America 83, 7147-7151 (1986).

117 Hirohama, T. et al. Copper(II) complexes of 1,10-phenanthroline-derived ligands: Studies on DNA binding properties and nuclease activity. Journal of Inorganic Biochemistry 99, 1205-1219, doi:https://doi.org/10.1016/j.jinorgbio.2005.02.020 (2005).

118 Lu, L.-P., Zhu, M.-L. & Yang, P. Crystal structure and nuclease activity of mono(1,10-phenanthroline) copper complex. Journal of Inorganic Biochemistry 95, 31-36, doi:https://doi.org/10.1016/S0162-0134(03)00049-7 (2003).

119 Ruíz, P. et al. Synthesis, structure, and nuclease properties of several binary and ternary complexes of copper(II) with norfloxacin and 1,10 phenantroline. Journal of Inorganic Biochemistry 101, 831-840, doi:https://doi.org/10.1016/j.jinorgbio.2007.01.009 (2007).

120 Efthimiadou, E. K. et al. Neutral and cationic mononuclear copper(II) complexes with enrofloxacin: Structure and biological activity. Journal of Inorganic Biochemistry 100, 1378-1388, doi:https://doi.org/10.1016/j.jinorgbio.2006.03.013 (2006).

121 Serafin, A. & Stańczak, A. The complexes of metal ions with fluoroquinolones. Russian Journal of Coordination Chemistry 35, 81-95, doi:10.1134/S1070328409020018 (2009).

122 Akinremi, C. A., Obaleye, J. A., Amolegbe, S. A., Adediji, J. F. & Bamigboye, M. O. Biological activities of some Fluoroquinolones-metal complexes. International Journal of Medicine and Biomedical Research 1, 24-34 (2012).

123 Ferreira, M. & Gameiro, P. Ciprofloxacin Metalloantibiotic: An Effective Antibiotic with an Influx Route Strongly Dependent on Lipid Interaction? Journal of Membrane Biology 248, 125-136, doi:http://dx.doi.org/10.1007/s00232-014-9749-6 (2015).

124 Lopes, S. C., Ribeiro, Carla, Gameiro, Paula. A New Approach to Counteract Bacteria Resistance: A Comparative Study Between Moxifloxacin and a New Moxifloxacin Derivative in Different Model Systems of Bacterial Membrane. Chemical Biology & Drug Design 81, 265-274, doi:http://dx.doi.org/10.1111/cbdd.12071 (2013).

125 Ribeiro, C., Lopes, S. C. & Gameiro, P. New insights into the translocation route of enrofloxacin and its metalloantibiotics. Journal of Membrane Biology 241, 117-125, doi:http://dx.doi.org/10.1007/s00232-011-9368-4 (2011).

126 Lakowicz, J. R. Principles of fluorescence spectroscopy. 3. edn, (Springer, 2006).

127 McClare, C. W. F. An accurate and convenient organic phosphorus assay. Analytical Biochemistry 39, 527-530, doi:https://doi.org/10.1016/0003-2697(71)90443-X (1971).

128 Bartlett, G. R. Phosphorus Assay in Column Chromatography. Journal of Biological Chemistry 234, 466-468 (1959).

129 Wiechelman, K. J., Braun, R. D. & Fitzpatrick, J. D. Investigation of the bicinchoninic acid protein assay: Identification of the groups responsible for color formation. Analytical Biochemistry 175, 231-237, doi:http://dx.doi.org/10.1016/0003-2697(88)90383-1 (1988).

130 Smith, P. K. et al. Measurement of protein using bicinchoninic acid. Analytical Biochemistry 150, 76-85, doi:http://dx.doi.org/10.1016/0003-2697(85)90442-7 (1985).

131 Haldar, S., Kombrabail, M., Krishnamoorthy, G. & Chattopadhyay, A. Depth-Dependent Heterogeneity in Membranes by Fluorescence Lifetime Distribution Analysis. Journal of Physical Chemistry Letters 3, 2676-2681, doi:http://dx.doi.org/10.1021/jz3012589 (2012).

132 Bhattacharya, B. & Samanta, A. Excited-State Proton-Transfer Dynamics of 7-Hydroxyquinoline in Room Temperature Ionic Liquids. Journal of Physical Chemistry B 112, 10101-10106, doi:http://dx.doi.org/10.1021/jp802930h (2008).

133 Cox, L. et al. Effect of Organic Amendments on Herbicide Sorption as Related to the Nature of the Dissolved Organic Matter. Environmental Science & Technology 34, 4600-4605, doi:10.1021/es0000293 (2000).

134 Ohno, T. Fluorescence Inner-Filtering Correction for Determining the Humification Index of Dissolved Organic Matter. Environmental Science & Technology 36, 742-746, doi:10.1021/es0155276 (2002).

135 Santos, N. C., Prieto, M. & Castanho, M. A. R. B. Quantifying molecular partition into model systems of biomembranes: an emphasis on optical spectroscopic methods. Biochimica et Biophysica Acta (BBA) - Biomembranes 1612, 123-135, doi:http://dx.doi.org/10.1016/S0005-2736(03)00112-3 (2003).

136 Lucio, M. et al. Influence of some anti-inflammatory drugs in membrane fluidity studied by fluorescence anisotropy measurements. Physical Chemistry Chemical Physics 6, 1493-1498, doi:10.1039/b314551b (2004).

137 Abrams, F. S. & London, E. Extension of the parallax analysis of membrane penetration depth to the polar region of model membranes: Use of fluorescence quenching by a spin-label attached to the phospholipid polar headgroup. Biochemistry 32, 10826-10831, doi:10.1021/bi00091a038 (1993).

138 Santos, N. C., Prieto, M. & Castanho, M. A. R. B. Interaction of the Major Epitope Region of HIV Protein gp41 with Membrane Model Systems. A Fluorescence Spectroscopy Study. Biochemistry 37, 8674-8682, doi:10.1021/bi9803933 (1998).

139 Teixeira, V. et al. Influence of Lysine Nε-Trimethylation and Lipid Composition on the Membrane Activity of the Cecropin A-Melittin Hybrid Peptide CA(1−7)M(2−9). The Journal of Physical Chemistry B 114, 16198-16208, doi:10.1021/jp106915c (2010).

140 Castanho, M. & Prieto, M. Filipin fluorescence quenching by spin-labeled probes: studies in aqueous solution and in a membrane model system. Biophysical Journal 69, 155-168, doi:http://dx.doi.org/10.1016/S0006-3495(95)79886-1 (1995).

141 Marsh, D. Handbook of lipid bilayers. Second edn, (CRC Press, 2013).

142 Rodrigues, C., Gameiro, P., Prieto, M. & de Castro, B. Interaction of rifampicin and isoniazid with large unilamellar liposomes: spectroscopic location studies. Biochimica et Biophysica Acta (BBA) - General Subjects 1620, 151-159, doi:http://dx.doi.org/10.1016/S0304-4165(02)00528-7 (2003).

143 de Almeida, R. F. M., Loura, L. M. S. & Prieto, M. Membrane lipid domains and rafts: current applications of fluorescence lifetime spectroscopy and imaging. Chemistry and Physics of Lipids 157, 61-77, doi:http://dx.doi.org/10.1016/j.chemphyslip.2008.07.011 (2009).

144 Merino-Montero, S., Montero, M. T. & Hernández-Borrell, J. Effects of lactose permease of Escherichia coli on the anisotropy and electrostatic surface potential of liposomes. Biophysical Chemistry 119, 101-105, doi:http://dx.doi.org/10.1016/j.bpc.2005.09.005 (2006).

145 Neves, P., Leite, A., Rangel, M., de Castro, B. & Gameiro, P. Influence of structural factors on the enhanced activity of moxifloxacin: a fluorescence and EPR spectroscopic study. Analytical and Bioanalytical Chemistry 387, 1543-1552, doi:10.1007/s00216-006-1009-x (2007).

146 Vázquez, J. L., Montero, M. T., Trias, J. & Hernàndez-Borrell, J. 6-Fluoroquinolone–liposome interactions: fluorescence quenching study using

iodide. International Journal of Pharmaceutics 171, 75-86, doi:https://doi.org/10.1016/S0378-5173(98)00154-9 (1998).

147 Chalpin, D. B. & Kleinfeld, A. M. Interaction of fluorescence quenchers with the n-(9-anthroyloxy) fatty acid membrane probes. Biochimica et Biophysica Acta (BBA) - Biomembranes 731, 465-474, doi:https://doi.org/10.1016/0005-2736(83)90042-1 (1983).

148 Neves, P. et al. Characterization of membrane protein reconstitution in LUVs of different lipid composition by fluorescence anisotropy. Journal of Pharmaceutical and Biomedical Analysis 49, 276-281, doi:http://dx.doi.org/10.1016/j.jpba.2008.11.026 (2009).

149 Mach, T. et al. Facilitated Permeation of Antibiotics across Membrane Channels − Interaction of the Quinolone Moxifloxacin with the OmpF Channel. Journal of the American Chemical Society 130, 13301-13309, doi:10.1021/ja803188c (2008).

150 Coutinho, A. & Prieto, M. Ribonuclease T1 and alcohol dehydrogenase fluorescence quenching by acrylamide: A laboratory experiment for undergraduate students. Journal of Chemical Education 70, 425, doi:10.1021/ed070p425 (1993).

151 Neves, P., Sousa, I., Winterhalter, M. & Gameiro, P. Fluorescence quenching as a tool to investigate quinolone antibiotic interactions with bacterial protein OmpF. J Membr Biol 227, 133-140, doi:10.1007/s00232-008-9152-2 (2009).

152 Neves, P., Berkane, E., Gameiro, P., Winterhalter, M. & de Castro, B. Interaction between quinolones antibiotics and bacterial outer membrane porin OmpF. Biophys Chem 113, 123-128, doi:10.1016/j.bpc.2004.08.004 (2005).

153 Larsson, T., Wedborg, M. & Turner, D. Correction of inner-filter effect in fluorescence excitation-emission matrix spectrometry using Raman scatter. Analytica Chimica Acta 583, 357-363, doi:http://dx.doi.org/10.1016/j.aca.2006.09.067 (2007).

154 Puchalski, M. M., Morra, M. J. & von Wandruszka, R. Assessment of inner filter effect corrections in fluorimetry. Fresenius' Journal of Analytical Chemistry 340, 341-344, doi:10.1007/BF00321578 (1991).

155 Castanho, M. A. R. B. & Prieto, M. J. E. Fluorescence quenching data interpretation in biological systems. Biochimica et Biophysica Acta (BBA) - Biomembranes 1373, 1-16, doi:http://dx.doi.org/10.1016/S0005-2736(98)00081-9 (1998).

156 Working Party of the British Society for Antimicrobial Chemotherapy. in A guide to sensitivity testing. Report of the Working Party of the British Society for Antimicrobial Chemotherapy. Vol. 27 Ch. 2.3. Standardization of inocula for sensitivity tests, 13-17 (Journal of Antimicrobial Chemotherapy, 1991).

157 Clinical and Laboratory Standards Institute (CLSI). Methods for Dilution Antimicrobial Susceptibility Tests for Bacteria That Grow Aerobically. CLSI document M07-A9. Approved Standard - Ninth edn, (Clinical and Laboratory Standards Institute, 2012).

158 Hall, B. G., Acar, H., Nandipati, A. & Barlow, M. Growth Rates Made Easy. Molecular Biology and Evolution 31, 232-238, doi:10.1093/molbev/mst187 (2014).

159 Reller, L. B., Weinstein, M., Jorgensen, J. H. & Ferraro, M. J. Antimicrobial Susceptibility Testing: A Review of General Principles and Contemporary Practices. Clinical Infectious Diseases 49, 1749-1755, doi:10.1086/647952 (2009).

160 Gibbons, S., Oluwatuyi, M. & Kaatz, G. W. A novel inhibitor of multidrug efflux pumps in Staphylococcus aureus. Journal of Antimicrobial Chemotherapy 51, 13-17, doi:10.1093/jac/dkg044 (2003).

161 Seral, C., Van Bambeke, F. & Tulkens, P. M. Quantitative Analysis of Gentamicin, Azithromycin, Telithromycin, Ciprofloxacin, Moxifloxacin, and Oritavancin (LY333328) Activities against Intracellular Staphylococcus aureus in Mouse J774 Macrophages. Antimicrobial Agents and Chemotherapy 47, 2283-2292, doi:10.1128/aac.47.7.2283-2292.2003 (2003).

162 Ba, B. B. et al. Activity of Gatifloxacin in an In Vitro Pharmacokinetic-Pharmacodynamic Model against Staphylococcus aureus Strains either Susceptible to Ciprofloxacin or Exhibiting Various Levels and Mechanisms of Ciprofloxacin Resistance. Antimicrobial Agents and Chemotherapy 50, 1931-1936, doi:10.1128/aac.01586-05 (2006).

163 Barcia-Macay, M., Seral, C., Mingeot-Leclercq, M.-P., Tulkens, P. M. & Van Bambeke, F. Pharmacodynamic Evaluation of the Intracellular Activities of Antibiotics against Staphylococcus aureus in a Model of THP-1 Macrophages. Antimicrobial Agents and Chemotherapy 50, 841-851, doi:10.1128/aac.50.3.841-851.2006 (2006).

164 Schedletzky, H., Wiedemann, B. & Heisig, P. The effect of moxifloxacin on its target topoisomerases from Escherichia coli and Staphylococcus aureus. Journal of Antimicrobial Chemotherapy 43, 31-37, doi:10.1093/jac/43.suppl_2.31 (1999).

165 Orhan, D. D., Özçelik, B., Özgen, S. & Ergun, F. Antibacterial, antifungal, and antiviral activities of some flavonoids. Microbiological Research 165, 496-504, doi:http://dx.doi.org/10.1016/j.micres.2009.09.002 (2010).

166 Nguyen, H. A. et al. Factors influencing the intracellular activity of fluoroquinolones: a study using levofloxacin in a Staphylococcus aureus THP-1 monocyte model. Journal of Antimicrobial Chemotherapy 57, 883-890, doi:10.1093/jac/dkl079 (2006).

167 Patel, M. V. et al. Antistaphylococcal Activity of WCK 771, a Tricyclic Fluoroquinolone, in Animal Infection Models. Antimicrobial Agents and Chemotherapy 48, 4754-4761, doi:10.1128/aac.48.12.4754-4761.2004 (2004).

168 Rey-Mellano, M. E., Senoro, D. B., Tayo, L. L. & Wan, M.-W. in 6th International Conference on Biological, Chemical & Environmental Sciences (BCES-2016) (Pattaya, Thailand, 2016).

169 Clinical and Laboratory Standards Institute (CLSI). Performance Standards for Antimicrobial Susceptibility Testing. CLSI document M100-S24., Vol. Twenty-Fourth Informational Supplement (Clinical and Laboratory Standards Institute, 2014).

170 The European Committee on Antimicrobial Susceptibility Testing. Routine and extended internal quality control for MIC determination and disk diffusion as ecommended by EUCAST. Version 8.0. (2018).

171 The European Committee on Antimicrobial Susceptibility Testing (EUCAST). Breakpoint tables for interpretation of MICs and zone diameters. Version 8.1. (http://www.eucast.org, 2018).

172 Blondeau, J. M. Fluoroquinolones: mechanism of action, classification, and development of resistance. Survey of Ophthalmology 49, S73-S78, doi:http://dx.doi.org/10.1016/j.survophthal.2004.01.005 (2004).

173 Gomez Perez, M., Fourcade, L., Mateescu, M. A. & Paquin, J. Neutral Red versus MTT assay of cell viability in the presence of copper compounds. Analytical Biochemistry 535, 43-46, doi:https://doi.org/10.1016/j.ab.2017.07.027 (2017).

174 Grassi, L., Maisetta, G., Maccari, G., Esin, S. & Batoni, G. Analogs of the Frog-skin Antimicrobial Peptide Temporin 1Tb Exhibit a Wider Spectrum of Activity and a Stronger Antibiofilm Potential as Compared to the Parental Peptide. Frontiers in Chemistry 5, doi:10.3389/fchem.2017.00024 (2017).

175 Tavanti, A. et al. Fungicidal activity of the human peptide hepcidin 20 alone or in combination with other antifungals against Candida glabrata isolates. Peptides 32, 2484-2487, doi:https://doi.org/10.1016/j.peptides.2011.10.012 (2011).

176 Cramariuc, O. et al. Mechanism for translocation of fluoroquinolones across lipid membranes. Biochimica et Biophysica Acta (BBA) - Biomembranes 1818, 2563-2571, doi:http://dx.doi.org/10.1016/j.bbamem.2012.05.027 (2012).

177 Ross, D. L., Elkinton, S. K. & Riley, C. M. Physicochemical properties of the fluoroquinolone antimicrobials. III. 1-Octanol/water partition coefficients and their relationships to structure. International Journal of Pharmaceutics 88, 379-389, doi:https://doi.org/10.1016/0378-5173(92)90336-Z (1992).

178 Garrison, M. D., Doh, L. M., Potts, R. O. & Abraham, W. Fluorescence spectroscopy of 9-anthroyloxy fatty acids in solvents. Chemistry and Physics of Lipids 70, 155-162, doi:https://doi.org/10.1016/0009-3084(94)90083-3 (1994).

179 Villalaín, J. & Prieto, M. Location and interaction of N-(9-anthroyloxy)-stearic acid probes incorporated in phosphatidylcholine vesicles. Chemistry and Physics of Lipids 59, 9-16, doi:http://dx.doi.org/10.1016/0009-3084(91)90058-J (1991).

180 de Castro, B., Gameiro, P., Lima, J. L. F. C., Matos, C. & Reis, S. Location and partition coefficients of anti-inflammatory drugs in EPC liposomes. A fluorescence quenching study using n-(9-anthroyloxy)-stearic probes. Colloids and Surfaces A: Physicochemical and Engineering Aspects 190, 205-212, doi:http://dx.doi.org/10.1016/S0927-7757(01)00680-X (2001).

181 Sikaris, K. A. & Sawyer, W. H. The interaction of local anaesthetics with synthetic phospholipid bilayers. Biochemical Pharmacology 31, 2625-2631, doi:http://dx.doi.org/10.1016/0006-2952(82)90709-2 (1982).

182 Mazák, K., Kökösi, J. & Noszál, B. Lipophilicity of zwitterions and related species: A new insight. European Journal of Pharmaceutical Sciences 44, 68-73, doi:https://doi.org/10.1016/j.ejps.2011.06.009 (2011).

183 Esteves, F., Moutinho, C. & Matos, C. Correlation between octanol/water and liposome/water distribution coefficients and drug absorption of a set of pharmacologically active compounds. Journal of Liposome Research 23, 83-93, doi:10.3109/08982104.2012.742539 (2013).

184 Esquembre, R., Ferrer, M. L., Gutiérrez, M. C., Mallavia, R. & Mateo, C. R. Fluorescence Study of the Fluidity and Cooperativity of the Phase Transitions of Zwitterionic and Anionic Liposomes Confined in Sol−Gel Glasses. The Journal of Physical Chemistry B 111, 3665-3673, doi:10.1021/jp068685y (2007).

185 Nicolini, C. et al. Temperature and pressure effects on structural and conformational properties of POPC/SM/cholesterol model raft mixtures—a FT-IR, SAXS, DSC, PPC and Laurdan fluorescence spectroscopy study. Biochimica et Biophysica Acta (BBA) - Biomembranes 1758, 248-258, doi:https://doi.org/10.1016/j.bbamem.2006.01.019 (2006).

186 Kaiser, R. D. & London, E. Location of Diphenylhexatriene (DPH) and Its Derivatives within Membranes: Comparison of Different Fluorescence Quenching Analyses of Membrane Depth. Biochemistry 37, 8180-8190, doi:10.1021/bi980064a (1998).

187 do Canto, A. M. T. M. et al. Diphenylhexatriene membrane probes DPH and TMA-DPH: A comparative molecular dynamics simulation study. Biochimica et Biophysica Acta (BBA) - Biomembranes 1858, 2647-2661, doi:https://doi.org/10.1016/j.bbamem.2016.07.013 (2016).

188 Epand, R. F., Tokarska-Schlattner, M., Schlattner, U., Wallimann, T. & Epand, R. M. Cardiolipin Clusters and Membrane Domain Formation Induced by Mitochondrial Proteins. Journal of Molecular Biology 365, 968-980, doi:https://doi.org/10.1016/j.jmb.2006.10.028 (2007).

189 Domènech, Ò., Morros, A., Cabañas, M. E., Montero, M. T. & Hernández-Borrell, J. Thermal response of domains in cardiolipin content bilayers. Ultramicroscopy 107, 943-947, doi:https://doi.org/10.1016/j.ultramic.2007.04.009 (2007).

190 Polishchuk, A. V., Karaseva, E. T., Emelina, T. B. & Karasev, V. E. Spectroscopic and Photophysical Properties of Protonated Forms of Some Fluoroquinolones in Solutions. Journal of Fluorescence 22, 373-379, doi:10.1007/s10895-011-0969-1 (2012).

191 Sousa, C. et al. The binding of free and copper-complexed fluoroquinolones to OmpF porins: an experimental and molecular docking study. Vol. 7 (2017).

192 Balouiri, M., Sadiki, M. & Ibnsouda, S. K. Methods for in vitro evaluating antimicrobial activity: A review. Journal of Pharmaceutical Analysis 6, 71-79, doi:https://doi.org/10.1016/j.jpha.2015.11.005 (2016).

193 Chalkley, L. J. & Koornhof, H. J. Antimicrobial activity of ciprofloxacin against Pseudomonas aeruginosa, Escherichia coli, and Staphylococcus aureus determined by the killing curve method: antibiotic comparisons and synergistic interactions. Antimicrobial Agents and Chemotherapy 28, 331 (1985).

194 Prilipov, A., Phale, P. S., Van Gelder, P., Rosenbusch, J. P. & Koebnik, R. Coupling site-directed mutagenesis with high-level expression: large scale production of mutant porins from E. coli. FEMS Microbiology Letters 163, 65-72 (1998).

195 Mulcahy, L. R., Burns, J. L., Lory, S. & Lewis, K. Emergence of Pseudomonas aeruginosa Strains Producing High Levels of Persister Cells in Patients with Cystic Fibrosis. Journal of Bacteriology 192, 6191-6199, doi:10.1128/jb.01651-09 (2010).

196 Leonard, S. N., Kaatz, G. W., Rucker, L. R. & Rybak, M. J. Synergy between gemifloxacin and trimethoprim/sulfamethoxazole against community-associated methicillin-resistant Staphylococcus aureus. Journal of Antimicrobial Chemotherapy 62, 1305-1310, doi:10.1093/jac/dkn379 (2008).

197 Cao, B. et al. Concentration-dependent cytotoxicity of copper ions on mouse fibroblasts in vitro: effects of copper ion release from TCu380A vs TCu220C intra-uterine devices. Biomedical Microdevices 14, 709-720, doi:10.1007/s10544-012-9651-x (2012).

198 Bunetel, L. et al. In vitro chemical and biological effects of Ag, Cu and Cu + Zn adjunction in 46S6 bioactive glasses. Materials Research Express 2, 095402, doi:10.1088/2053-1591/2/9/095402 (2015).

199 Bongers, M., Rusch, B. & van Gestel, C. A. M. The effect of counterion and percolation on the toxicity of lead for the springtail Folsomia candida in soil. Environmental Toxicology and Chemistry 23, 195-199, doi:doi:10.1897/02-508 (2004).

Supplementary Data

6

Table S1 - Antibiotic resistance profiles of the MDR isolates used in microbiological assays, determined according to EUCAST guidelines. [171]

Characteristics	Bacterial Strain					
	Ec1-SA1 [a]	**Ec2-SA1** [a]	**Ec3-SA1** [a]	**Ec4-SA** [a]	**HSJ Ec001**	**HSJ Ec002**
Sample						
Resistant to	ATM-CAZ-CTX-TE-AMP-SXT-CIP-CN	ATM-CAZ-CTX-TE-AMP-CIP	CAZ-CTX-TE-AMP-CIP-CN	ATM-CTX-AMP	AMP- CXM-CET-CIP-SXT-LVX	AMC-AMP-CAZ-CXM-CTX-CIP-GEN-TZP-TOB-SXT-LVX
	Bacterial Strain					
Characteristics	**HSJ Ec003**	**HSJ Ec004**	**Pa1-SA2** [b]	**Pa2-SA2** [b]	**Pa3-SA2** [b]	**Pa4-SA2** [b]
Sample						
Resistant to	CXM-CIP-LVX	AMC-AMP-CXM-CIP-TZP-LVX	CAZ-IPM-CIP	IPM-CN-CIP-FEP	CN-CIP-FEP	CAZ-IPM-CIP-FEP

[a] All strains were tested to: AMC-ATM-CAZ-CTX-TE-CHL-AMP-FOX-SXT-CIP-IPM-CN.

[b] All strains were tested to: CAZ-ATM-IPM-CN-CIP-FEP.

Antibiotic abbreviation: AMC - Amoxicillin-Clavulanate (2:1); AMP – Ampicillin; ATM – Aztreonam; CAZ – Ceftazidime; CET - Cefalotin; CHL – Chloramphenicol; CIP - Ciprofloxacin; CN – Cephalexin; CTX - Cefotaxime; CXM - Cefuroxime; DA - Clindamycin; DPT – Daptomicin; E - Eritromycin; FEP – Cefepime; FOX – Cefoxitin; GEN - Gentamicin; IPM – Imipenem; LNZ – Linezolid; LVX - Levofloxacin; OX - Oxacillin; RD – Rifamin; SXT - Trimethoprim-Sulphamethoxazole; TE – Tetracycline; TEC – Teicoplanin; TGC – Tygecicline; TOB – Tobramycin; TZP – Piperacillin - azobactam; VA – Vancomicin;

Table S2 - Antibiotic resistance profiles of the MRSA isolates used in microbiological assays, determined according to EUCAST guidelines. [171]

Characteristics	Bacterial Strain					
	Sa1-SA3 [c]	**Sa2-SA3** [c]	**Sa3-SA3** [c]	**Sa4-SA3** [c]	**17/05** [d]	**17/08** [d]
Sample					P.E.G. (cateter)	foreskin buffer
Resistant to	VA-AMP-FOX-CIP-OX	AMC-AMP-FOX-IPM-CIP-OX	VA-AMC-AMP-FOX-IPM-CIP-OX	AMP-FOX-CIP-OX	OXA-CTX-DA-E-CIP-LEV	OXA-CTX-CN-DA-E-CIP-LEV-DPT^{NS}
Clone					ST228/SCCmecIV	ST228/SCCmecI
	Bacterial Strain					
Characteristics	**37/3** [d]	**38/13 bis** [d]	**59/57** [d]	**27/17** [d]	**5/41** [d]	**58/01** [d]
Sample	bronchial lavage	umbical cord	buffer wound	unknown	Emoculture	buffer wound
Resistant to	OXA-CTX-CN-E-CIP-LEV	OXA-CTX-CN-CIP-LEV	OXA-CXT-DA-E-CIP-LEV-DPTNS-LNZ	CTX-CIP-LEV	OXA-CXT-CN-DA-E-CIP-LEV-DPTNS-LNZ	OXA-CXT-CIP-LEV-RD
Clone	ST22/SCCmecIV.h	ST22/SCCmecIV.h	ST22/SCCmecIV.h	IV.h/ST22/E-MRSA15/t20	ST5/SCCmecII	ST5/SCCmecII

[c] All strains were tested to: SXT-VA-AMC-CHL-TE-AMP-FOX-IPM-CN-CIP-OX.

[d] All strains were tested to: OXA-CTX-CN-DA-E-CIP-LEV-LNZ-DPT-TGC-RD-VA-TEC.

Antibiotic abbreviation: AMC - Amoxicillin-Clavulanate (2:1); AMP – Ampicillin; ATM – Aztreonam; CAZ – Ceftazidime; CET - Cefalotin; CHL – Chloramphenicol; CIP - Ciprofloxacin; CN – Cephalexin; CTX - Cefotaxime; CXM - Cefuroxime; DA - Clindamycin; DPT – Daptomicin; E - Eritromycin; FEP – Cefepime; FOX – Cefoxitin; GEN - Gentamicin; IPM – Imipenem; LNZ – Linezolid; LVX - Levofloxacin; OX - Oxacillin; RD – Rifamin; SXT - Trimethoprim-Sulphamethoxazole; TE – Tetracycline; TEC – Teicoplanin; TGC – Tygecicline; TOB – Tobramycin; TZP – Piperacillin - azobactam; VA – Vancomicin;

Table S2 – Continued.

Characteristics	Bacterial Strain					
	26/01 [d]	**16/01** [d]	**6/16 bis** [d]	**3/146** [d]	**7/21 bis** [d]	**19/35** [d]
Sample	unknown	scalp injury	buffer wound	ulcer	Emoculture	Pus
Resistant to	OXA-CTX-CN-CIP-LEV	OXA-CTX-CN-CIP-LEV	OXA-CXT-DA-E-CIP-LEV-DPT^{NS}-RD	OXA-CTX-CN-E-CIP-LEV	OXA-CXT-CN-CIP-LEV	OXA-CXT-CN-DA-E-CIP-LEV-DPT^{NS}-RD
Clone	ST239/SCCmecIII	ST772/SCCmec IV.c PVL+	ST5/SCCmecII	ST8/SCCmecIV	ST8/SCCmecIV	ST63/SCCmecIV

[d] All strains were tested to: OXA-CTX-CN-DA-E-CIP-LEV-LNZ-DPT-TGC-RD-VA-TEC.

Antibiotic abbreviation: AMC - Amoxicillin-Clavulanate (2:1); AMP – Ampicillin; ATM – Aztreonam; CAZ – Ceftazidime; CET - Cefalotin; CHL – Chloramphenicol; CIP - Ciprofloxacin; CN – Cephalexin; CTX - Cefotaxime; CXM - Cefuroxime; DA - Clindamycin; DPT – Daptomicin; E - Eritromycin; FEP – Cefepime; FOX – Cefoxitin; GEN - Gentamicin; IPM – Imipenem; LNZ – Linezolid; LVX - Levofloxacin; OX - Oxacillin; RD – Rifamin; SXT - Trimethoprim-Sulphamethoxazole; TE – Tetracycline; TEC – Teicoplanin; TGC – Tygecicline; TOB – Tobramycin; TZP – Piperacillin - azobactam; VA – Vancomicin;